ISSN 1984-6428

JANUARY-MARCH
2013
VOLUME 5
NUMBER 1

Orbital

The Electronic Journal of Chemistry

BODIPY DYES FOR CONJUGATION WITH PROTEINS

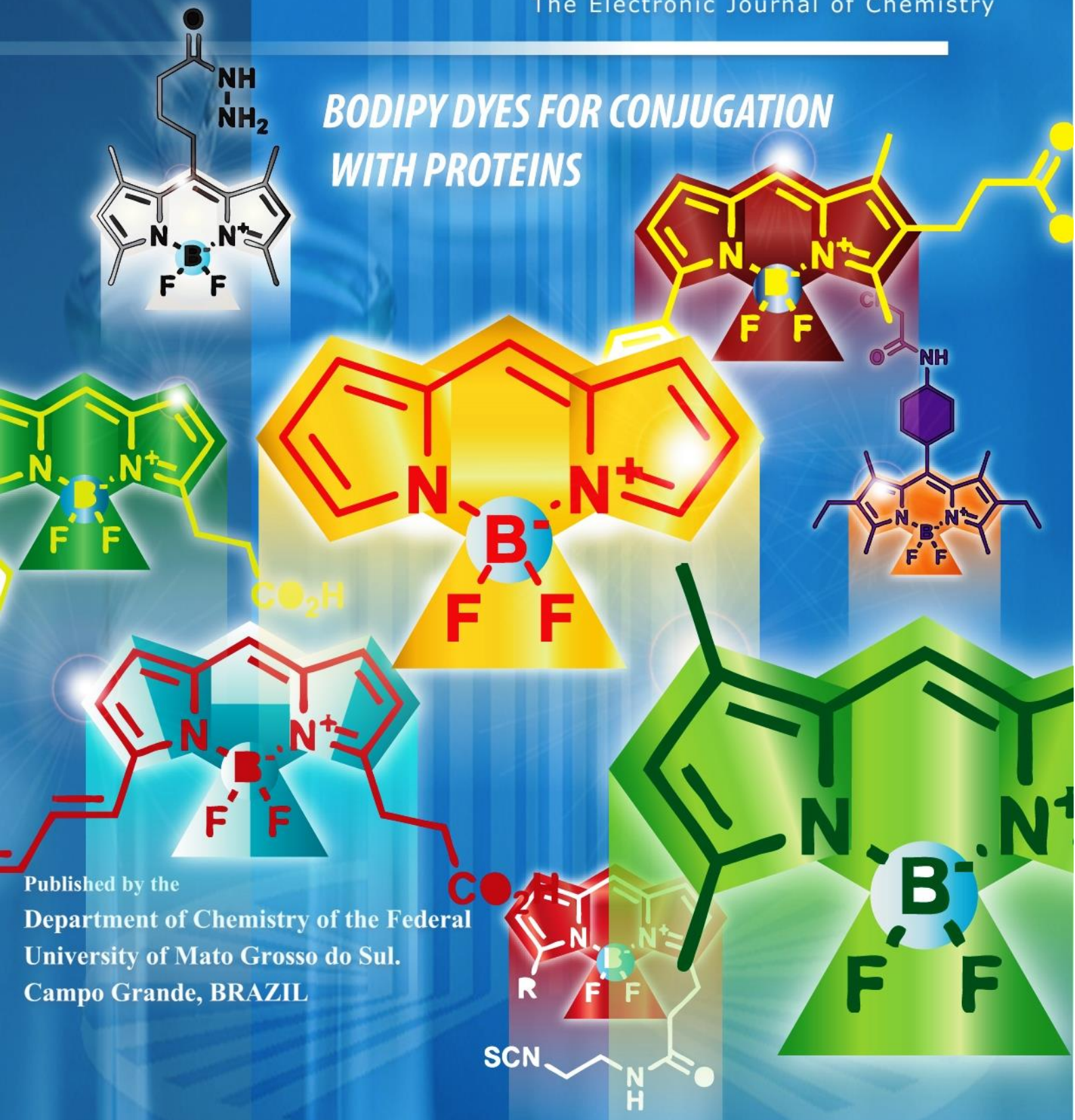

Published by the
Department of Chemistry of the Federal
University of Mato Grosso do Sul.
Campo Grande, BRAZIL

www.orbital.ufms.br

UFMS

Orbital - Vol. 5 No. 1 - January-March 2013

Table of Contents

FULL PAPERS

REVIEWS

Orbital: The Electronic Journal of Chemistry
journal homepage: www.orbital.ufms.br
ISSN 1984-6428

| Vol 5 | | No. 1 | | January-March 2013 |

Full Paper

Dielectric Behaviour of Binary Mixture of 2-Chloroaniline with 2-Methoxyethanol and 2-Ethoxyethanol

Bhupesh G. Nemmaniwar, Namdeo V. Kalyankar and Potaji L. Kadam*

Physics Research Laboratory, Yeshwant Mahavidyalaya, Nanded – 431605, Maharashtra, India.

Article history: Received: 04 April 2012; revised: 05 January 2013; accepted: 21 January 2013. Available online: 17 April 2013.

Abstract: Densities, viscosities, refractive indices, dielectric constant (ε') and dielectric loss (ε") of 2-chloroaniline (2CA) + 2-methoxyethanol (2ME) and 2-chloroaniline (2CA) + 2-ethoxyethanol (2EE) for different mole fractions of 2-chloroaniline in binary mixture have been measured at single microwave frequency 10.985 GHz at 30^0C by Surber method using microwave X-band. The values of dielectric parameters (ε' and ε") have been used to evaluate the molar polarization (P_{12}) loss tangent (tanδ), viscosity (η), activation energy (Ea), excess permittivity (Δε'), excess dielectric loss (Δε"), excess viscosities (Δη), excess polarization (ΔP_{12}) and excess activation energy (ΔE_a) have also been estimated. These parameters have been used to explain the formation of complexes in the system. It is found that dielectric constant (ε'), dielectric loss (ε"), loss tangent (tanδ), molar polarization (P_{12}) varies non-linearly but activation energy (Ea) , viscosity (η) ,density (ρ), and refractive index (n) varies linearly with increasing mole fraction in binary mixture of 2-chloroaniline (2-CA) + 2-methoxyethanol (2-ME) and 2-chloroaniline (2-CA) + 2-ethoxyethanol (2-EE). Hence, solute-solvent molecular associations have been reported.

Keywords: molecular interaction; polar liquids; binary mixture; excess parameters.

1. INTRODUCTION

Effects of molecular orientations are very sensitive to all kinds of interactions. Experimental investigation of dielectric properties of polar liquids from microwave absorption is of great value in understanding the nature of complex formation. When a binary mixture is formed the viscosity, density, refractive index, thermodynamic parameters and dielectric parameters do not vary linearly. The deviation from linearity of these parameters is termed as excess parameters which are useful to understand the nature of bonding between the two liquid mixtures.

The nature of complex formation between the molecules may be ascertained by studying apparent molar polarization and is useful in determine the nature of molecular interactions in the liquid systems. In past, several workers have made dielectric studies of liquid mixtures by taking amines as one of the constituent components in the binary mixture [1-7]. Vural *et al*. [8] have studied the excess molar volumes to refractive index of binary mixture glycerol + methanol and glycerol + water at 298.15 K and 303.15 K, respectively and Kamble *et al*. [9] have studied the excess parameters of binary systems of cyclohexane and methyl acetate.

Dielectric study of 2-CA + 2-ME and 2-CA + 2-EE mixture have not been carried out in the past. As such it was felt that the present study provides most useful information regarding the molecular interaction and the formation of complexes in the mixture of 2-CA + 2-ME and 2-CA + 2-EE.

2-Methoxyethanol (2-ME) is also called as methyl cellosolve and used as a solvent for mainly different purpose, such as varnishes, dyes, resins and an additive in airplane deicing solutions while 2-ethoxyethanol (2-EE) commercially known as “Cello solves” and widely used as complexes of solvents, coemulsifiers so stabilizers of emulsions, dyes and lacquers.

2. MATERIAL AND METHODS

* Corresponding author. E-mail: pothajikadam@yahoo.com

2.1. Materials

2-Chloroaniline (GC Grade) from Merck Schuchardt, Germany. 2-Methoxyethanol and 2-ethoxyethanol (AR Grade) were obtained from M/S Sd. Fine chemical, Mumbai, India without further purification. The two liquids according to their proportions by volume were mixed well and kept 6h in well stoppered bottles to ensure good thermal equilibrium. These liquids used as solute and solvent.

2.2. Measurements

The dielectric constant (ε') and dielectric loss (ε") have been measured using microwave X-band bench oscillating frequency of 10.985 GHz [10] at 30^0C using source of Reflex kystron 2 K 25 (USSR). The densities and viscosities of the pure components and their mixtures were measured by using DMA 35 portable vibrating density meter. Anton paar Autria (Europe) having accuracy of density 0.001 gm/cm^3 and viscosity by Oswald viscometer.

Refractive indices for sodium D-line were measured by using Abbe's refractometer, having accuracy up to the third place of decimal microwave power measured by PM-437 (Attest) power meter, Chennai, India. Rectangular wave guide working TE_{10} mode, 10 dB, Vidyut Vantra Udyog, India. To hold the liquid sample in the liquid cell, thin mica window whose VSWR and attenuation were neglected is introduced between the cell and rest of microwave bench.

The values of ε' and ε" for present investigation, for low loss liquids according to Heston *et al*. [11].

$$\varepsilon' = (\lambda_0/\lambda_c)^2 + (\lambda_0/\lambda_d)^2 \quad \ldots\ldots\ldots\ldots\ldots\ldots (1)$$

$$\varepsilon'' = 2/\pi\,(\lambda_g/\lambda_d)\,(\lambda_0/\lambda_d)^2\,(d\rho/dn) \quad \ldots\ldots\ldots\ldots\ldots\ldots (2)$$

Where λ_c is the cut-off wavelength, λ_o is the free space wavelength, λ_d is the wavelength in dielectric medium and λ_g is the wavelength in empty wave guide parameters ρ is inverse voltage standing wave ratio, n is the number of minima.

The precision of measurements for the wavelength with the available X-band microwave test bench is $\pm$0.001 cm corresponding to this accuracy value, the error in the measurements of ε' is estimated. For simplification, involved errors due to non zero impedance of the short circuit plunger are ignored. The errors of measurements are calculated by using the conventional method of error analysis [12]. Over all estimated accuracy of measurements for ε' and ε" by this method is about $\pm$1% and $\pm$5%, respectively.

The ε' and ε" were measured by reflectometric technique by measuring reflection coefficient from the air dielectric boundary of the liquid [13-18]. The ε' and ε" for different mole fractions of 2CA in the binary mixture of 2-CA+2-ME and 2-CA+2-EE are measured at 30^0C.

In order to determine the dielectric wavelength (λ_d), dielectric constant (ε'),dielectric loss (ε"), loss tangent (tanδ) and molar polarization (P_{12}), the movable short of the liquid cell was moved in and out and corresponding reflection coefficient was measured using crystal detector in the directional coupler [19].

The relationship between the reflected power and depth of liquid columns is given by a damped sinusoidal curve. The distance between two adjacent minima of this curve gives $\lambda_d/2$. Thus the knowing the values of wavelength in dielectric medium λ_d, free space wavelength (λ_0) cut off wavelength (λ_c), waveguide wavelength (λ_g) and molar polarization (P_{12}), were determined by Surber relations [10, 19-21]

3. RESULTS AND DISCUSSION

The values of viscosity (η), Refractive index (n), density (ρ), dielectric constant (ε'), dielectric loss (ε"), loss tangent (tanδ) and activation energy (E_a) for viscous flow with increasing mole fraction (X) of 2 CA for the binary mixtures of 2-CA + 2-ME and 2-CA+2-EE are reported in (Tables 1 and 2).

The variation of the dielectric constant (ε') with mole fraction of (2-CA) in mixture is as in Fig. 1a. A pronounced minima is observed in the curve at X=0.42771 for the (2-CA) + 2-ME, binary system and at X = 0.35551 for the (2-CA + 2-EE) which indicates the formation of complex in these binary mixture as for the amine + alcohol mixture observed by Combs *et al*. [22].

3.1. Microwave absorption

It is seen from Fig.1b that the absorption in the mixture is greater than that in pure liquids, a maxima in the tan δ curve occurring at X=0.0964 and X=0.4277 (2-ME and 2-EE) mole fraction of 2-CA in to our case the formation of complex will increases

the dielectric absorption due to the following consideration. In the complex, the dipole moment can be taken as, $(\mu_{D1+}\ \mu_{D2})$, μ_{D1} and μ_{D2} being the dipole moments of the constituent molecules. For n molecules of each liquid forming the complex the absorption would be proportional to n $(\mu_{D1}^{2}+\ \mu_{D2}^{2})$, for pure liquids, assuming no interaction. On the other hand, in the mixture absorption would be proportional to the greater term n $(\mu_{D1}^{2}+\ \mu_{D2}^{2})$.

Table 1. Values of mole fraction (X) of 2-CA density (ρ), viscosity (η), refractive index (n),dielectric constant (ε'),dielectric loss (ε''),loss tangent (tanδ) and activation energy (E_a) for binary liquid system at 30^0C.

System 1 (2CA+2ME)

X	ρ gm/cm^3	η CP	n	ε'	ε''	tanδ	E_a (Kcal/mol)
0	0.9569	1.3577	1.391	6.6882	0.5752	0.0806	3.5430
0.09647	0.9914	1.5502	1.417	5.9745	0.6942	0.1162	3.6229
0.19944	1.0260	1.7984	1.440	5.8212	0.5287	0.0908	3.7123
0.30959	1.0596	2.0753	1.466	6.2272	0.6895	0.1107	3.7986
0.42771	1.0903	2.1779	1.490	4.1455	0.4037	0.0974	3.8276
0.55469	1.1210	3.9268	1.511	6.8956	0.7655	0.1101	4.1826
0.69156	1.1506	4.0572	1.535	4.9912	0.4570	0.0916	4.2023
0.83953	1.170	4.0727	1547	4.4318	0.2975	0.0671	4.2046
1	1.2056	2.6800	1.575	4.1455	0.2585	0.0624	3.8931

Table 2. Values of mole fraction (X) of 2-CA density (ρ), viscosity (η), refractive index (n),dielectric constant (ε'),dielectric loss (ε''),loss tangent (tanδ) and activation energy (E_a) for binary liquid system at 30^0 C

System 2 (2CA + 2EE)

X	ρ gm/cm^3	η CP	n	ε'	ε''	tanδ	E_a (Kcal/mol)
0	0.9236	1.5462	1.395	3.2563	0.1294	0.0397	3.6213
0.11609	0.9664	1.8552	1.422	4.9915	0.2929	0.0587	3.7310
0.23457	1.0007	3.4450	1.445	4.4318	0.1394	0.0315	4.1038
0.35551	1.0391	3.7185	1.472	2.4142	0.0440	0.0182	4.1498
0.47899	1.0739	3.9080	1.492	5.5157	0.5279	0.0951	4.1797
0.60510	1.1064	4.0073	1.512	3.0420	0.1901	0.0625	4.1948
0.73391	1.1403	4.1158	1.534	4.0136	0.2387	0.0595	4.2109
0.86551	1.8056	4.2856	1.554	4.2848	0.3000	0.0700	4.2353
1	1.2056	2.6800	1.575	4.1456	0.2780	0.0671	3.8931

3.2. Maxima in the viscosity curve

When the viscosity (η) is plotted against mole fraction, the curve shows sharp maxima in Fig.1c. The maxima for the 2-CA+2-ME mixture accuracy at X=0.691 mole fraction of (2-CA) and for 2-CA+2-EE mixture it occur curve at X=0.839 mole fraction of (2-CA) the maxima for the 2-EE is much pronounced than that for 2-ME. Huyskens *et al.* [8] have explained the increases in viscosity for the acid amine and 2-ME or 2-EE mixture due to the formation of dissociated ions in the mixture. Which is exothermic and depends upon the acidic strength of 2-ME and 2-EE Since in the present case 2-EE react with (2-CA) by an exothermic reaction, the pronounced maxima for the 2-ME may be associated with the formation of dissociated ions in the mixture and due to the more acidic character of 2-ME than 2-EE. The spectacular increases in viscosity (η) may also be attributed to the mutual that viscosity of the alcohols and amine molecules, as provided by the Andrade's theory [20].

3.3. Excess parameters

The excess values of dielectric permittivity $\Delta\varepsilon'$, excess viscosity $\Delta\eta$, excess square of refractive index Δn^2D, excess activation energy ΔE_a for 2-CA+2-ME and 2-CA+2-EE system are presented in Fig. 2.

The excess value calculated by using the relation:

$$\Delta Y=Y_m-(X_1Y_1+X_2Y_2) \quad \text{..... (3)}$$

Where ΔY any excess parameters and Y is refers to the above mentioned quantities the subscripts m, 1 and 2 used in the above equation are respectively for the mixture, component 1 and component 2. X_1 and X_2 are the mole fraction of two components in the liquids mixture.

The excess viscosities, excess square of refractive index and excess activation energy are all positive indicating strong interaction between the alcohols and amines molecules. For all there excess parameters the maxima for the 2-CA+2-ME mixture occur at X=0.55469 mole fraction of 2-CA and for 2-CA+2-EE mixture maxima occur at about X= 0.35551 mole fraction of 2CA (Fig. 2a, 2b, 2c).

The dipole moment of 2-ME and 2-EE calculated by formula [21]:

$$\mu_D = 0.0127 \times 10^{-18} \sqrt{(P_{12} - P_0)T} \quad \text{..... (4)}$$

The values of dipole moment μ_D obtained for 2- ME and 2-EE are μ_D =0.8994 esu and μ_D =0.5580 esu, respectively. The higher μ_D value of 2-ME indicates that dipole-dipole interaction in 2-ME is stronger than 2-EE. This behavior of 2-ME is supported by the higher values of activation energy and excess activation energy of 2-ME as compared to 2-EE. The deviation of excess activation energy of viscous flow in these systems indicates the increases the internal energy of viscous flow thus, supporting the presence of strong interaction in the system of alcohols and amines (Fig. 2c).

The variation of the square of refractive indices on mixing with the mole fraction of 2-CA it can be seen that in (Fig. 2b) That the changes in refractive index of 2-CA+2-ME and 2-CA + 2-EE are positive throughout the entire composition range, and that as the hydrogen bonding of the interactions increases the change in refractive index becomes more negative.

The excess dielectric constant of the mixture was plotted against the mole fraction of 2-CA in the mixture at 30^0C and is shown in Fig. 2d from the figure it can be seen that negative (2-ME) $0 \leq X \leq 0.27, 0.38 \leq X \leq 0.53$ and at $0.78 \leq X \leq 1$. Positive at $X=0.27 \leq X \leq 0.38$ and $0.58 \leq X \leq 0.72$. (2-EE) positive at $0 \leq X \leq 0.28$, $0.40 \leq X \leq 0.58$ and again at $0.72 \leq X \leq 1$. Negative at $0.28 \leq X \leq 0.40$ and $0.58 \leq X \leq 0.72$, respectively and again showing a positive value of 50% of 2-EE and 55% of 2-ME concentration of 2-CA, for both the systems. At the concentration for which $\Delta\varepsilon'$ is negative indicates that molecules of the mixtures form multimer structure via hydrogen bonding in such a way that the effective dipole movement is reduced where as the concentrations for which $\Delta\varepsilon'$ is positive indicates that the molecules of the mixture form multimer structure via hydrogen bonding in such a way that the effective dipole moments are increased.

4. CONCLUSION

The dielectric constant, dielectric loss, loss tangent, viscosity, density, refractive index and excess parameters have been reported for 2-CA+2-ME and 2-CA+2-EE binary mixture at the various concentrations. These suggest the strong interaction between the alcohols and amine molecules. The excess parameter curves suggest the more acidic

character of 2-ME than 2-EE.

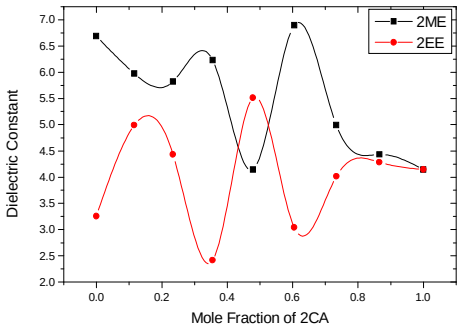

1a

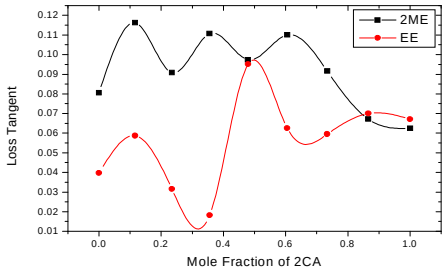

1b

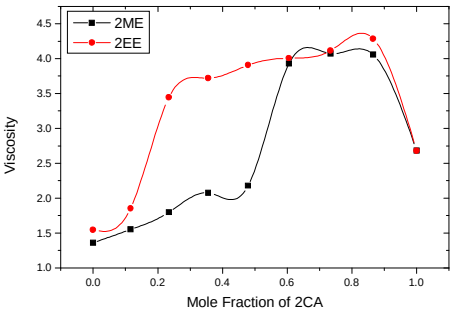

1c

Figure 1. Variation of (a) dielectric constant (ε'**)** (b) Loss Tangent (tanδ) and (c) Viscosity (η) mole fraction of 2-CA.

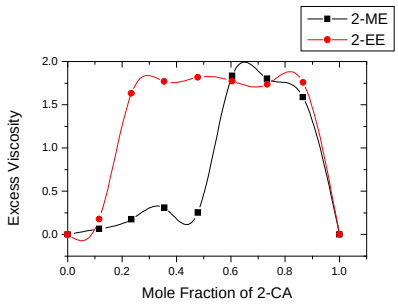

2a

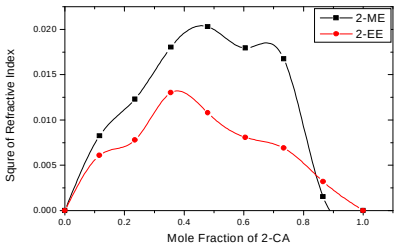

2b

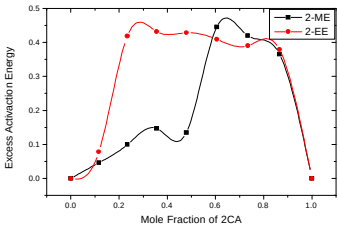

2c

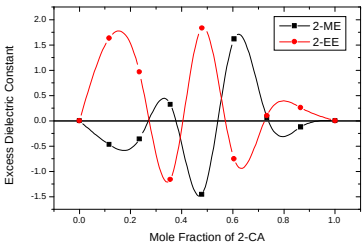

2d

Figure 2. Variation of (a) Excess viscosity (Δη) (b) Excess square of refractive index (n^2D) (c) Excess activation energy (ΔE_a) and (d) Excess dielectric constant (Δε') mole fraction of 2-CA.

5. ACKNOWLEDGMENTS

The authors thanks to the Principal, Yeshwant Mahavidyalaya Nanded for providing necessary laboratory facilities.

6. REFERENCES AND NOTES

[1] Mahendran, G.; Palaniappan, L. *Indian J. of Pure & App. Phys.* **2011**, *49*, 803.

[2] Vishwam,T.; Chitra, M.; Subramanian, V.; Murty, V.R.K. *J.Molecular Structure*. **2008**, *872*, 93. [CrossRef]

[3] Vijaya, K. T.; Madhumohan, T. *J. Chem. Thermodynamics*

2012, *47*, 267. [CrossRef]

[4] Tucker, S. W.; Walkar, S. *Canadian J. Chem.* **1969**, *47*, 681. [CrossRef]

[5] Gupta, K. K.; Bansal, A. K.; Sing, P. J.; Shrama, K. S. *Indian J. Pure App. Phys.* **2004**, *42*, 849.

[6] Kalaivani,T.; Kumar S.; Krishnan, S. *Indian J. Pure App. Phys.* **2005**, *43*, 542.

[7] Oster, G.; *J. Am. Chem. Soc.* **1946**, *68*, 2036. [CrossRef][PubMed]

[8] Huyskens, P.; Fellx, N.; Janssens, N.; Broeck, F.V.; Kapuku, F. *J. Phys. Chem.* **1980**, *84*, 1387. [CrossRef]

[9] Kamble, S.; Sudake, Y. S.; Mehrotra, S. C. *J. Koren. Chem. Soc.* **2011**, *55*, 3.

[10] Surber, W. H. *J. Appl. Phys.* **1948**, *19*,514.

[11] Hestone, W. H.; Frankline, A. D.; Hennely, E. L.; Smyth, C. P. *J. Am. Chem. Soc.* **1950**, *72*, 3443. [CrossRef]

[12] Jain, R.; Bhargava, N.; Sharma, K.S.; Bhatnagar, D. *Indian J. Pure App. Phys.* **2011**, *49*, 401.

[13] Govindan, K.; Ravichandran, *Indian J. Pure Appl. Phys.* **1994**, *32*, 852.

[14] Sengwa, R. J.; Madhvi, Abhilasha, Sonukhla, *Indian J. Chem.* **2006**, *44A*, 943.

[15] Vasan, S. T.; Sannaninganvar, F. M.; Ayachit, N. H.; Deshpande, D. K. *J. Mol. Liq.* **2007**, *135*, 115. [CrossRef]

[16] Kalamse, G. M.; Pande, R. *Asian J. Chem.* **2005**, *17*, *3*, 1698.

[17] Sharma, A.; Sharma, D. R. *Indian J. Pure App. Phys.* **1993**, *31*, 841.

[18] Sharma, A.; Shrama, D. R. *Indian J. Pure App. Phys.* **1993**, *31*, 744.

[19] Sisodia, M. L.; Raghuvanshi, G. S.; Basic microwave Techniques and Lab manual.Wiley Eastern Ltd, New Delhi: **1990**, chapter 6.

[20] Hill, N. E.; Waughan, W. E.; Price, A. H.; Davils, M.; Dielectric properties and molecular Behaviour,Van Nostrand, London: **1969**, chapter 1.

[21] Debye, P.; (a) Polar molecular, The chemical Catalog Company, Inc, NewYork: **1929**. (b) The Dipole moment and Chemical Struture, Blackie and Son Ltd, London: **1931**, chapter 3.

[22] Combs, L. L.; McMahan,W. H.; Farish, S. H. *J. Phys. Chem.* **1971**, *75*, 2133. [CrossRef]

Orbital: The Electronic Journal of Chemistry
journal homepage: www.orbital.ufms.br
ISSN 1984-6428

| Vol 5 | | No. 1 | | January-March 2013 |

Full Paper

Determinação da Estrutura de Diferentes Álcoois Terpênicos: Um Estudo Teórico e Experimental

Naiara Letícia Marana[a], Lucas C. Ducati[b] e Luiz Carlos da Silva Filho[a]*

[a]*Departamento de Química, Faculdade de Ciências, Universidade Estadual Paulista (UNESP), Bauru, São Paulo, Brasil.*
[b]*Instituto de Química, Universidade de Campinas (Unicamp), Campinas, São Paulo, Brasil.*

Article history: Received: 19 November 2012; revised: 05 January 2013; accepted: 21 January 2013. Available online: 17 April 2013.

Abstract: Terpene compounds is a major class of natural products found in nature, although having a relatively simple structure, their ^{1}H-NMR spectra and ^{13}C are complex and have many overlapping signals. The present study aimed to conduct a theoretical and experimental study in order to determine the structure of different chiral alcohols through the use of theoretical calculations of NMR shielding tensors (δ) and their comparison with the experimental chemical shifts. The results show that the level of theory adopted in our studies to describe the structure of the alcohol was adequate, with a good theoretical and experimental correlation assists in determining what structure.

Keywords: terpenic alcohol; correlation study; NMR; ab-initio calculations

1. INTRODUÇÃO

Os compostos terpênicos constituem uma das maiores classes de produtos naturais encontrados na natureza, sendo que mais de 55.000 tipos destes compostos já foram descritos na literatura [1, 2]. Dentre as inúmeras funções biológicas que são atribuídas aos derivados terpênicos podemos citar: atrair insetos para promover polinização das flores, repelente natural, proteção contra doenças, pigmentos naturais, entre outras. Industrialmente os terpenos podem ser utilizados como aromatizantes, medicamentos, intermediários sintéticos [1, 2]. Dentre os álcoois terpênicos mais utilizados o mentol ($C_{10}H_{20}O$) vem ganhando destaque, pois é o maior constituinte do óleo essencial Labiaceae (encontrado na peppermint e spearmint) [3], e é o mais empregado no ramo da indústria devido a suas propriedades anestésicas e anti-inflamatórias [4, 5]. O pinanodiol ($C_{10}H_{18}O_2$), um diol derivado do α-pineno é utilizado amplamente como reagente quiral na preparação de α-hidroxicetonas, β-hidroxialilsilanos e reagentes quirais com dupla alilação [6, 7].

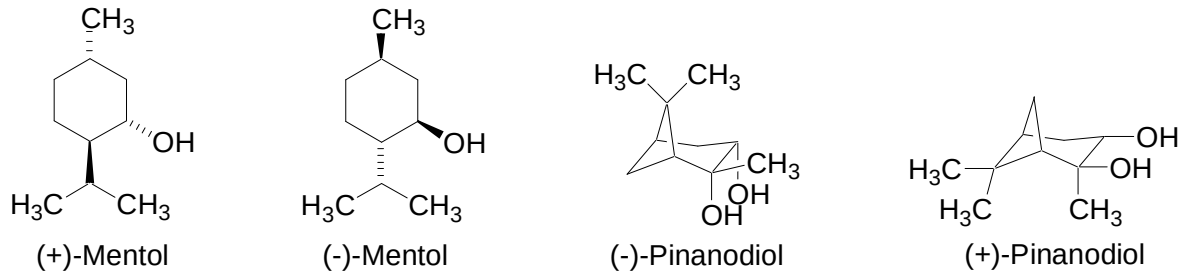

Figura 1. Estrutura do álcoois quirais (+) e (-)-mentol e (+) e (-)-pinanodiol.

O desenvolvimento e a utilização dos derivados terpênicos como novos produtos, é baseado no conhecimento de sua estrutura e de suas propriedades físicas e químicas e, apesar dos álcoois

* Corresponding author. E-mail: lcsilva@fc.unesp.br

mostrados na Figura 1 possuírem uma estrutura relativamente simples, seus espectros de RMN-^{1}H e ^{13}C são complexos e possuem muitos sinais sobrepostos (multipletos – espectros de segunda ordem) e muitos acoplamentos. Portanto, o presente trabalho tem como objetivo realizar um estudo teórico e experimental para determinar inequivocamente a estrutura destes álcoois quirais através da utilização cálculos teóricos de tensores blindagem de RMN (δ), como ferramenta auxiliar que nos permitirá uma atribuição correta de todos os sinais de Ressonância Magnética Nuclear de Hidrogênio-1 e Carbono-13, e correlacionando estes dois métodos.

Nos últimos anos, a Ressonância Magnética Nuclear (RMN) tem sido um dos métodos mais poderosos em elucidação estrutural e vem provando ser uma técnica versátil para solução de muitos tipos de problemas na Química. Os dados obtidos a partir de espectros de RMN, em particular deslocamentos químicos, são amplamente utilizados para caracterizar o ambiente químico individual de átomos [8]. No entanto, a atribuição correta do sinal do RMN, bem como a compreensão da relação entre o deslocamento químico e estrutura molecular podem ser problemas difíceis de solucionar e com o desenvolvimento de cálculos *ab initio* que estão cada vez mais precisos, é possível utiliza-los como ferramenta para auxiliar na solução destes problemas. Assim sendo, o uso das duas técnicas em conjunto pode ser uma ferramenta bastante útil para fazer atribuições corretas e entender a estrutura química de moléculas [8, 9].

2. MATERIAL E MÉTODOS

A estrutura dos álcoois foi otimizada e após a minimização de energia, os dados teóricos de RMN-^{13}C e ^{1}H foram obtidos pelo método *Gauge-Independent Atomic Orbital* (GIAO) [10]. Os cálculos foram realizados com o programa Gaussian09 [11] aplicando-se o funcional de densidade B3LYP [12], que vem demonstrando ótimo desempenho na simulação de diferentes tipos de compostos [13-15], com o conjunto de funções de base cc-pVDZ [16] para todos os átomos sendo todos sob o efeito do solvente (clorofórmio) pelo método *Polarizable Continuum Model* using the integral equation (IEFPCM).[17] Ao final, os resultados teóricos e experimentais foram comparados por um gráfico de correlação, obtendo-se o coeficiente de correlação, que indica se os valores obtidos teoricamente estão em boa concordância com os dados experimentais.

Os espectros de RMN-^{1}H de 500 MHz e de RMN-^{13}C de 125 MHz foram obtidos em um espectrômetro Bruker DRX-500. Os deslocamentos químicos (δ) estão relatados em parte por milhão (ppm) em relação ao tetrametilsilano (TMS), utilizado como padrão interno, utilizando $CDCl_3$ como solvente.

Os compostos analisados {(-)-mentol, (+)-mentol, (-)-pinanodiol e (+)-pinanodiol} foram adquiridos comercialmente (Sigma-Aldrich Co.).

3. RESULTADOS E DISCUSSÃO

Os dados de RMN experimental dos compostos estudados neste trabalho foram obtidos através técnicas de RMN 1D (RMN-^{1}H e ^{13}C) e 2D (COSY, HSQC e HMBC) e estão mostrados nas tabelas 1 a 4.

Tabela 1. Deslocamento químico e acoplamento para o (+) e (-)-Mentol.

Atribuição	δC (ppm)	Atribuição	δH (ppm)	Multiplicidade	*J* (Hz)
C1	71,6	**H1**	3,40	dt	J_1= J_2= 10,4; J_3= 4,2.
C2	50,2	**H2**	1,10	ddt	J_1= 12,3; J_2= 10,4; J_3=J_4= 2,8.
C6	45,0	**H6'**	1,95	dddd	J_1= 12,1; J_2= 4,2; J_3= 3,6; J_4= 2,0.
		H6"	0,95	m	-
C4	34,6	**H4'**	1,64	m	-
		H4"	0,85	m	-
C5	31,6	**H5**	1,43	m	-
C8	25,8	**H8**	2,16	dh_{ept}	J_1=J_2=J_3=J_4=J_5= J_6= 7,0; J_7=2,8.
C3	23,2	**H3'**	1,59	ddt	J_1= 11,5; J_2= 3,4; J_3=J_4= 3,0.
		H3"	1,00	m	-
C7	22,2	**H7**	0,90	d	J_1= 6,5
C10	21,0	**H10**	0,92	d	J_1= 7,0
C9	16,1	**H9**	0,80	d	J_1= 7,0

Tabela 2. Correlações ^{1}H / ^{1}H and ^{1}H / ^{13}C para o (+) e (-)-Mentol.

C	HSQC	COSY	HMBC
C1	H1	H2, H6', H6''	H2, H3', H3'', H6', H6'', H8
C2	H2	H1, H3', H3'', H8	H1, H3', H3'', H6', H6'', H8, H9, H10
C6	H6'	H1, H4', H5, H6''	H1, H2, H4'', H5, H7
	H6''	H1, H5, H6'	
C4	H4'	H3', H3'', H4'', H5, H6'	H2, H3', H3'', H5, H6', H6''
	H4''	H3', H3'', H4', H5,	
C5	H5	H4', H4'', H6', H6'', H7	H1, H3', H3'', H4', H4'', H6', H6'', H7
C8	H8	H2, H9, H10	H1, H2, H3', H3'', H9, H10
C3	H3'	H2, H3'', H4', H4''	H1, H2, H4', H4'', H8
	H3''	H2, H3', H4', H4''	
C7	H7	H5	H5, H6'
C10	H10	H8	H2, H8, H9
C9	H9	H8	H2, H8, H10

Tabela 3: Deslocamento químico e acoplamento para o (+) e (-)-Pinanodiol.

Atribuição	δC (ppm)	Atribuição	δH (ppm)	Multiplicidade	*J* (Hz)
C6	73,9	-	-	-	-
C1	69,3	**H1**	3,99	ddd	J_1= 9,4; J_2(OH)= 6,5; J_3= 5,3.
C5	54,0	**H5**	2,01	t	J_1=J_2= 6,0
C3	40,5	**H3**	1,92	tdd	J_1=J_2= 6,0; J_3= 3,6; J_4=2,5
C8	38,9	-	-	-	-
C2	38,2	**H2'**	2,45	dddd	J_1= 14,0; J_2= 9,4; J_3= 3,6; J_4= 2,5
		H2"	1,64	ddd	J_1= 14,0; J_2= 5,3; J_3= 2,5
C7	29,6	**H7**	1,31	s	-
C4	28,0	**H4'**	2,20	dtd	J_1= 10,5; J_2=J_3= 6,0; J_4=2,5
		H4"	1,36	d	J_1= 10,5
C9	27,8	**H9**	1,27	s	-
C10	24,1	**H10**	0,94	s	-

Tabela 4. Correlações ^{1}H / ^{1}H and ^{1}H / ^{13}C para o (+) e (-)-Pinanodiol.

C	HSQC	COSY	HMBC
C6	-	-	H1, H2', H2'', H5, H7
C1	H1	H2', H2''	H2', H2'', H6, H7
C5	H5	H3, H4''	H3, H4', H4'', H9, H10
C3	H3	H2', H2'', H3, H4'	H2', H2'', H4', H4'', H5, H9, H10
C8	-	-	H3, H5, H9, H10
C2	H2'	H1, H2'', H3, H4'	H1, H3, H4'
	H2"	H1, H2', H3	
C7	H7	-	H1, H5
C4	H4'	H2', H3, H4'', H5	H2', H3, H5
	H4"	H4'	
C9	H9	-	H3, H5, H10
C10	H10	-	H3, H5, H9

Os espectros de RMN 1D e 2D dos álcoois terpênicos foram bastantes úteis na atribuição dos deslocamentos químicos dos hidrogênios. Para o (+) e o (-)-mentol não foi possível determinar todas as constantes de acoplamento (J) presentes nas moléculas, devido a alta incidência de sobreposição entre os sinais no espectro de RMN-^{1}H, mas foi possível verificar um acoplamento em W entre os hidrogênios 4' e 6', verificado pelo espectro de COSY, apresentando um acoplamento de 2,0 Hz.

Para o (+) e o (-)-pinanodiol, algumas das constantes de acoplamento medidas mostraram-se interessantes, como por exemplo, o acoplamento em W entre H3 e H5 na ordem de 6,0 Hz, também verificado no espectro de COSY, e a inexistência de acoplamento entre H3 e H4'', e entre H5 e H4''. Isto pode ser explicado devido aos ângulos diedros (H3/H4'' e H-5/H4'') serem próximos de 90º no

pinanodiol. Todos estes resultados concordam com a conformação obtida por modelagem molecular.

Paralelamente às análises experimentais, foi realizado um estudo de minimização de energia dos álcoois quirais estudados, utilizando o programa Gaussian09 e aplicando-se o funcional de densidade B3LYP com o conjunto de funções de base cc-pVDZ para todos os átomos sendo todos sob o efeito do solvente, as estruturas obtidas estão mostradas na Figura 2.

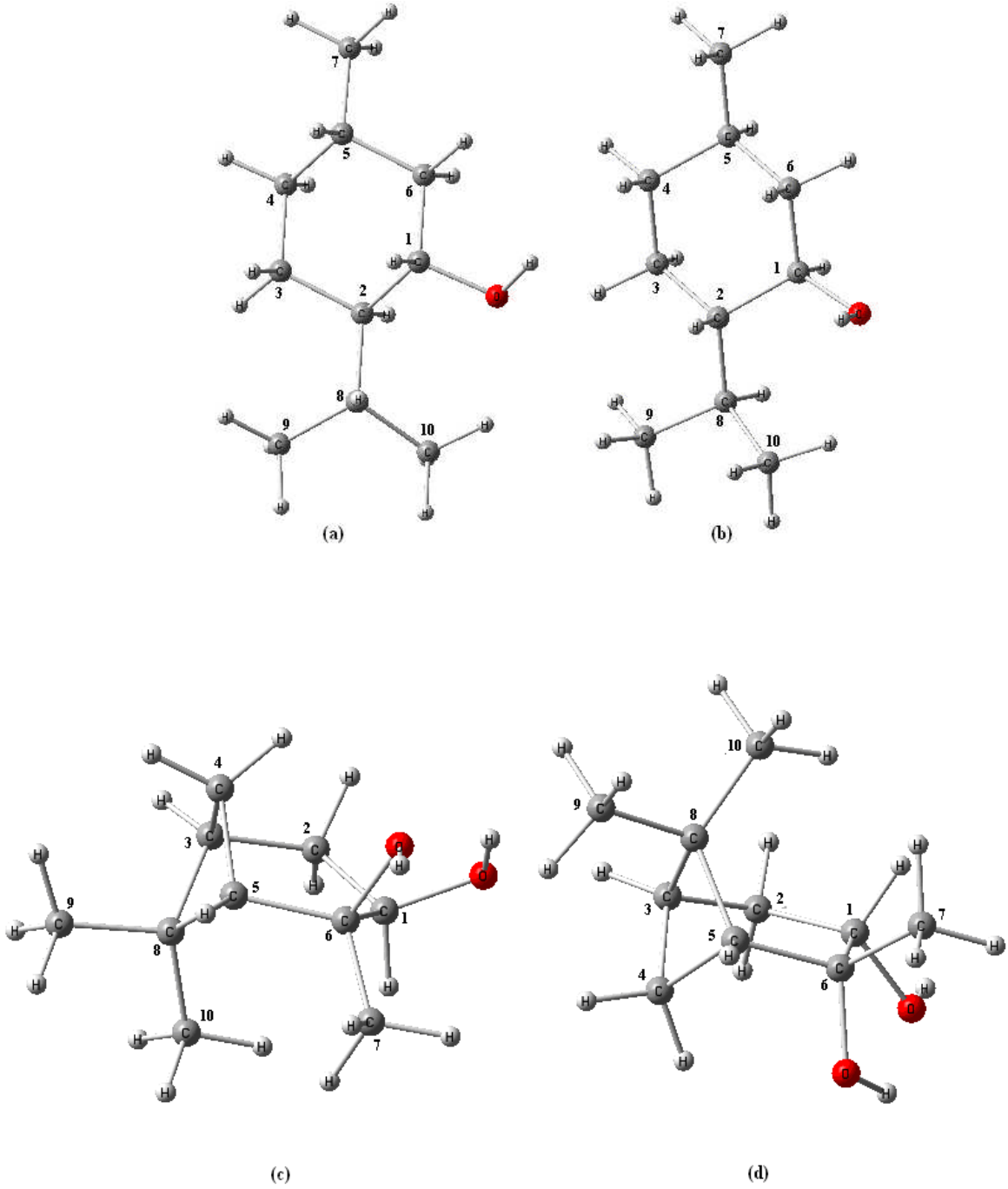

Figura 2. Estruturas minimizadas: (a) (+)-mentol, (b) (-) mentol, (c) (+) pinanodiol e (d) (-) pinanodiol.

Após a otimização das estruturas, foram obtidos os dados teóricos dos tensores blindagem de RMN (δ) para carbono e hidrogênio e comparados com os deslocamentos químicos obtidos experimentalmente. Os dados dos deslocamentos químicos teóricos e experimental estão dispostos nas tabelas 5 a 8.

Tabela 5. Deslocamento químico teórico/experimental para o (-)-Mentol.

Atribuição	δC[a] (ppm)	δC[b] (ppm)	Desvio Ponderado δC	Atribuição	δH[a] (ppm)	δH[b] (ppm)	Desvio Ponderado δH
C1	83,9	71,6	0,17	**H1**	3,96	3,40	0,16
C2	60,2	50,2	0,20	**H2**	1,17	1,10	0,06
C6	54,5	45,0	0,21	**H6'**	2,77	1,95	0,42
				H6"	1,35	0,95	0,42
C4	42,3	34,6	0,22	**H4'**	2,40	1,64	0,46
				H4"	1,60	0,85	0,88
C5	41,3	31,6	0,31	**H5**	2,16	1,43	0,51
C8	44,1	25,8	0,71	**H8**	2,29	2,16	0,06
C3	37,6	23,2	0,62	**H3'**	2,61	1,59	0,64
				H3"	1,74	1,00	0,74
C7	30,8	22,2	0,39	**H7**	1,48	0,90	0,64
C10	28,9	21,0	0,38	**H10**	1,69	0,92	0,84
C9	28,3	16,1	0,76	**H9**	1,45	0,80	0,81
Desvio Médio			0,40				0,51

[a]valores teóricos
[b]valores experimentais

Tabela 6. Deslocamento químico teórico/experimental para o (+)-Mentol.

Atribuição	δC[a] (ppm)	δC[b] (ppm)	Desvio Ponderado δC	Atribuição	δH[a] (ppm)	δH[b] (ppm)	Desvio Ponderado δH
C1	84,87	71,6	0,19	**H1**	4,16	3,40	0,22
C2	56,37	50,2	0,12	**H2**	2,51	1,10	1,28
C6	54,07	45,0	0,20	**H6'**	2,33	1,95	0,19
				H6"	1,83	0,95	0,93
C4	42,23	34,6	0,22	**H4'**	2,41	1,64	0,46
				H4"	1,68	0,85	0,98
C5	40,46	31,6	0,28	**H5**	2,16	1,43	0,51
C8	43,11	25,8	0,67	**H8**	2,31	2,16	0,07
C3	36,89	23,2	0,59	**H3'**	2,51	1,59	0,58
				H3"	1,77	1,00	0,77
C7	28,70	22,2	0,29	**H7**	1,53	0,90	0,70
C10	31,45	21,0	0,50	**H10**	1,44	0,92	0,57
C9	27,39	16,1	0,70	**H9**	1,51	0,80	0,89
Desvio Médio			0,38				0,82

[a]valores teóricos
[b]valores experimentais

Tabela 7. Deslocamento químico teórico/experimental para o (-)-pinanodiol.

Atribuição	δC[a] (ppm)	δC[b] (ppm)	Desvio Ponderado δC	Atribuição	δH[a] (ppm)	δH[b] (ppm)	Desvio Ponderado δH
C6	80,1	73,9	0,08	-	-	-	-
C1	76,7	69,3	0,11	**H1**	4,7	3,99	0,18
C5	61,7	54,0	0,14	**H5**	2,8	2,01	0,33
C3	49,7	40,5	0,23	**H3**	2,7	1,92	0,41
C8	48,6	38,9	0,23	-	-	-	-
C2	46,3	38,2	0,21	**H2'**	3,1	2,45	0,27
				H2"	2,4	1,64	0,46
C7	36,5	29,6	0,23	**H7**	1,9	1,31	0,45
C4	37,6	28,0	0,34	**H4'**	2,9	2,20	0,32
				H4"	2,6	1,36	0,91
C9	34,2	27,8	0,23	**H9**	1,78	1,27	0,40
C10	30,5	24,1	0,27	**H10**	1,76	0,94	0,87
Desvio Médio			0,21				0,46

[a]valores teóricos
[b]valores experimentais

Tabela 8. Deslocamento químico teórico/experimental para o (+)-Pinanodiol

Atribuição	δC[a] (ppm)	δC[b] (ppm)	Desvio Ponderado δC	Atribuição	δH[a] (ppm)	δH[b] (ppm)	Desvio Ponderado δH
C6	82,08	73,9	0,11	-	-	-	-
C1	74,48	69,3	0,07	**H1**	4,77	3,99	0,20
C5	62,54	54,0	0,16	**H5**	2,62	2,01	0,30
C3	49,58	40,5	0,22	**H3**	2,74	1,92	0,43
C8	49,33	38,9	0,27	-	-	-	-
C2	46,96	38,2	0,23	**H2'**	3,33	2,45	0,36
				H2"	2,40	1,64	0,46
C7	35,30	29,6	0,19	**H7**	2,21	1,31	0,69
C4	37,35	28,0	0,33	**H4'**	2,97	2,20	0,35
				H4"	2,42	1,36	0,78
C9	33,99	27,8	0,22	**H9**	1,80	1,27	0,42
C10	29,73	24,1	0,23	**H10**	1,81	0,94	0,93
Desvio Médio			0,20				0,49

[a]valores teóricos
[b]valores experimentais

Pode-se observar pela análise das tabelas 5 a 8 de deslocamentos químicos que a média dos desvios ponderados referentes ao carbono e hidrogênio dos compostos deu valores baixos, sendo que o maior valor do desvio foi de 0,82 que se refere ao deslocamento químico do hidrogênio para o (+)-mentol. Considerando os valores dos desvios ponderados, o átomo de carbono-1 do (-)-pinanodiol, foi o que apresentou o menor desvio em comparação com o deslocamento químico experimental e o átomo de hidrogênio-2 do (+)-mentol, foi o que apresentou o maior desvio. Porém, analisando os desvios médios, podemos observar que estes valores indicam uma boa correlação entre os dados experimentais e teóricos,

sendo que, o (-)-mentol apresentou um desvio menor que o (+)-mentol e o (+)-pinanodiol apresentou um desvio menor que o (-)-pinanodiol, mas comparando os quatro compostos, os compostos pinanodiol apresentaram o menor desvio, o que pode ser confirmado pelo estudo de correlação dos dados experimentais com os dados teóricos, possibilitando a obtenção de um coeficiente de correlação para cada um dos compostos estudados. Os gráficos de correlação estão demonstrados nas figuras 3 e 4 para carbono e hidrogênio, respectivamente, e os coeficientes de correlação estão dispostos na Tabela 9.

Pela análise dos resultados teóricos e experimentais apresentados, podemos observar que o modelo teórico empregado B3LYP/cc-pVDZ descreveu bem o deslocamento químico de RMN-^{1}H e de ^{13}C dos álcoois estudados, visto que a variação entre os valores teóricos e experimentais foi pequena, já que os valores dos coeficientes de correlação deram bem próximos de 1, sendo que o (-)-pinanodiol apresentou o melhor resultado, com coeficiente de correlação para deslocamento químico de carbono de 0,9888 e de hidrogênio de 0,9429. Assim, podemos concluir que as análises teóricas realizadas para os compostos estudados foram eficientes para descrever e auxiliar na atribuição das estruturas dos álcoois terpênicos estudados com bons resultados comparativos.

Tabela 9. Coeficientes de correlação RMN-^{1}H e RMN-^{13}C

Composto	Coeficiente de correlação ^{1}H-RMN	Coeficiente de correlação ^{13}C-RMN
(+) mentol	0,8547	0,9577
(-) mentol	0,8918	0,9592
(+) pinanodiol	0,9538	0,9873
(-) pinanodiol	0,9429	0,9888

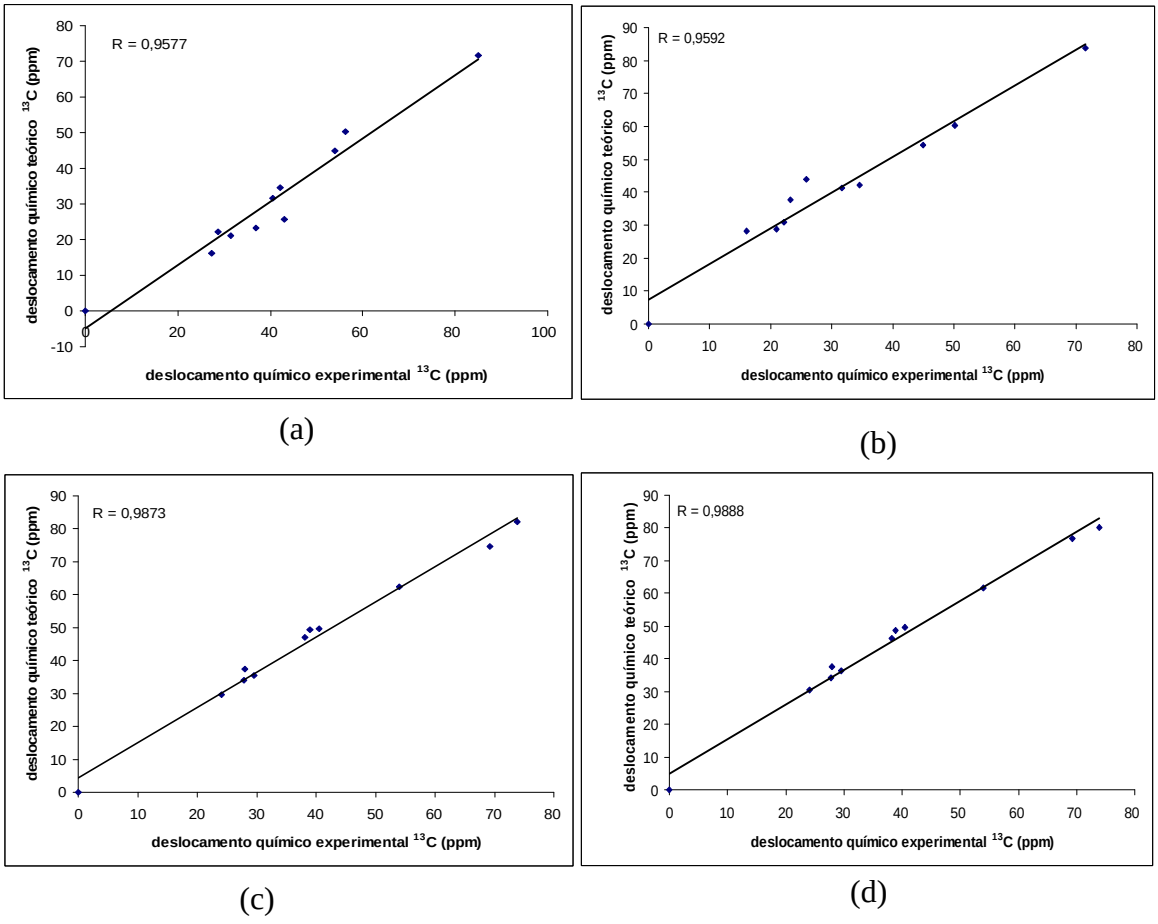

Figura 3. Gráficos de correlação para deslocamento químico de Carbono-13: (a) (+)-mentol, (b) (-)-mentol, (c) (+)-pinanodiol e (d) (-)-pinanodiol.

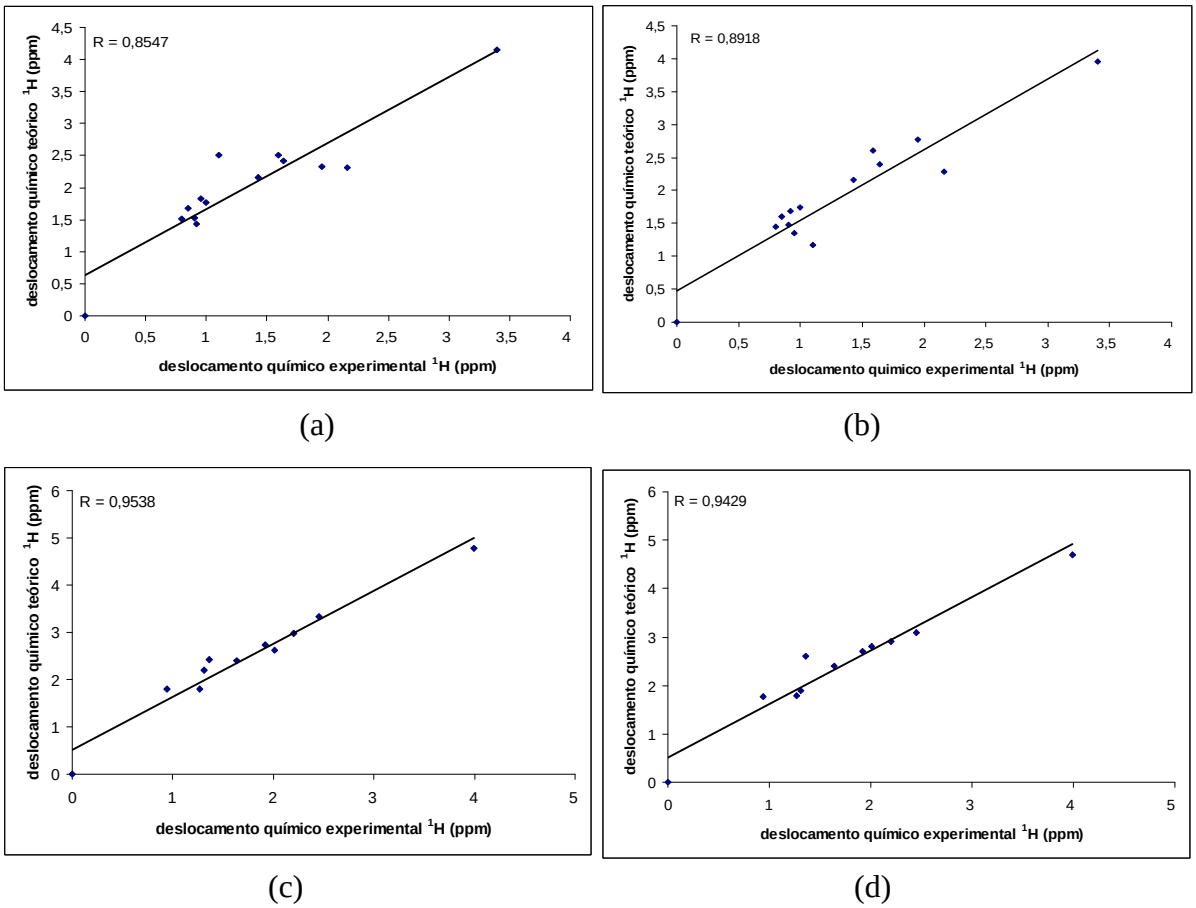

Figura 4. Gráficos de correlação para deslocamento químico de Hidrogênio-1 (a) (+)-mentol, (b) (-)-mentol, (c) (+)-pinanodiol e (d) (-)-pinanodiol.

4. CONCLUSÃO

Podemos concluir que o nível de teoria adotado em nossos estudos para descrever a estrutura dos álcoois foi adequado, apresentando uma boa correlação teórico-experimental o que nos auxiliou na determinação da estrutura dos álcoois estudados.

A correlação entre os dados experimentais e teóricos mostra ser uma excelente ferramenta para auxiliar a elucidação estrutural e atribuição inequívoca de sinais de RMN dos álcoois estudados. Outro ponto a ser destacado neste trabalho é que os valores teóricos de deslocamento químico de RMN obtidos com o nível de teoria B3LYP/cc-pVDZ possibilita associar um custo computacional não tão elevado a uma precisão apurada dos resultados obtidos.

5. AGRADECIMENTOS

Os autores agradecem à Fundação de Amparo à Pesquisa do Estado de São Paulo (FAPESP), Conselho Nacional de Desenvolvimento Científico e Tecnológico (CNPq), ao curso de Pós-Graduação em Ciência e Tecnologia de Materiais (POSMAT), pelo apoio e auxilio financeiro.

6. REFERÊNCIAS E NOTAS

[1] Springob, K.; Kutchan, T. M. In: Plant-derived Natural Products Synthesis, Function, and Application. Springer US: London, 2009.

[2] Richardson, A. In: The Chemistry of Fragrances, In Pybus D.H.; Sell C.S. Eds.; The Royal Society of Chemistry: Cambridge, 1999, chapter 8. [CrossRef]

[3] World Health Organization - Monographs on Selected Medicinal Plants, Vol. 2, Geneva: WHO, 2002. [Link]

[4] Galeottia, N.; Mannellia, L. D. C.; Mazzantib, G.; Bartolinia, A.; Ghelardini, C. *Neurosci. Lett.* **2002**, *322*, 145. [CrossRef]

[5] Eccles, R. *J. Pharm. Pharmacol*. **1994**, *46*, 618. [CrossRef]

[6] Kelly, T. A.; Fuchs, V. U.; Perry, C. W.; Snow, R. J.

Tetrahedron **1993**, *49*, 1009. [CrossRef]

[7] Peng, F.; Hall, D. G. *J. Am. Chem. Soc*. **2007**, *129*, 3070. [CrossRef]

[8] Sebastiani, D.; Parrinello, M. *J. Phys. Chem. A* **2001**, *105*, 1951. [CrossRef]

[9] Constantino, M. G.; Silva-Filho, L. C.; Cunha Neto, A.; Heleno, V. C. G.; da Silva, G. V. J.; Lopes, J. L. C. *Spectrochim. Acta, Part A: Molec Biomol. Spec. (SAA)* **2005**, *61*, 171. [CrooRef]

[10] Cheeseman, J. R.; Frisch, M. J.; Devlin, F. J.; Stephens, P. J. *Chem. Phys. Lett.* **1996**, *252*, 211. [CrossRef]

[11] Frisch, M. J.; Trucks, G. W.; Schlegel, H. B.; et. al. Gaussian 09, Revision A.1, Inc., Wallingford CT, 2009.

[12] Becke, A. D. *Phys. Rev. A* **1988**, *38*, 3098. [CrossRef][PubMed]

[13] Winter, N. O. C.; Graf, N. K.; Leutwyler, S.; Hättig, C. *Phys. Chem. Chem. Phys.*, **2012**.

[14] Torres, E.; DiLabio, G. *J. Phys. Chem. Lett.* **2012**, *13*, 1738. [CrossRef]

[15] Jimenez-Izal, E.; Chiatti, F.; Corno, M.; Rimola A.; Ugliengo, P. *J. Phys. Chem. C* **2012**, *27*, 14561. [CrossRef]

[16] Dunning, T. H. *J. Chem. Phys.* **1989**, *90*, 1007. [CrossRef]

[17] Tomasi, J.; Mennucci, B.; Cammi, R. *Chem. Rev.* **2005**, *105*, 2999. [CrossRef][PubMed]

Orbital: The Electronic Journal of Chemistry
journal homepage: www.orbital.ufms.br
ISSN 1984-6428

| Vol 5 | | No. 1 | | January-March 2013 |

Full Paper

Silica Sulfuric Acid Catalyzed One-pot Synthesis of Biginelli Reaction in Water

Digambar D. Gaikwad[a], Tirpude Haridas[b], Hussain Sayyed[b], Mazahar Farooqui*[d]

[a]*Department of Chemistry, Govt. College of Arts & Sciences, Aurangabad-4310001, India.*
[b]*Department of Chemistry, Sir Sayyed College, Aurangabad-4310001, India.*
[c]*Dr Rafiq Zakaria College for Women, Aurangabad-43100,1 India.*

Article history: Received: 16 January 2012; revised: 29 December 2012; accepted: 23 January 2013. Available online: 17 April 2013.

Abstract: Silica sulphuric acid-catalyzed, simple, one-pot, cost effective and environmentally benign process for the synthesis of dihydropyrimidones is described. The novel compounds were tested for antibacterial activity and was found to be effective against some gram positive and gram negative bacteria.

Keywords: aryl aldehyde; β-ketoester; urea; thiourea; antibacterial activity

1. INTRODUCTION

The development of simple and eco-friendly synthetic procedures constitutes an important goal in green chemistry. Solvent-free reactions are the subject of constant development because of its ease set-up, mild conditions, increased yields of products, cost efficiency and environment friendliness compared to their solution counterparts.

The Biginelli reaction is a well-known multicomponent reaction involving a one-pot cyclocondensation of an aldehyde, β-ketoester and urea/thiourea [1, 2]. Multicomponent reactions (MCRs) have recently gained tremendous importance in organic and medicinal chemistry. The main contributing factors are the high atom economy, wide application in combinatorial chemistry and diversity-oriented synthesis [3]. Organic solvent free reaction has attracted considerable interest due to increasing awareness about environmental problems in chemical research and industry [4]. In general, the dihydropyrimidones (DHPMs) and their derivatives are known for their diverse important biological activities and pharmacological properties [5] including antiviral, antitumor, antibacterial , anti-inflammatory, analgesic, blood palette aggregation inhibitor, cardiovascular activity, and potent calcium channel blockers [6, 7]. The biological activity of some recently isolated alkaloids has also been attributed to the presence of dihydropyrimidinones moiety in the molecules. Notable among these are the batzelladine alkaloids, which have been found to be potent HIV gp-120-CD4 inhibitors [8].

The first report of the Biginelli reaction in 1893, which is one of the most important reactions for the synthesis of dihydropyrimidinones based on acid catalyzed three-component condensation of 1,3-dicarbonyl compounds, aldehydes and urea [9]. Nowadays many methods have been reported for the preparation DHPMs. But unfortunately these methods led to low to moderate yields particularly when substituted aromatic or aliphatic aldehydes and thiourea were employed. To overcome this problem, various homogeneous as well as heterogeneous catalysts have been utilized. Such as $Sr(OTf)_2$ [10], $In(OTf)_3$ [11], $Yb(OTf)_3$ [12], $Bi(OTf)_3$ [13], $Cu(OTf)_2$ [14], $Ln(OTf)_3$ [15], $CuCl_2$ [16] , LiBr [17], $MgBr_2$ [18], BF_3 [19], $FeCl_3$ [20], $BiCl_3$ [21], $InCl_3$ [22], $ZrCl_4$ [23], $ZrOCl_2$ [24], PPE [25], polymer supported ytterbium reagents [26], baker's yeast [27], The heterogeneous catalysts used in this reaction involve the use of KSF (montmorillonite) [28], Zeolite (TS-1) [29] , HZSM-5 [30]. The limitations in using the above mentioned catalysts were elevated reaction temperatures, solvent mediated reactions and moderate yields of the products. We report the silica

* Corresponding author. E-mail: mazahar_64@rediffmail.com

sulfuric acid (SSA, Scheme 1) as an efficient catalyst for the preparation of DHPMs.

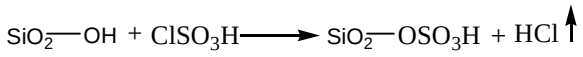

Scheme 1. SSA preparation.

This acid-catalyzed, three-component reaction between an aldehyde, a ß-ketoester and urea constitutes a rapid and facile synthesis of dihydropyrimidones, which are interesting compounds with a potential for pharmaceutical application (Scheme 2). This method has been developed for the synthesis of region and steroselective synthesis of DHPMs without using any chiral catalyst.

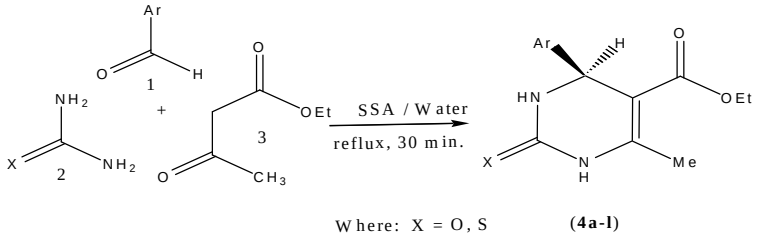

Scheme 2. SSA catalyzed synthesis of dihydropyrimidinones.

The first step in the mechanism is believed to be the condensation between the aldehyde and urea, with some similarities to the Mannich condensation. The iminium intermediate generated acts as an electrophile for the nucleophilic addition of the ketoester enol and the ketone carbonyl of the resulting adduct undergoes condensation with the urea NH_2 to give the cyclized product (Scheme 2).

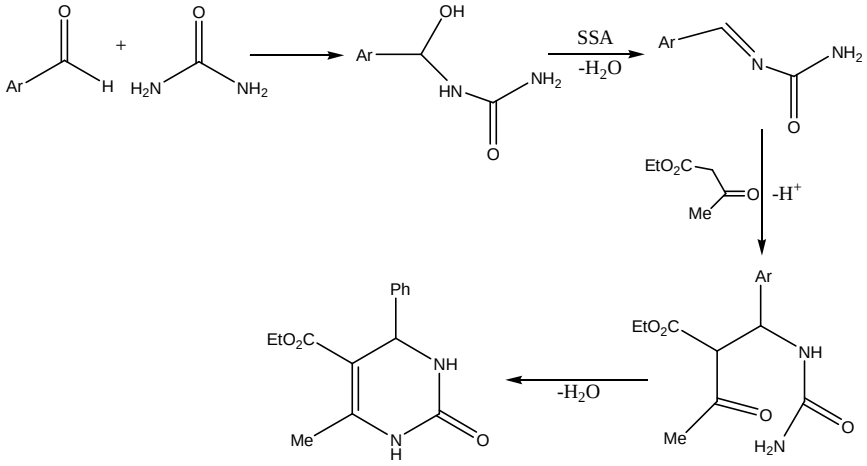

Scheme 2. Mechanism.

2. MATERIAL AND METHODS

TLC routinely checked the purity of the synthesized compounds on silica gel coated plates. IR spectra are recorded in KBr pellets on a Perkin-Elmer FTIR, PMR spectra are recorded on Perkin-Elmer Jeol FX 90 QC 300 MHz instrument in $CDCl_3$, chemical shifts are reported in d values using TMS as an internal standard. Organic solutions were dried over anhydrous Na_2SO_4 and concentrated below 40 °C in vacuum.

2.1. Typical procedure for the synthesis of DHPM

A mixture of benzaldehyde (0.50 g, 4.71 mmol), ethyl acetoacetate (0.613 g, 4.71 mmol), urea (0.424 g, 7.07 mmol), water (5 mL) and catalytic amount of silica sulphuric acid was reflux

for 30 min (TLC check). The reaction mixture after cooling to room temperature was poured into crushed ice and stirred for 5-10 min. The solid separated was filtered and washed with ice-cold water. To separate the catalyst from the product, the mixture was treated with hot ethanol and filtered. The residue, being the catalyst, was dried and reused. The filtrate on concentration afforded the product, which was found to be sufficiently pure to obtain analytical data.

3. RESULTS AND DISCUSSION

The results, summarized in Table 1, indicated that this protocol is able to tolerate the structural variety. Aromatic aldehydes are subjected to this condensation very efficiently. Besides the β-ketoester have been employed in the present study, thiourea has been used with similar success to provide the corresponding dihydropyrimidines. Solventless Biginelli reaction acid no special precaution was needed in handling. The catalyst can be reused for several times. When the reactions were preceded without catalyst, low yield was obtained for acyl acetate as a substrate; no product was detected for β–diketones.

In summary, a new and efficient modified Biginelli reaction has been described. The advantages of this environmentally benign reaction include the simple reaction set-up, high product yields, short reaction time and needless reaction solvents. In addition, the catalyst can be recovered and reused, so it is valuable in the economic point of view.

The reusability of the catalyst is an important factor from economical and environmental point of views and has attracted much attention in recent years. Therefore, the reusability of silica sulfuric acid was examined in the Biginelli reaction under optimized reaction conditions. As silica sulfuric acid is a heterogeneous catalyst, it was separated by simple filtration after dilution of the reaction mixture with $CHCl_3$, dried at 60 ^oC and reused. The results showed that the catalyst can be used 5 times without loss of its activity.

We could achieve the synthesis of this compound in one step using 3-hydroxybenzaldehyde, thiourea, ethyl acetoacetate and SSA under the above mentioned reaction conditions. Monastrol (Figure 1) was obtained in 94% yield. The most important and salient feature of the present reaction is the recyclability of the catalyst and the scalability of the reaction. It was observed that the catalyst could be reused at least five times. Use of the recycled catalyst in the reaction had no effect either on the yield of the product or the quality of the product. Moreover, no side products were observed in these reactions. Furthermore, the reaction can be scaled up to a multigram scale. This was demonstrated by preparing 11.2 g of monastrol starting with 5.0 g of 3-hydroxybenzaldehyde. Thus an efficient one-step, solvent-free synthesis of DHPMs was achieved in very good yields.

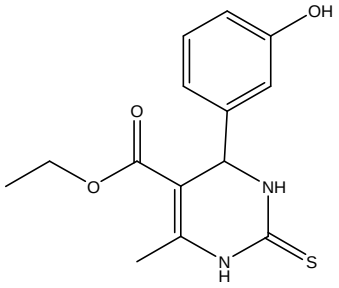

Figure 1. Example of biologically active monastrol.

3.1. Antibacterial activity

Antibacterial activities of synthesized compounds were examined in vitro by known agar diffusion cup method (**4a-l**). All the compounds were tested for activity against gram-positive bacteria and gram-negative bacteria like *Neisseria gonorrhoeae*, *Proteus vulgaris*, *Bacillus subtilis*, *Escherichia coli*, *Pseudomonas aeruginosa*, *Staphylococcus aureus*. The culture medium was nutrient agar. All the compounds were dissolved in DMF (500 ppm concentration) and DMF used as control. Streptomycin and Neomycin were employed as the standard drug. The results are summerised in Table 5.

*5-Ethoxycarbonyl-6-methyl-4-phenyl-3,4 -dihydropyridin-2(1H)-one (**4a**):* IR (KBr): 1606, 1647, 1664, 3215, 3319 cm -1, 1H-NMR (300 MHz, DMSO-d6): δ 1.10 (t, J = 7.1 Hz, 3H), 2.24 (s, 3H), 3.98 (q, J = 7.1 Hz, 2H), 5.13 (s, 1H), 7.30 (m, 5H), 7.74 (s, NH), 9.19 (s, NH).

*5-Ethoxycarbonyl-6-methyl-4(4-chlorophenyl)-3,4-dihydropyridin-2(1H)-one (**4b**):* IR (KBr): 1649, 1704, 1723, 3242 cm -1, 1H-NMR (300 MHz, DMSO-d6): δ 1.06 (t, J = 7.2 Hz, 3H), 2.24 (s, 3H), 3.98 (q, J = 7.2 Hz, 2H), 5.13 (s, 1H), 7.30 (d,

J=8.4Hz, 2H), 7.40 (d, J=8.4Hz, 2H), 7.74 (s, NH), 9.19 (s, NH).

5-Ethoxycarbonyl-6-methyl-4(2,3-dichlorophenyl)-3,4-dihydropyridin-2(1H)-one ***(4c):*** IR (KBr): 1640, 1690, 1700, 3100, 3360 cm -1, 1H-NMR (300 MHz, DMSO-d6): δ 0.97 (t, J = 7.5 Hz, 3H), 2.31 (s, 3H), 3.89 (q, J = 7.5 Hz, 2H), 5.69 (s, 1H), 7.25-7.43 (d, J=8.4Hz, 2H), 7.40 (d, J=8.4Hz, 1H), 7.80 (s, NH), 9.19 (s, NH).

5-Ethoxycarbonyl-4(4-methylphenyl)-6-methyl-3,4-dihydropyridin-2(1H)-one ***(4d):*** IR (KBr): 1650, 1725, 2981, 3114, 3245 cm-1, 1H-NMR (300 MHz, DMSO-d6): δ 1.08 (t, J = 7.5 Hz, 3H), 2.21 (s, 3H), 3.95 (q, J = 7.5 Hz, 2H), 5.08 (s, 1H), 7.09 (m, 4H), 7.70 (s, NH), 9.13 (s, NH).

5-Ethoxycarbonyl-4-(4-methoxyphenyl)-6-methyl-3,4-dihydropyridin-2(1H)-one ***(4e):*** IR (KBr): 1644, 1748, 2926, 3084, 3224 cm-1, 1H NMR (300 MHz, DMSO-d6): δ 1.12 (t, J = 7.1 Hz, 3H), 2.26 (s, 3H), 3.72 (s, 3H), 3.99 (q, J = 7.1 Hz, 2H), 5.09 (s, 1H), 6.90 (d, J=8.6 Hz, 2H), 7.16 (d, J=8.6 Hz, 2H),7.69 (s, NH), 9.20 (s, NH).

5-Ethoxycarbonyl-4-(2-hydroxyphenyl)-6-methyl-3,4-dihydropyridin-2(1H)-one ***(4f):*** IR (KBr): 1705, 1748, 2926, 3084, 3224 cm-1, 1H-NMR (300 MHz, DMSO-d6): δ 1.22 (t, J = 7.1 Hz, 3H), 2.72 (s, 3H), 4.49 (q, J=7.1Hz, 2H), 5.10 (s, 1H), 6.77(d, J = 8.1 Hz, 1H), 6.90 (t, J = 7.5Hz, 1H), 7.23-7.14 (m, 2H), 7.62 (s, NH), 9.02 (s, NH), 9.31 (s, OH).

5-Ethoxycarbonyl-4-(4-hydroxyphenyl)-6-methyl-3,4-dihydropyridin-2(1H)-one ***(4g):*** IR (KBr): 1641, 1690, 2982, 3290 cm-1, 1H NMR (300 MHz, DMSO-d6): δ 1.08 (t, J = 7.2Hz, 3H), 2.20 (s, 3H), 3.96 (q, J=7.2Hz, 2H), 5.05(s, 1H), 6.67 (d, J = 6.9 Hz, 2H), 7.00 (d, J=6.9Hz, 2H), 7.60 (s, NH), 9.06 (s, NH), 9.31 (s, OH).

5-Ethoxycarbonyl-6-methyl-4-(2-nitrophenyl)-3,4-dihydropyridin-2(1H)-one ***(4h):*** IR (KBr): 1650, 1710, 3110, 3240 cm-1. 1H NMR (300 MHz, DMSO-d6): δ 0.94 (t, J = 7.5 Hz, 3H), 2.30(s, 3H), 3.88 (q, J = 7.5 Hz, 2H), 5.81 (s, 1H), 7.49-7.98 (m, 5H), 7.87 (s, NH), 9.31 (s, NH).

5-Ethoxycarbonyl-6-methyl-4-(4-nitrophenyl)-3,4-dihydropyridin-2(1H)-one ***(4i):*** IR (KBr): 1650, 1710, 1730, 3230cm-1, 1H NMR (300 MHz, DMSO-d6): δ 1.04 (t, J = 7.1 Hz, 3H), 2.21 (s, 3H), 3.95 (q, J = 7.1 Hz, 2H), 5.24 (s, 1H), 7.50 (d, J=8.7 Hz, 2H), 7.87 (s, NH), 8.20 (d, J=8.7 Hz, 2H), 9.31 (s, NH).

5-Ethoxycarbonyl-6-methyl-4-phenyl-3,4-dihydropyrimidin-2(1H)-thione ***(4j):*** IR (KBr): 1186, 1467, 1571, 1662, 1705, 2988, 3180 cm-1, 1H NMR (300 MHz, DMSO-d6): δ 1.09(t, J=6.0Hz, 3H), 2.28 (s, 3H), 3.96 (q, J = 6.0 Hz, 2H), 5.19 (s, 1H), 7.28-7.18 (m, 5H), 9.66 (br, s, NH), 10.32 (br, NH).

5-Ethoxycarbonyl-4-(3-hydroxyphenyl)-6-methyl-3,4-dihydropyridin-2(1H)-thione ***(4k):*** IR (KBr): 3300, 3180, 2900, 2600, 1680, 1651, 1570 cm-1. 1H NMR (300 MHz, DMSO-d6): δ 1.10 (t, J = 7.50 Hz, 3H), 2.36 (s, 3H), 4.08 (q, J = 7.50 Hz, 2H), 5.22(s, 1H), 6.64-6.78 (m, 3H), 7.02-7.15 (m, 1H), 7.87(s, NH), 9.18 (s, NH), 9.82 (s, OH).

5-Ethoxycarbonyl-4(4-methylphenyl)-6-methyl-3,4-dihydropyridin-2(1H)-thione ***(4l):*** IR (KBr): 3245, 3114, 2981, 1725, 1706, 1650 cm-1. 1H NMR (300 MHz, DMSO-d6): δ 1.08 (t, J = 7.03 Hz, 3H), 2.21 (s, 3H), 2.48 (s, 3H), 3.95 (q, J = 7.03 Hz, 2H), 5.08 (s, 1H), 7.09 (m, 4H), 7.89 (s, NH), 9.13 (s, NH).

Table1. Silica-sulphuric acid catalyzed synthesis of DHPMs.

Entry	R	X	m. p. (^{0}C)	% Yield
4a	Ph-	O	204 lit[8]	98
4b	4-Cl-Ph-	O	214 lit[8]	95
4c	2,3(Cl)$_2$-Ph-	O	245 lit[25]	96
4d	4-CH$_3$-Ph-	O	212 lit[25]	94
4e	4-OMe-Ph-	O	202 lit[8]	94
4f	2-HO-Ph-	O	200 lit[8]	97
4g	4-HO-Ph-	O	227 lit[8]	94
4h	2-NO$_2$-Ph	O	220 lit[25]	95
4i	4-NO$_2$-Ph	O	208 lit[25]	92
4j	Ph-	S	205 lit[8]	95
4k	3-OH-Ph-	S	188	97
4l	3-CH$_3$-Ph-	S	222	96

Table 2. Effect of solvent on the yield of DHPMs.

Entry	Solvent	Yields %
1	Ethanol	60
2	THF	65
3	DMF	60
4	DMSO	60
5	Water	98

Table 3. Recovery of SSA catalyst.

Entries	Product	% Yield of SSA		
		Recycle-1	Recycle-2	Recycle-3
1	4a	98	90	85
2	4b	95	93	87
3	4c	96	89	83
4	4d	94	87	82

Table 4. Optimization of the reaction conditions.

Entries	Catalyst	Temp (^{0}C)	Time	Yield %
1	$InBr_3$	reflux	7 hr	75
2	PPE	reflux	15 hr	94
3	TEBA	reflux	2hr	90
4	SSA	rt	20hr	**0**
5	**SSA**	reflux	30 mints	**98**

Table 5. Antibacterial activity of DHPMs (Minimum Inhibitory Concentration).

Entry	R	X	Zone of inhibition (mm)					
			Ng	Pv	Bs	Ec	Sa	Pa
4a	Ph-	O	28	21	18	20	24	29
4b	4-Cl-Ph-	O	25	23	22	19	32	24
4c	3,4-$(Cl)_2$-Ph-	O	25	19	24	15	21	18
4d	4-CH_3-Ph-	O	28	23	18	30	29	23
4e	4-OMe-Ph-	O	30	39	38	28	30	33
4f	2-HO-Ph-	O	28	31	32	39	34	29
4g	4-HO-Ph-	O	29	27	24	21	27	30
4h	2-NO_2-Ph	O	30	35	26	28	30	24
4i	4-NO_2-Ph	O	35	23	25	26	28	32
4j	Ph-	S	37	36	30	18	32	27
4k	3-OH-Ph-	S	30	37	28	39	30	28
4l	3-CH_3-Ph	S	39	38	26	25	37	28
	Streptomycin		40	40	40	40	40	40
	Neomycin		10	10	10	10	10	10

Neisseria gonorrhoeae (Ng), Proteus vulgaris (Pv), Bacillus subtilis (Bs), Escherichia coli (Ec), Pseudomonas aeruginosa (Pa), Staphylococcus aureus (Sa)

4. CONCLUSION

The reaction is carried out ecofriendly and good yield is obtained. The novel compounds are tested for antibacterial activity against gram-positive bacteria and gram-negative bacteria like *Neisseria gonorrhoeae, Proteus vulgaris, Bacillus subtilis, Escherichia coli, Pseudomonas aeruginosa, Staphylococcus aureus.* The compounds show appreciable activities between the alcohols and amine molecules. The excess parameter curves suggest the more acidic character of 2 ME than 2 EE.

5. ACKNOWLEDGMENTS

The authors thanks to the Principal, Yeshwant Mahavidyalaya Nanded for providing necessary laboratory facilities.

6. REFERENCES AND NOTES

[1] Kappe, C. O. *Acc. Chem. Res.* **2000**, *33*, 879. [CrossRef][PubMed]

[2] Lusch, M. J.; Tallarico, J. A. *Org. Lett.* **2004**, *6*, 3237. [CrossRef][PubMed]

[3] Li, C. J. *Chem Rev.* **2005**, *105*, 3095. [CrossRef][PubMed]

[4] Sheldon, R. A. *Green Chem.* **2005**, *7*, 267. [CrossRef]

[5] Kappe, C. O. *Eur. J. Med Chem.* **2000**, *35*, 1043. [CrossRef]

[6] Lindstrom, U. M. *Chem. Rev.* **2002**, *102*, 2751. [CrossRef][PubMed]

[7] Yu Xia, L. I.; Wei Liang, B. A. O. *Chin. Chem. Lett.* **2003**, *14*, 993.

[8] Kundu, S. K.; Majee, A.; Hajra, A. *Ind. J. Chem.* **2009**, *48B*, 408. [Link]

[9] Kappe, C. O.; Stadler, A. *Org. React.* **2004**, *63*, 1. [CrossRef]

[10] Su, W.; Li, j.; Zheng, Z.; Shen, Y. *Tetrahedron Lett*. **2005**, 46, 6037. [CrossRef]

[11] Ghosh, R.; Maiti, S.; Chakarborty, A. *J. Mol. Catal A.*, **2004**, *210*, 53. [CrossRef]

[12] Ma, Y.; Qian, C.; Wang, L.; Yang, M. *J. Org. Chem.* **2000**, *65*, 3864. [CrossRef][PubMed]

[13] Varala, R.; Alam, M. M.; Adapa, S. R. *Synlett.* **2003**, 67. [CrossRef]

[14] Paraskar, A. S.; Dewkar, G. K.; Sudalai, A. *Tetrahedron Lett*. **2003**, *44*, 3305. [CrossRef]

[15] Ma, Y.; Qian, C.; Wang, L.; Yang, M. *J. Org. Chem.* **2000**, *65*, 3864. [CrossRef][PubMed]

[16] Gohain, M.; Prajapati, D.; Sandhu, J. S. *Synlett* **2004**, 235. [CrossRef]

[17] Maiti, G.; Kundu, P.; Guin, C. *Tetrahedron Lett*. **2003**, *44*, 2757. [CrossRef]

[18] Salehi, H.; Guo, Q. X. *Synth. Commun*. **2004**, *34*, 171. [CrossRef]

[19] Hu, E. P.; Sidler, D. R.; Dolling, U. H. *J. Org. Chem*. **1998,** *63*, 3454. [CrossRef]

[20] Lu, J.; Ma, H. *Synlett* **2000**, 63. [CrossRef]

[21] Ramalinga, K.; Vijavalakshmi, P.; Kaimal, T. N. B. *Synlett.* **2001**, 863. [CrossRef]

[22] Ranu, B. C.; Hajra, A.; Jana, U. *J. Org. Chem.* **2000**, *65*, 6270. [CrossRef][PubMed]

[23] Reddy, C. V.; Mahesh, M.; Raju, P. V. K.; Babu, T. R.; Reddy, V. V. N. *Tetrahedron Lett.* **2002**, *43*, 2657. [CrossRef]

[24] Rodriguez, D.; Bemardi, O.; Kirsch, G. *Tetrahedron Lett.* **2007**, *48*, 5777. [CrossRef]

[25] Fabio, S. F.; Kappe, O. C. *ARKIVOC,* **2001**, *(II)*, 122.

[26] Dondoni, A.; Massi, A. *Tetrahedron Lett.* **2001**, *42*, 7975. [CrossRef]

[27] Kumar, A.; Maurya, R. A. *Tetrahedron Lett.* **2007**, *48*, 4569. [CrossRef]

[28] Lin, H.; Ding, J.; Chen, X.; Zhang, Z. *Molecules* **2000**, *5*, 1240. [CrossRef]

[29] Kulkarni, M. G.; Chavhan, S. W.; Shinde, M. P.; Gaikwad, D. D.; Borhade, A. S.; Dhondge, A. P.; Shaikh, Y. B.; Ningdale, V. B.; Desai, M. P.; Birhade, D. R. *Beilst. J. Org. Chem.* **2009**, *5*, 04.

[30] Radha, R. V.; Shrinivas, N.; Kishan, R.; Kulkarni, S. J.; Raghavan, K. V. *Green Chem.* **2001**, *3*, 305.

Orbital: The Electronic Journal of Chemistry
journal homepage: www.orbital.ufms.br
ISSN 1984-6428

| Vol 5 | | No. 1 | | January-March 2013 |

Full Paper

Comparison among Different pH Values of Rhodamine B Solution Impregnated into Mesoporous Silica

Juliana Jorge[a], Gustavo R. Castro[b], Marco A. U. Martines[a]*

[a]*Instituto de Química, Universidade Federal de Mato Grosso do Sul, Av. Filinto Muller, 1555, Cidade Universitária, 79074-460, Campo Grande, MS. Brazil.*
[b]*IBB, Universidade Estadual Paulista, P.O.Box 510, CEP 18618-000, Botucatu, SP, Brazil.*

Article history: Received: 05 October 2012; revised: 20 February 2013; accepted: 28 February 2013. Available online: 17 April 2013.

Abstract: We studied the behavior of different pH values of Rhodamine B solution impregnated into pores of mesoporous silica, through structural characterization techniques, such as scanning electron microscopy and porosity measurements, and spectroscopic characterization techniques, such as infrared and luminescence spectroscopy; in order to applications in luminescence. Because, Rhodamine B is an interesting xanthene dye whose optical properties depend of many factors, dye concentration and pH values. MSU-4 type mesoporous silica has been synthesized with Tween 60 surfactant as directing-structure agent and tetraethyl orthosilicate (Si(OEt)4, TEOS) as silica source. The mesoporous structures doped with dyes are promissory materials for several applications, for example, optical sensors and biomarkers.

Keywords: biological markers; xanthenes dye; photoluminescence; pH effect

1. INTRODUCTION

Xanthenes dyes are widely used, mainly for optical sensing of O_2, CO_2, H_2S, organic compounds containing sulfur and NH_3, and also pH sensors, immunoassays, and many others applications [1].

Rhodamine B is a xanthene dye whose optical properties depend of several factors, such as solvent, concentration and pH value [2]. The carboxyl group participates of typical acid-base balance, wherein the acidic and basic forms are strongly luminescent and colored [2]. Rhodamine B and others xanthenes dyes have been extensively studied in solution, the molecular structure and the solvent have an important role on deactivation of non-radiactive pathways of the first excited state these dyes [3]. By emission spectra of Rhodamine B it's possible to detect changes on surface pH [2]. So, Rhodamine B is an interesting molecule with spectral luminescence properties that makes it useful as a biomarker, important for studies of biological systems and sensors [4], and also as sensing probe for detection of heavy metals [5].

Discovery of mesoporous crystalline materials, in 1992 [6, 7], arouse the interest of scientists working in the field of synthesis of zeolites and materials, catalysis and materials science [8, 9]. This new class of materials attracted great attention due potentials applications [10], including in biology and medicine areas.

Mesoporous materials possess high surface area due narrow distribution size pores that promotes space, like as a host for chemical controlled inclusion into the pores. Mesoporous materials enable new and promising applications of these materials in several areas, such as chemistry, materials science, biology and medicine [11, 12], for example, catalysis; adsorption of heavy metals (environmental decontamination) and ultrafiltration membranes [13]; gas storage; HPLC columns [14]; and drug delivery and materials for bone regeneration and tissue. Dyes molecules encapsulated in mesoporous materials are promising for applications in medicine area as self-diagnostic kits; and developing of biomarkers [15].

Dye and inorganic component may be mixed in nanometric scale, such hybrids are extremely versatile in their processing and composition, as well optical and mechanical properties [16]. Incorporation promotes isolation and protection against

* Corresponding author. E-mail: marcomartines@gmail.com

intermolecular interactions, rearrangement and photodegradation.

Then in this work, we studied the behavior of different pH values (2.0; 7.0, and 11.0) of Rhodamine B solution impregnated into pores of mesoporous silica, through structural and spectroscopic characterization techniques in order to applications in luminescence.

2. MATERIAL AND METHODS

All reagents were purchased from Sigma-Aldrich, Acros Organic or Fluka and used as received.

2.1. Preparation of mesoporous silica

Mesoporous silica MSU-4 type was synthesized with polyoxyethylene sorbitan monostearate (Tween 60®), as structure directing agent, and tetraethyl orthosilicate (TEOS), as silica source, in a two-step procedure. Micellar solution was prepared at room temperature mixing $2x10^{-2}$ mol of Tween 60® and water, the pH was adjusted with hydrochloric acid (HCl 1 $mol.L^{-1}$) and $16x10^{-2}$ mol of TEOS was added. The final step of condensation was performed by addition of sodium fluoride (NaF 0.25$mol.L^{-1}$), and finally, the reaction remained in condensation for 72 h and 65 °C under stirring, elapsed this time the obtained precipitate was filtered [14]. After the filtering, the obtained silica was calcined at 600 °C for complete removal of the surfactant.

2.3. Preparation of Rhodamine B solutions

Aqueous solution of Rhodamine B ($2x10^{-4}$ $mol.L^{-1}$) was prepared with 0.01 g of Rhodamine B in a flask balloon. The pH values (2.0; 7.0; 11.0) were adjusted with HCl (0.09 $mol.L^{-1}$) solution, and sodium hydroxide (NaOH 0.05 $mol.L^{-1}$) solution.

2.3. Impregnation of Rhodamine B solutions in mesoporous silica

Were mixing with calcined silica, 5 mL of each solution of Rhodamine B prepared in different pH values, until solubilization, after this, each mix of silica and Rhodamine B solution was washed three times with distilled water and dry at 50 °C in a stove.

2.4. Characterization

The obtained material passed through the following characterization techniques: Scanning Electron Microscopy (SEM), to observe morphology and size of the particles, was carried out in an electronic microscope ZEISS DSM 960 at 20 kV. The SEM measurements was carried out in Brazilian Nanotechnology National Laboratory - LNNANO. Porosity measurements, to collect information about surface area and pores diameter, was performed in a Micromeritcs 2010 using standard continuous proceeding, initial degassing of samples at 150 °C for 15 h. Surface areas were determined by the Brunnauer-Emmett-Teller (BET) method within a relative pressure range of 0.05–0.2. Pore size distributions were calculated only for sizes above 2.5 nm from the desorption branch, using a polynomial correlation between relative pressure and pore diameter deduced from the Broekhoff and Boer (BdB) model [17, 18]. To facilitate comparisons, the reduced adsorption curves (isotherms divided by the amount adsorbed at a relative pressure of 0.8) were displayed [19]. The absorption effect was corrected for all the samples. Small-angle X-ray scattering (SAXS), in order to analyze pores' arrangement and organization, was measured on National Laboratory Synchroton Light (LNLS Campinas, Brazil), using asymmetric slit and silicon monochromator (111), with monochromatic beam (λ= 1.488 Å) and horizontal focus. The scattered intensity was collected with "imaging plate" at 849.64 mm of the sample. The camera length corresponds to a scattering vector q ranging from 0.018 to 0.39 Å-1. Horizontal and vertical beam stoppers were used to absorb the direct and the totally reflected X-ray beam, respectively. Most of the patterns exhibited three diffraction peaks that were assigned to a pore correlation length. This pore center to pore center correlation length is herein after referred to as ''d-spacing''. The absorption effect was corrected for all the samples. Fourier Transform Infrared (FT-IR) spectra, to observe impregnation of Rhodamine B into silica pores, were acquired within the 4000 to 500 cm^{-1} range using KBr pellets with a 2 cm^{-1} resolution, using a BOMEM MB 100 spectrometer. Luminescence spectroscopy, to study luminescence properties and possible interactions between dye and silica surface, was recorded with a spectrofluorimeter SPEX-FluoroLog, with xenon lamp of 450 W.

3. RESULTS AND DISCUSSION

SEM image (Figure 1) of pure mesoporous

silica displays particles micrometric size with heterogenic shape, going from sticks to spherical, characteristic of MSU-X type of mesoporous silica. The material was named Michigan State University type material, or MSU-X silica (X refers to the nature of the surfactant: 1 for alkyl-PEO, 2 for alkylaryl-PEO, 3 for polypropyleneoxyde-PEO block copolymer, and 4 for Tween-type nonionic ethoxylated sorbitan esters) is prepared under neutral or mild acidic conditions. The final structure and the morphology of MSU-X type material are highly dependent on the parameter of the reactional mean, such as a local interaction created by the lipophilic/hydrophilic equilibrium, the Brownian motion that destroys the network, the hydrolysis kinetic and polymerization of silica. Synthesis of MSU-X type mesoporous silica based on hydrogen bonding illustrates perfectly the versatility of this approach, since the final material structure (pore diameter, particle size) can be readily modified by adjusting several synthesis parameters, with the same reaction medium [20].

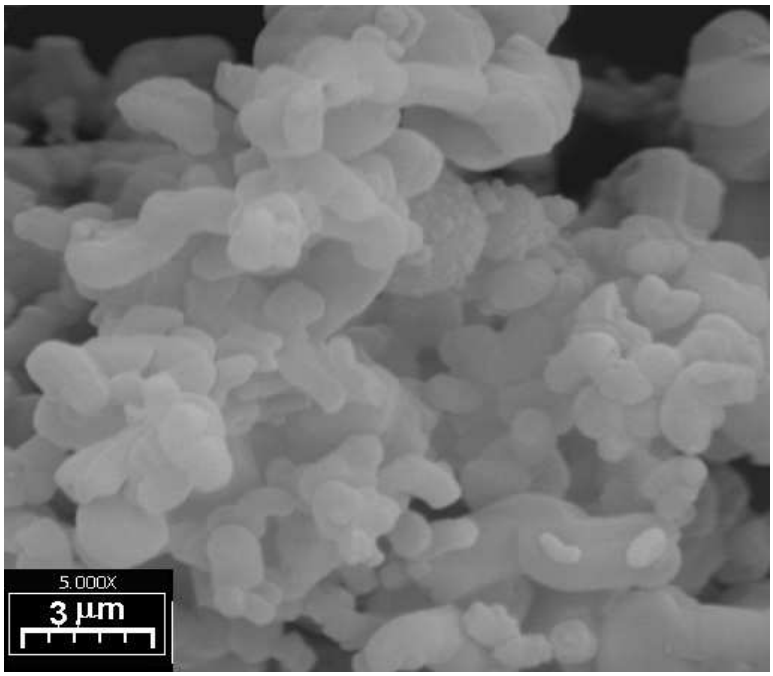

Figure 1. SEM image of calcined pure silica.

The porosity measurements presented in the Figure 2 is characteristic of micelle-templated structures (MTS) [20]. Therefore, the sample displays a substantial structure of confined mesopores. The adsorption isotherm for silica pure no exhibits hysteresis, feature of uniform pores, the adsorption not increase in high relative pressure, feature of textural porosity, like as the curve of adsorption that not exhibits hysteresis, which is characteristic of pore necking. The sample shows fine distribution pores, typical of MTS, with type IV nitrogen adsorption-desorption isotherm [20]. The graphics inserted shows a high specific surface of 1200 $m^2.g^{-1}$ and pore average size of 4.6 nm.

The SAXS measures in the Figure 3, were performed in order to collect information about structure and arrangement of pores, the spectra of silica impregnated with Rhodamine B in different pH values are shown below. A view of the spectra displays the diffraction peaks d_{100}, d_{110} and d_{200} for silica with Rhodamine B in pH 2 (d_1= 5.21 nm; d_2= 3.01 nm, and d_3= 2.59 nm) and pH 7 (d_1= 5.21 nm; d_2= 3.03 nm, and d_3= 2.64 nm). The presence of three diffraction peaks, for all the silica, except silica with Rhodamine B in pH 11, denotes hexagonal porous arrangement material, ordered mesostructure, and the quality of the sample may be estimated by diffraction line intensity [18, 21].

The IR spectra in Figure 4 are typical of noncrystalline silica [22]. The bands assignments from the spectra are described. Asymmetric stretching Si-O and Si-O-(Si) vibrations occur in the 1233-1041 cm^{-1} wavenumber range. $Si-O^-$ asymmetric and SiO symmetric stretchings appear in 957 and 803 cm^{-1}, respectively. Deformation O-Si-O appears at 464 cm^{-1} [22]. All the spectra show typical water molecule

stretching bands in the 3622-3323 cm^{-1} region. The water molecule deformation band generally observed at ca. 1625 cm^{-1} appears between 1639 and 1661 cm^{-1} for each sample. This shift to a larger wavenumber can be attributed to the presence of H_3O^+ ions in the silica samples [23]. There is a weak peak at about 1453 cm^{-1} and another peak at about 2900 cm^{-1}, assigned ascribed to the C–H stretching modes that might be attributed to aromatic rings of Rhodamine B [24].

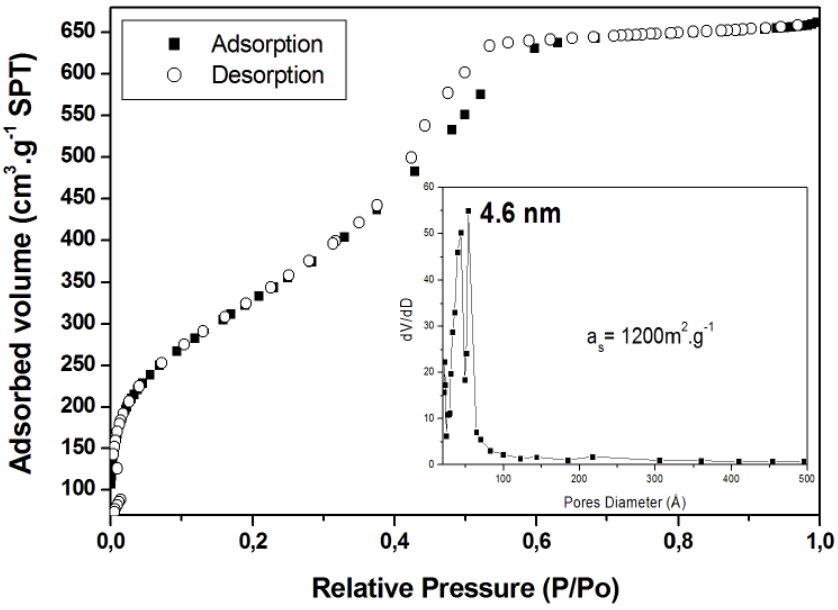

Figure 2. Adsorption/desorption isotherm of calcined mesoporous silica, with distribution pores diameter inserted.

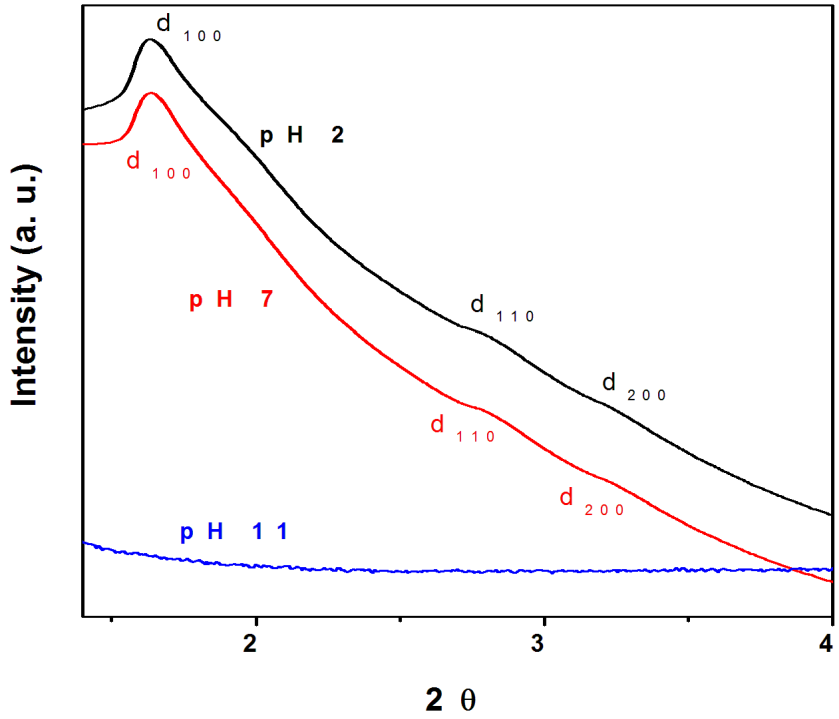

Figure 3. SAXS of mesoporous silica impregnated with Rhodamine B solution in pH 2, pH 7 and pH 11.

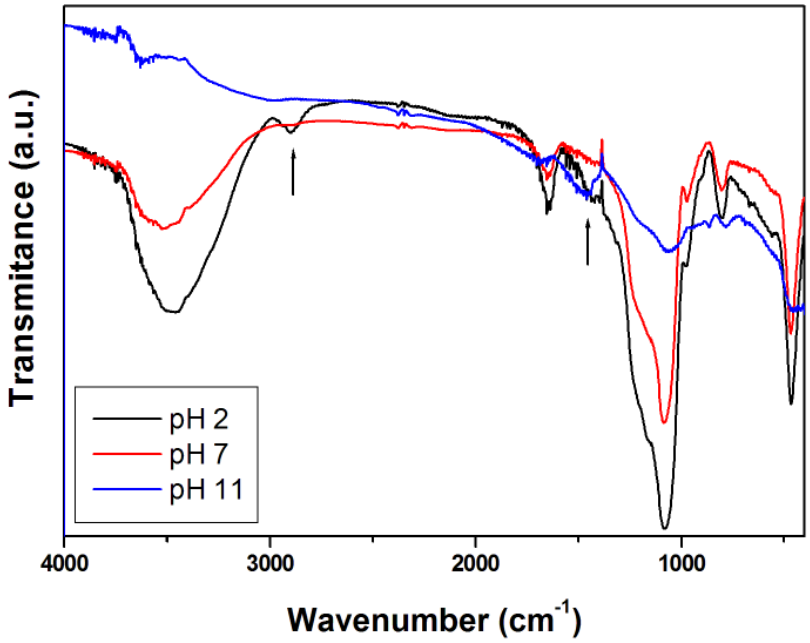

Figure 4. Fourier Transform Infrared spectra of mesoporous silica impregnated with Rhodamine B solution in pH 2, pH 7 and pH 11.

In the Figure 5, excitation spectra, is found a maximum intensity located between 500 to 550 nm, that corresponds to $S_0 \rightarrow S_1$ transition [25], in addition to others bands that appear for all spectra.

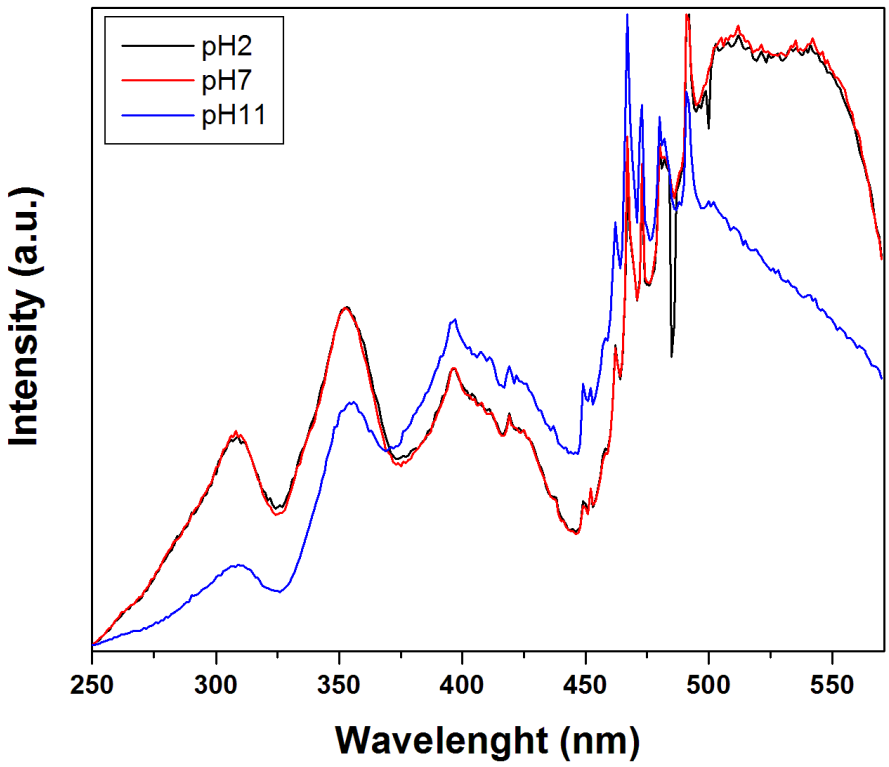

Figure 5. Spectra of excitation, λ_{em} = 593 nm, of mesoporous silica impregnated with Rhodamine B solution in pH 2, pH 7 and pH 11.

The emission spectra (Figure 6) depict that there is a broad band with a maximum of intensity located to 580 nm that corresponds to $S_1 \rightarrow S_0$ transition [25]. A significant shift occurs for silica impregnated with Rhodamine B solution in pH 11, indicating changes must be related to removing dimers when increase the pH, leading to the observation of monomer emission [26], consequently influences the spectroscopic properties of Rhodamine B, which also observed for the others techniques used.

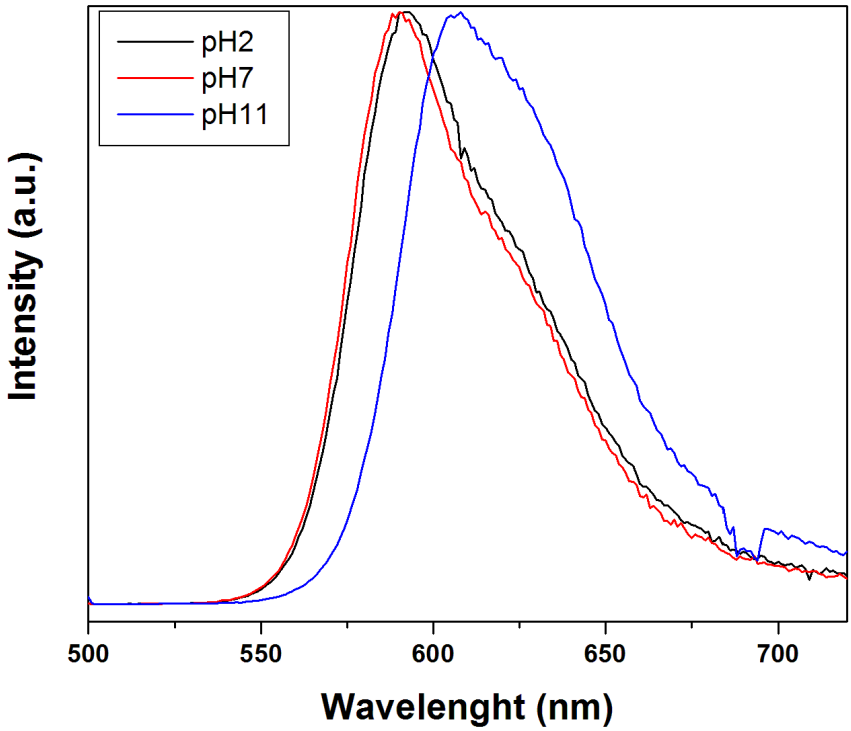

Figure 6. Spectra of emission, λ_{exc} = 480 nm of mesoporous silica impregnated with Rhodamine B solution in pH 2, pH 7 and pH 11.

4. CONCLUSION

Results show that, in acidic medium, Rhodamine B impregnated in silica has a stable behavior. However, in alkaline medium, there is a change in physical and spectroscopic properties of Rhodamine impregnated in silica, which may be associated to changes in the dimer equilibrium of Rhodamine B in aqueous solution and a possible interaction of Rhodamine B with the silanol groups in mesoporous silica surface. These behavior open new prospects about explorations in the field of photoluminescence, as new biomarkers and chemical sensors.

5. ACKNOWLEDGMENTS

The authors would like to thank all governments' agencies and institutions which made possible this research. JJ thanks the CAPES foundation for its fellowship. The authors gratefully acknowledge CNPq, FUNDECT-MS and the Brazilian Synchrotron Light Laboratory - LNLS for the SAXS, and the Brazilian Nanotechnology National Laboratory - LNNANO for the SEM measurements.

6. REFERENCES AND NOTES

[1] Mchedlov-Petrossyan, N. O.; Kukhtik, V. I.; Bezugliy, V. D. *J. Phys. Org. Chem.* **2003**, *16*, 380. [CrossRef]

[2] Silva, A. A.; Flor, J.; Davolos, M. R. *Surf. Sci.* **2007**, *601*, 4. [CrossRef]

[3] Vieira Ferreira, L. F.; Lemos, M. J.; Reis, M. J.; Botelho do Rego, A. M. *Langmuir* **2000**, *16*, 5673. [CrossRef]

[4] Moreno-Villoslada, I.; Jofré, M.; Miranda, V.; González, R.; Sotelo, T.; Hess, S.; Rivas, B. L. *J. Phys. Chem. B* **2006**, *110*, 11809. [CrossRef]

[5] Ghosh, K.; Sarkar, T.; Samadder, A.; Khuda-Bukhsh, A.R. *New J. Chem.* **2012**, *36*, 2121. [CrossRef]

[6] Beck, J. S.; Vartuli, J. C.; Roth, W. J.; Leonowicz, M. E.; Kresge, C. T.; Schmitt, K. D.; Chu, C. T-W.; Olson, D. H.; Sheppard, E. W.; Mccullen, S. B.; Higgins, J. B.; Schlenker, J. L. *J. Am. Chem. Soc.* **1992**, *114*, 10834. [CrossRef]

[7] Kresge, C. T.; Leonowicz, M. E.; Roth, W. J.; Vartuli, J. C.; Beck, J. S. *Nature* **1992**, *359*, 710. [CrossRef]

[8] Sayari, A. *Chem. Mater.* **1996**, *8*, 1840. [CrossRef]

[9] Beck, J. S.; Vartuli, J. C. *Curr. Opin. Solid State Mater. Sci.* **1996**, *1*, 76. [CrossRef]

[10] Shen, J. L.; Cheng, C. F. *Curr. Opin. Solid State Mater. Sci.* **2004**, *7*, 427. [CrossRef]

[11] Kim, J. Y.; Park, S. H.; Yu, J. *Opt. Mater.* **2002**, *21*, 349. [CrossRef]

[12] Wirnsberger, G.; Scott, B. J.; Stucky, G. D. *Chem. Commun*. **2001**, 119. [CrossRef]

[13] Boissiere, C.; Martines, M. A. U.; Kooyamn, P. J.; Kruijff, T. R.; Larbot, A.; Prouzet, E. *Chem Mater* **2003**, *15*, 460. [CrossRef]

[14] Martines, M. A. U.; Yeong, E.; Persin, M.; Larbot, A.; Voorhout, W. F.; Kübel, C. K. U.; Kooyman, P.; Prouzet, E. *C. R. Chim.* **2005**, *8*, 627. [CrossRef]

[15] Hoffmann, F.; Cornelius, M.; Morell, J.; Fröba, M. *Angew. Chem. Int. Ed.* **2006**, *45*, 3216. [CrossRef]

[16] Seçkin, T.; Gültek, A.; Kartaca, S. *Dyes and Pigments* **2003**, *56*, 51. [CrossRef]

[17] Broekhoff, J. C. P.; de Boer J. H. *J. Catal.* **1968**, *10*, 377. [CrossRef]

[18] Prouzet, E.; Cot, F.; Nabias, G.; Larbot, A.; Kooyman, P.; Pinnavaia, T. J. *Chem. Mater.* **1999**, *11*, 1498. [CrossRef]

[19] Ryoo, R.; Ko, C. H.; Kruk, M.; Antochshuk, V.; Jaroniec, M. *J. Phys. Chem. B* **2000**, *104*, 11465. [CrossRef]

[20] Boissiere C.; Martines M. A. U.; Tokumoto M.; Larbot A.; Prouzet E. *Chem. Mater.* **2003**, *15*, 509. [CrossRef]

[21] Prouzet E.; Pinnavaia T.J. *Angew Chem Int Ed* **1997**, *36*, 516. [CrossRef]

[22] Martines, M. A. U.; Davolos, M. R.; Jafelicci Jr., M; Souza, D. F.; Nunes L. A. O. *J. Lumin.* **2008**, *128*, 1787. [CrossRef]

[23] Martines, M. A. U.; Pecoraro E.; Simoneti J. A.; Davolos M. R.; Jafelicci Jr., M. *Separ. Sci. Technol.* **2000**, *35*, 287. [CrossRef]

[24] Pavia, D. L.; Lampman G. M.; Kriz G. S.; Vyvyan J. R. Introduction to Spectroscopy. Brooks/Cole, Belmont: **2009**.

[25] Bockstette, M.; Wohrle, D.; Braun, I.; Ekloff, G. S. *Microporous Mesoporous Mater*, **1998**, *23*, 83. [CrossRef]

[26] Rocha, L. A.; Caiut, J. M. A.; Messaddeq, Y.; Ribeiro, S. J. L.; Martines, M. A. U.; Freiria, J. C.; Dexpert-Ghys, J.; Verelst, M. *Nanotechnology* **2010**, *21*, 155603. [CrossRef][PubMed]

Orbital: The Electronic Journal of Chemistry
journal homepage: www.orbital.ufms.br
ISSN 1984-6428

| Vol 5 | | No. 1 | | January-March 2013 |

Full Paper

Omega-6/Omega-3 and PUFA/SFA in *Colossoma macropomum* Grown in Roraima, Brazil

Antonio Alves de Melo Filho[a*], Hamilton Hermes de Oliveira[a], Ricardo Carvalho dos Santos[b]

[a]*Programa de Pós-Graduação em Química, Universidade Federal de Roraima, Av. Capitão Ene Garcez, 2413, Campus Paricarana, CEP 69312-000, Boa Vista, Roraima, Brazil.*
[b]*Programa de Pós-Graduação em Biodiversidade e Biotecnologia, BIONORTE, Doutorado em Biotecnologia. Coordenação Estadual de Roraima – Universidade Federal de Roraima – UFRR, Campus Cauamé, BR 174, s/n, Km 12 (sentido Pacaraima), Distrito do Monte Cristo, CEP 69310-250, Boa Vista, Roraima, Brasil.*

Article history: Received: 11 October 2012; revised: 08 February 2013; accepted: 18 February 2013. Available online: 17 April 2013.

Abstract: In this study was evaluated the fatty acids composition of tambaqui (Colossoma macropomum) fillet, fish species cultivated in Roraima State, Brazil. For the extraction of tambaqui oil was used Sohxlet device and then it was methylated. The oil was identified using a gas chromatograph and were identified 24 acids and these were divided into characteristic groups such as: saturated fatty acids (SFA), monounsaturated fatty acids (MUFA), polyunsaturated fatty acids (PUFA) and series fatty acids omega-6 and omega-3. The ratios obtained were PUFA/SFA and omega-6/omega-3. The results of chromatographic analysis were subjected to tests by variance ANOVA and multiple comparisons of Tukey at 5%. The ratios omega-6/omega-3 and PUFA/SFA showed values of 8.58 and 0.75 respectively.

Keywords: Colossoma macropomum; fatty acids; fish oil; omega-3; omega-6; tambaqui

1. INTRODUCTION

The tambaqui (*Colossoma macropomum*) is a fish native from Amazon and Orinoco basins and their effluents. This species has attracted interest in pisciculture in Roraima State, Brazil, because it has been successfully adapted in fish-farming, for its ability to have various types of food, and also to have rapid growth, about eight months, and still serves as excellent filter feeders of plankton [1-4].

The fish bred in the wild undergo various environmental influences. The tambaqui can gain weight up to 3.0 times more in semi-intensive system under stable and controlled diet composition, as in the nursery, which in intensive system in the stream channel. Thus, the lipid content can be modified to improve that fish qualitatively and quantitatively [1, 5].

According to Henderson and Tocher [6] fresh-water fish contains high proportions of saturated and polyunsaturated fatty acids with 18 carbon atoms, but low levels of unsaturated fatty acids with 20 and 22 carbon atoms when compared to the lipids of marine fish.

To Visentainer et al. [7] the fatty acid intake of omega-3 series reduce the rate of total blood cholesterol, moreover, dietary interventions have shown that consumption of polyunsaturated fatty acids (PUFA) and/or fish oil reduces cardiovascular diseases.

According to Simopoulos [8] diets for humans, actually, have plenty of saturated fatty acids. However, these diets are low and present unequal amounts of polyunsaturated fatty acids of omega-3 and omega-6 and also some amount of *trans* fatty acids.

Simopoulos [8] looks at the diets in the Occident, which contain higher amount of omega-6 because of the indiscriminate recommendation to substitute saturated fatty acids by omega-6, with the purpose of reducing serum cholesterol. The ideal ratio of omega-6 and omega-3 in the daily diet is not well established, but it is recommended that the intake of linoleic acid should not exceed 10% of total calories. The same author insists on presenting Occident diets the ratio ω6/ω3 is about 20:1 to 30:1 and recommends that the proportion of fatty acids, ω6/ω3, is from 5:1 to 10:1, which are very high values compared to those

* Corresponding author. E-mail: antonio.melo@pq.cnpq.br (A. A. Melo Filho)

considered ideals 1:1 to 2:1.

The Department of Health in England recommends that the value of ratio ω6/ω3 is a maximum of four. Thus, observed that there is no consensus regarding the nutritional issue [9].

In this way, this paper has like main goal to evaluate the total composition of fatty acids, to calculate the ratio ω6/ω3 and PUFA/SFA in tambaqui fillet oil, at four localities in Roraima State, using the gas chromatographic technical.

2. MATERIAL AND METHODS

2.1. Obtained Samples

It was collected three specimens of fish at random from a lot with about two thousand specimens of tambaqui, which had been captured from four pools of semi-intensive. This procedure was performed in four localities in Roraima State, namely: Alto Alegre, Bonfim, Uraricoera and Boa Vista (in Passarão region). But, these samples were identified and analyzed separately.

2.2. Drying, Extraction and Oil Yeld

After killing the fish, the fillets were removed, crushed and taken to drying in a heating oven with air circulation. The method used for drying and oil extraction follows Duarte's method however with modifications [10]:

It was removed from the fish fillet and then mashed in a blender, weighed 100 g fillet is crushed, then taken to a drying temperature of 100 ^{o}C in a heating oven with air circulation during a time of approximately 8 hours to constant mass. The dry tissue was transferred to an Erlenmeyer of 1000 mL, which was added 20 g of anhydrous sodium sulfate and 400 mL of hexane, then taken to a mixer to promote agitation for one hour. After the agitation were made filtration and evaporation of the solvent in rotary evaporator. The extracted oil was packaged in amber bottle in nitrogen atmosphere for further analysis.

2.3. Preparation of Methyl Esters

It was weighed 4 g of oil phase in the distillation flask of 125 mL. After adding 5 mL of alcoholic potassium hydroxide 0.5 N put the flask under reflux for 3 minutes. Added to the balloon still hot, 15 mL of ammonium chloride / sulfuric acid in methanol (16 g of ammonium chloride, 480 mL of methanol and 24 mL of concentrated sulfuric acid) and put the flask back to reflux for 3 minutes. After the sample has cooled 10 mL of heptane was added. The mixture obtained was transferred to separating funnel 60 mL, shaking the funnel vigorously for 15 seconds. The phase was extracted with heptane and filtered through filter paper with ± 3.0 g of anhydrous sodium sulfate. The heptane phase was transferred to a 5 mL amber bottle with lid and in a nitrogen atmosphere for further analysis [11].

2.4. Identification Fatty Acids

The esters of fatty acid were separated in a gas chromatograph Varian CP High Resolution - 3380 equipped with a fused silica capillary column (DB-Wax 30 m × 0.25 mm) and flame ionization detector. The gas flow was 2.0 mL min^{-1} for the carrier gas H_2. The ratio of division (split) of the sample was 1:200. The column temperature was programmed to 100 °C at baseline was elevated to 240 °C at a rate of 7 °C min^{-1}. The injector and detector temperatures were 260 °C. The injection volume was 2 µL. The peak areas were determined by the method of standardization, using an integrator-processor (J & W Scientific) and identification of peaks was made by comparison of retention times (tr) patterns of fatty acid methyl esters, Supelco 37.

2.5. Statistical Analysis

The results were submitted to test of variance ANOVA and the multiple comparison Tukey's test at 5% level of probability using the software Statistic 6.0.

3. RESULTS AND DISCUSSION

The Table 1 shows the percentage of results in tambaqui oil in Roraima State in four different localities studied.

As can be seen, on Table 1, 24 fatty acids were identified and the area of concentration was greater with the 18-carbon acids (C18) in which *cis*-oleic acid (C18:1ω9c) omega-9 series, stands out with the highest percentage. Following in a descending percentage order of fatty acids majority comes soon after the palmitic acid (C16: 0), *cis*-linoleic acid (C18:2ω6c), stearic (C18:0), *trans*-9-octadecenoic

(C18:1ω9t), *trans*-linoleic acid (C18: 2ω6t), palmitoleic (C16:1ω7), α-linolenic acid (C18:3ω3) and *cis*-12-octadecenóico (C18: 1ω6c). The palmitic acid (C16: 0) presented the highest percentage among the saturated acids, however this sequence of results have not been the same in four localities studied.

Table 1. Results (%) of total lipid fatty acids in tambaqui fillet oil.

Name	Nomenclature	Alto Alegre	Bonfim	Uraricoera	Passarão
C14:0	myristic acid	1,05±0,03^{a}	0,83±0,03^{c}	0,90±0,03^{b}	0,96±0,01^{b}
C14:1	miristoleic acid	0,45±0,01^{c}	0,47±0,01^{bc}	0,57±0,01^{a}	0,48±0,01^{b}
C15:0	pentadecyclic acid	0,19±0,01^{b}	0,24±0,01^{a}	0,11±0,01^{c}	0,11±0,01^{c}
C15:1	6-pentadecenoic acid	Nd	0,13±0,01^{a}	Nd	0,09±0,01^{b}
C16:0	palmitic acid	20,48±0,01^{a}	18,11±0,01^{b}	16,16±0,06^{c}	16,78±0,012^{c}
C16:1ω7	palmitoleic acid	2,94±0,21^{a}	2,68±0,14^{ab}	2,30±0,14^{b}	2,73±0,09^{a}
C17:0	margaric acid	0,36±0,03^{a}	Nd	Nd	0,27±0,01^{b}
C17:1	*cis*-10-Heptadecenic acid	Nd	0,14±0,03^{a}	0,08±0,01^{b}	0,16±0,03^{a}
C18:0	stearic acid	9,60±0,17^{a}	8,03±0,13^{b}	9,29±0,13^{a}	9,75±0,07^{a}
C18:1ω9c	cis-oleic acid	26.84±0.48^{a}	23.17±0,14^{b}	23.77±0.12^{b}	25.54±0.81^{a}
C18:1ω6c	*cis*-12-octadecenoic acid	2.09±0.08^{a}	1.81±0.06^{b}	1.44±0.03^{c}	1.41±0.03^{c}
C18:1ω9t	*trans*-9-octadecenoic acid	3.86±0.24^{b}	4.34±0.25^{b}	5.59±0.28^{a}	5.22±0.08^{a}
C18:2ω6c	*cis*-linoleic acid	10.81±0.54^{d}	13.20±0.13^{c}	16.57±0.27^{a}	14.85±0.58^{b}
C18:2ω6t	*trans*-linoleic acid	5.47±0.31^{a}	3.95±0.07^{bc}	3.85±0.34^{c}	4.68±0.27^{ab}
C18:3ω3	α-linolenic acid	1.82±0.06^{b}	1.81±0.06^{b}	2.83±0.21^{a}	2.69±0,22^{a}
C20:0	arachidic acid	0.15±0.01^{a}	0.12±0.01^{b}	Nd	0.11±0.01^{b}
C20:1ω9c	*cis*-10-eicosaenoic acid	0.90±0.02^{b}	1.04±0.03^{a}	0.67±0.02^{c}	0.60±0.02^{c}
C20:3ω6	γ-linolenic acid	0.31±0.01^{c}	0.56±0.02^{a}	0.37±0.03^{b}	0.37±0.03^{b}
C20:3ω3	α-linolenic acid	Nd	0.33±0.02^{a}	0.08±0.03^{c}	0.13±0.01^{b}
C20:4ω6	arachidonic acid	Nd	0.11±0.01^{a}	Nd	0.11±0.01^{a}
C20:5ω3	eicosapentaenoic acid	Nd	0.09±0.003	Nd	Nd
C21:0	undocosaenoic acid	0.16±0.01^{b}	0.16±0.01^{b}	0.12±0.01^{c}	0.18±0.01^{a}
C22:1ω9c	*cis*-14-docosaenoic acid	0.25±0.02^{a}	0.18±0.01^{c}	0.22±0.02^{b}	0.14±0.01^{d}
C24:0	tetracosanoic acid	Nd	0.25±0.02	Nd	Nd

a, b, c, d: The following medias with same letter, at line, don't differ statisticaly by Tukey's test at 5% probability level. Nd: no determined.

Comparing the main fatty acids of the tambaqui fillet oil from four localities, it was observed that there was no significant difference ($p<0.05$) between acid *trans*-9-octadecenoic (C18:1ω9t), stearic (C18:0) and palmitoleic (C16:1ω7), but there are differences between the palmitic acid (C16:0) and *cis*-linoleic (C18:2ω6c). Therefore, can be noticed the presence of arachidonic acid (C20:4ω6) only in Bonfim and Passarão and the eicosapentaenoic acid (C20:5ω3) in Bonfim.

Figure 1 shows the four chromatograms pooled analysis of the esters of fatty acids of tambaqui fillet in Roraima State.

The Table 2 shows saturated fatty acids – SFA (myristic, pentadecyclic, palmitic, margaric, stearic, arachidic, undocosaenoic and tetracosanoic acids);

monounsaturated fatty acids – MUFA (miristoleic, 6-pentadecenoic, palmitoleic, *cis*-10-Heptadecenic, cis-oleic, *cis*-12-octadecenoic, *trans*-9-octadecenoic, *cis*-10-eicosaenoic and *cis*-14-docosaenoic acids); polyunsaturated fatty acids – PUFA (*cis*-linoleic, *trans*-linoleic, α-linolenic, γ-linolenic, α-linolenic, arachidonic and eicosapentaenoic acids) and unsaturated fatty acids – UFA (fatty acids present in MUFA and PUFA) determined from the data of Table 1 and the Table 3 show the ratio PUFA/SFA and omega-6/omega-3.

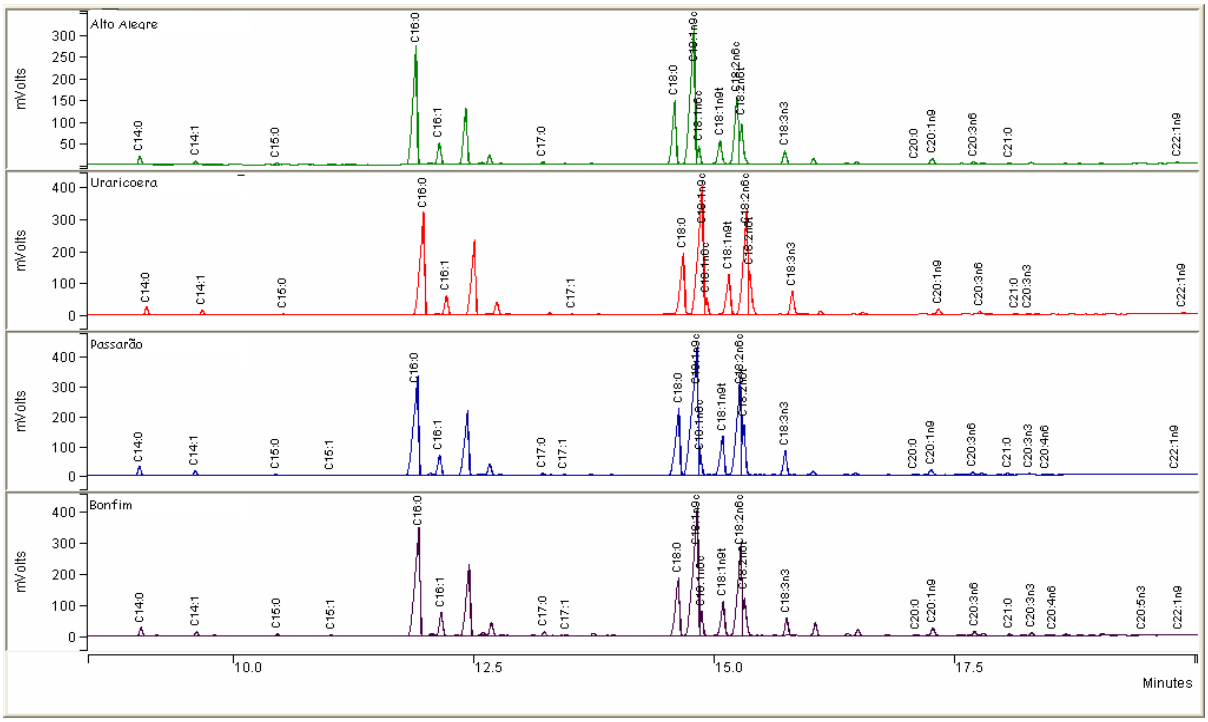

Figure 1. Cromatograms of esters of fatty acids in tambaqui.

Table 2. Groups and average SFA, MUFA, PUFA and UFA.

GROUPS	AA (%)	BO (%)	UA (%)	PS (%)	Average (%)
SFA	31.99	27.49	26.58	28.16	28.56±2.38
MUFA	37.33	33.96	34.64	36.37	35.58±1.55
PUFA	18.41	20.05	23.63	22.83	21.23±2.43
UFA	55.74	54.01	58.27	59.20	56.80±2.37
Omega-6	18.68	19.63	22.23	21.42	20.49±1.62
Omega-3	1.82	2.23	2.91	2.82	2.45±0.51

AA: Alto Alegre; BO: Bonfim; UA: Uraricoera; PS: Passarão.

The concentration of omega-6 series range was 18.68 to 22.23% while for the acids of the omega-3 series range was 1.82 to 2.91% for the oils of tambaqui in four localities (Table 2). The lowest ratio omega-6/omega-3 was observed for fish oil in Uraricoera and Passarão, 7.6:1 (Table 3). You could say that the value of ratio omega-6/omega-3 found in this work is within the recommended levels (5:1 to 10:1) to Occidental diets, however, is considered a high value in relation to those considered ideals (1:1

to 2:1) [8].

Table 3. Ratios of PUFA/SFA and omega-6/omega-3.

RATION	AA	BO	UA	PS	Average
PUFA/SFA	0.58	0.73	0.89	0.81	0.75±0.14
***ω*6/*ω*3**	10.30	8.80	7.60	7.60	8.58±1.28

The ratio of PUFA/SFA which shows the highest value was found in fish oil in Urariquera (0.89) and the lowest was for Alto Alegre (0.58), see Table 3. The Department of Health and Social Security [9] reported that diets with values lower than 0.45 of PUFA/SFA are unhealthy and that higher value this is considerably healthy. Based on this indicator can be said that the tambaqui oil from tambaqui reared in semi-intensive system of State of Roraima is considered healthy.

4. CONCLUSION

The *trans*-linoleic acid (C18: 2*ω*6t) known as CLA-*trans*-10,12, is being widely researched, because, it can possess anticarcinogenic properties. For this acid was found a significant value (4.49%) in fish oils of State of Roraima. The ratio of fatty acids omega-6 and omega-3 has been gaining much attention in scientific means at discussing about fatty acids, this is due to several factors involving beneficial to human health, in view of the Occidental diets, in which ratio omega-6/omega-3 range from 20:1 to 30:1 where the ideal would be 1:1 to 2:1. The ratio omega-6/omega-3 tambaqui oil analyzed in State of Roraima 8.58:1 may not be considered ideal, but is within the normal range.

From a technological standpoint the fractionation of tambaqui oil in Roraima State can be of great importance in the seafood industry in which this feature may be used into concentration of fatty acids in order to find food needs with these products, as well as serving like very healthy source in the human diet.

5. REFERENCES AND NOTES

[1] Almeida, N. M. Composição de acidos graxos e quantificação de EPA e DHA de matrinxã (*Brycon cephalus*) e tambaqui (*Colossoma macropomum*) cultivados e capturados na Amazonia Central. [Tese] Campinas: Faculdade de Engenharia de Alimentos, UNICAMP, 2004. [Link]

[2] Melo Filho, A. A.; Oliveira, H. H.; Panero, F. S.; Santos, R. C. Análisis físico-químico del aceite de filete de tambaqui (*Colossoma macropomum*) cultivado en el Estado de Roraima, Brasil. *Orbital Elec. J. Chem*. 2012, 4, 263. [Link]

[3] Chagas, E. C.; Gomes, L. C.; Júnior, H. M.; Roubach, R. Produtividade de tambaqui criado em tanque-rede com diferentes taxas de alimentação. *Ciên. Rural.* **2007**, *37*, 119. [CrossRef]

[4] Mendonça, P. P.; Ferreira, R. A.; Vidal Junior, M. V.; Andrade, D. R; Santos, M. V. B; Ferreira, A. V.; Rezende, F. P. *Archivos de Zootecnia.* **2009**, *58*, 323. [CrossRef]

[5] Arbeláez-Rojas, G. A.; Fracalossi, D. M.; Fim, J. D. I. *Ver. Bras. Zootecnia* **2002**, *31*, 1059. [CrossRef]

[6] Henderson, R. J; Tocher, D. R. *Prog. Lipid Research.* **1987**, *26*, 281. [CrossRef]

[7] Visentainer, J. V.; Sandra, T. M. G.; Carmino, H.; Oscar, O. S. J.; Adriano, B. M. S.; Karin, C. J.; Nilson, E. S.; Makoto, M. *Ciências e Tecnologia de Alimentos.* **2003**, *23*, 478. [CrossRef]

[8] Simopoulos, A. P. *American Journal of Clinical Nutrition.* **1991**, *54*, 438. [CrossRef]

[9] Department of Health. Nutritional aspects of cardiovascular disease. Report of the Cardiovascular Review Group Committee on Medical Aspects of Food Policy. Reports on Health and Social Subjects, n.46. H. M. Stationary Office: London, 1994.

[10] Duarte, G. R. M. Estudo da composição de ácidos graxos e colesterol em óleos de peixes do Rio Araguaia. [Dissertação] Goiânia: Instituto de Química, UFG, 2001.

[11] Hartman, L.; Lago, R. C. A. *Laboratory Practice.* **1973**, *22*, 475. [CrossRef]

Orbital: The Electronic Journal of Chemistry
journal homepage: www.orbital.ufms.br
ISSN 1984-6428

| Vol 5 | | No. 1 | | January-March 2013 |

Full Paper

Tannic acid Catalyzed an Efficient Synthesis of 2,4,5-Triaryl-1*H*-Imidazole

Nana V. Shitole[a], Balasahe V. Shitole[b], Gopal K. Kakde[b], Murlidhar S. Shingare[b]

[a]*Shri Shivaji College, Department of Chemistry Parbhani-431401 MS, India*
[b]*Dr. Babasaheb Ambedkar Marathwada University, Auranagabad-431004, MS, India.*

Article history: Received: 27 October 2012; revised: 20 February 2013; accepted: 28 February 2013. Available online: 17 April 2013.

Abstract: Tannic acid ($C_{76}H_{52}O_{46}$) has been found to be an efficient catalyst for one-pot synthesis of 2,4,5-triaryl substituted imidazoles by the reaction of an arylaldehyde, benzyl/benzoin and an ammonium acetate. The short reaction time and excellent yields making this protocol practical and economically attractive.

Keywords: ammonium acetate; benzyl; benzoin; imidazoles

1. INTRODUCTION

The steady growth in interest in heterocyclic compounds is basically connected with their raised biological activity and also with the fact that they enable the development of novel materials with unique properties. One very interesting and promising class of heterocycles is the triarylimidazole moiety due to both their use in medicinal chemistry as synthetic building block, and plays important role in biochemical process [1]. Imidazole ring system is one of the most important substructures found both in a large number of natural products and synthetic drugs along with the wide spectrum of physiological activities displayed by these compounds. For example, the antiulcerative agent cimetidine [2], the proton pump inhibitor omeprazole [3] and the benzodiazepine antagonist flumazenil [4] are Imidazole derivatives. In addition, the substituted imidazole ring systems are substantially used in the synthesis of some ionic liquids [5, 6], that have been given a new approach to 'Green Chemistry'. They are also used in photography as photosensitive compounds [7]. Hence, synthesis of the imidazole moiety has received extensive attention from several researcher groups [8-25].

Due to their great importance, many synthetic strategies have been developed. In 1882, Radziszewski and Japp reported the first synthesis of the imidazole from 1,2-dicarbonyl compound, various aldehydes and ammonia, to obtain the 2,4,5-triphenylimidazoles [8, 9]. Also, Grimmett et al. proposed the synthesis of the imidazole using nitriles and esters [10]. Recently, there are several methods reported in the literature for the synthesis of 2,4,5-triaryl-1*H*-imidazoles from benzyl/benzoin, aldehydes and ammonium acetate using different catalyst such as HY/silica gel [11], acidic Al_2O_3 [12], AcOH [13], $ZrCl_4$ [14], ionic liquid [15], iodine [16], NH_4OAc [17], $Yb(OTf)_3$ [18], $NiCl_2.6H_2O$ [19], sodium bisulfate [20], PEG-400 [21], boric acid [22], CAN [23] Fe_3O_4 nanoparticle [24] and poly(AMPS-co-AA) [25]. However, most of the reported methodologies still have certain limitations such as expensive catalysts, toxicity of solvents, restrictions for large scale applications, critical product isolation procedures, difficulty in recovery of high boiling solvents, excessive amounts of catalysts and generation of large amounts of toxic wastes in scaling up for industrial applications leading to environmental issues. Thus, the development of a simple and efficient method for the synthesis of 2,4,5-triaryl-1*H*-imidazole derivatives would be highly desirable.

The art of performing efficient chemical transformation coupling three or more components in a single operation by a catalytic process avoiding

* Corresponding author. E-mail: nvshitole@gmail.com

stoichiometric toxic reagents, large amounts of solvents and expensive purification techniques represents a fundamental target of the modern organic synthesis [26].

2. MATERIAL AND METHODS

Melting points were determined in an open capillary tube and are uncorrected. IR spectra were recorded in KBr on a Perkin-Elmer spectrometer. 1HNMR spectra were recorded on a Gemini 300-MHz instrument in CDCl3 as solvent and TMS as an internal standard. The purity of products was checked by thin-layer chromatography (TLC) on silica-gel.

2.1. Typical Procedure for the Synthesis of 2,4,5-Triaryl-1H-Imidazole 4(a-l)

A mixture of an aromatic aldehyde (1 mmol), benzil/benzoin (1mmol), ammonium acetate (2 mmol) and tannic acid (7.5 mol%) in ethanol (15 mL) was stirred at reflux temperature for 3-8 h. The progress of the reaction was monitored by TLC. After completion of reaction conversion, the reaction mixture was cooled to room temperature and poured on crushed ice. The obtained crude solid product was filtered, dried and crystallized from ethanol to get the corresponding 2,4,5-triaryl-1*H*-imidazoles **4(a-l).**

2.2. Spectroscopic data of synthesized some principal compounds

2,4,5-triphenyl-1H-imidazole (4a): IR (KBr, cm^{-1}): 3049, 1470, 1442, 1120, 698. ^{1}H-NMR (400 MHz, DMSO-d6, δ ppm): 12.62 (brs, 1H, NH), 8.12 (d, 2H, J = 7.6 Hz, Ar-H), 7.30–7.42 (m, 13H, Ar-H). MS (EI): m/z (%) = 296 (46) [M+]. Anal. calcd. for $C_{21}H_{16}N_2$: C, 85.11; H, 5.44; N, 9.45. Found: C, 85.02; H, 5.42; N, 9.42.

2-(2-chlorophenyl)-4,5-diphenyl-1H-imidazole (4b): IR (KBr, cm^{-1}): 3421, 3046, 1620, 1512, 1500. ^{1}H-NMR (400 MHz, DMSO-d6, δ ppm): 12.38 (brs, 1H, NH), 7.11–7.39 (m, 14H, Ar-H). MS (EI): m/z (%) = 330 (36), 332 (12) [M+]. Anal. calcd. for $C_{21}H_{15}ClN_2$: C, 76.24; H, 4.57; N, 8.47. Found: C, 76.20; H, 4.55; N, 8.51.

2-(4-chlorophenyl)-4,5-diphenyl-1H-imidazole (4c): IR (KBr, cm^{-1}): 3052, 1626, 1451, 1076, 761, 692. ^{1}H-NMR (400 MHz, DMSO-d6, δ ppm): 12.71 (brs, 1H, NH), 8.09 (d, 2H, J = 8.4 Hz, Ar-H), 7.21–7.50 (m, 12H, Ar-H). MS (EI): m/z (%) = 330 (36), 332 (12) [M+]. Anal. calcd. for $C_{21}H_{15}ClN_2$: C, 76.24; H, 4.57; N, 8.47. Found: C, 76.25; H, 4.45; N, 8.52.

2-(4-methoxyphenyl)-4,5-diphenyl-1H-imidazole (4e): IR (KBr, cm^{-1}): 3030, 1612, 1492, 1250, 1032, 695. ^{1}H-NMR (400 MHz, DMSO-d6, δ ppm): 12.51 (brs, 1H, NH), 8.11 (d, 2H, J = 8.0 Hz, Ar H), 7.52 (d, 4H, J = 6.8 Hz, ArH), 7.13–7.23 (m, 6H, Ar H), 7.05 (d, 2H, J = 7.6 Hz, Ar H), 3.71 (s, 3H, CH3). MS (EI): m/z (%) = 326 (36) [M+]. Anal. calcd. for $C_{22}H_{18}N_2O$: C, 80.96; H, 5.56; N, 8.58. Found: C, 80.90; H, 5.51; N, 8.53.

4-(4,5-diphenyl-1H-imidazol-2-yl)phenol (4i): IR (KBr, cm^{-1}): 3267, 3046,1698, 1600, 1491, 686. ^{1}H-NMR (400 MHz, DMSO-d6, δ ppm): 12.38 (s, 1H, NH), 9.61 (s, 1H, OH), 7.87 (d, 2H, J = 8.4 Hz, Ar-H), 7.54 (d, 2H, J = 7.6 Hz, Ar-H), 7.49 (d, 2H, J= 7.2 Hz, Ar-H), 7.42 (t, 2H, J = 7.6 Hz, Ar-H), 7.35 (t, 1H, J= 7.6 Hz, Ar-H), 7.29 (t, 2H, J = 7.6 Hz, Ar H), 7.21 (t, 1H, J = 7.2 Hz, Ar H), 6.85 (d, 2H, J = 8.4 Hz, Ar H). MS (EI): m/z (%) = 312 (40) [M+]. Anal. calcd. for $C_{21}H_{16}N_2O$: C, 80.75; H, 5.16; N, 8.97. Found: C, 80.71; H, 5.08; N, 8.91.

2-(4-fluorophenyl)-4,5-diphenyl-1H-imidazole (4j): IR (KBr, cm^{-1}): 3021, 1490, 1221, 827, 755, 685. ^{1}H-NMR (400 MHz, DMSO-d6, δ ppm): 12.71 (brs, 1H, NH), 8.13 (d, 2H, J = 4.2 Hz, Ar-H), 7.57 (d, 4H, J = 5.6 Hz, Ar-H), 7.21–7.34 (m, 8H, ArH). MS (EI): m/z (%) = 314 (44) [M+]. Anal. calcd. for $C_{21}H_{15}FN_2$: C, 80.24;H, 4.81; N, 8.91. Found: C, 80.27; H, 4.74; N, 8.87.

3. RESULTS AND DISCUSSION

As part of our ongoing investigation in developing a versatile and efficient method for synthesis of heterocyclic compounds [27], we report here an efficient synthetic method for the synthesis of 2,4,5-triarylimidazoles from benzyl/benzoin, aldehydes and ammonium acetate in the presence of tannic acid (Scheme 1).

We initially studied the reaction of benzaldehyde (**2a**) as a representative aldehyde, compound **1** and ammonium acetate (**3**) in the presence of tannic acid was considered as a standard model reaction for the optimization of reaction condition.

To evaluate the effect of solvent, we have screened different solvents such as dichloromethane, tetrahydrofuran, acetonitrile, chloroform, dioxane methanol and ethanol at reflux temperature. Ethanol

stood out as the solvent of choice among the solvents tested because of the rapid conversion and excellent 90% yield of desired product, whereas the product formed in lower yields (20-82%) by using other solvents (Table1).

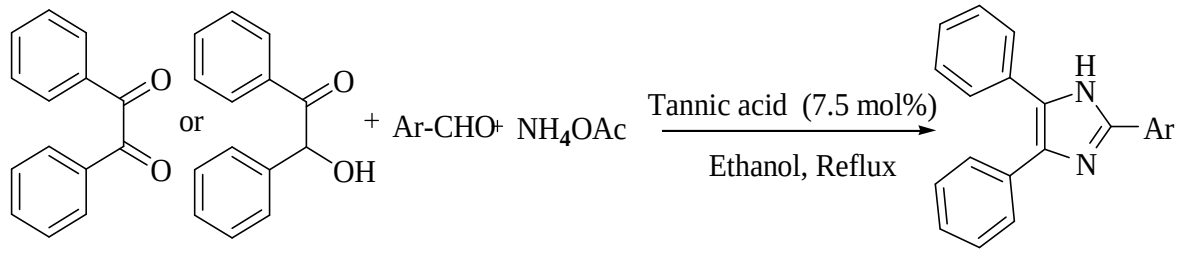

1 **2(a-k)** **3** **4(a-k)**

Scheme1. Synthesis of 2,4,5-Triaryl-1*H*-Imidazole.

Table 1. Screening of solvents[a]

Entry	Solvent	Yield[b] (%)
1	Dioxane	20
2	Acetonitrile	43
3	Tetrahydrofuran	49
4	Dichloromethane	54
5	Chloroform	67
6	Methanol	82
7	Ethanol	90

[a]Reaction conditions: 1 (1 mmol), **2a** (1 mmol), **3** (2 mmol), tannic acid (7.5 mol %) at reflux temperature. [b]Isolated yields.

To determine the exact concentration of catalyst, we have investigated the model reaction at 2.5, 5, 7.5 and 10 mol% of tannic acid in ethanol at reflux temperature. The product was obtained in 62, 80, 90 and 90 % of yield respectively. This indicates that the use of just 7.5 mol% of tannic acid is sufficient to push the reaction forward (Table 2).

The catalyst plays a crucial role in the success of the reaction in terms of the rate and the yield of product. To study the generality of this process various examples were illustrated for the synthesis of 2,4,5-triaryl imidazoles and these results are summarized in Table 3. The reaction is compatible with various substituents such as -CH_3, -OCH_3, -OH, -$N(CH_3)_2$, -Cl, -F. This method is also effective for heteroaromatic aldehydes which form their corresponding 2,4,5-triarylimidazole derivatives in 85-92% of yields (Table 3). The formation of desired product was confirmed by ^{1}H-NMR, IR and mass spectroscopic analysis technique. Also the melting points recorded and compared with the corresponding literature data.

Table2. Effect of concentration[a]

Entry	Solvent	Yield[b] (%)
1	2.5	62
2	5	80
3	7.5	90
4	10	90

[a]Reaction conditions: 1 (1 mmol), **2a** (1 mmol), **3** (2 mmol) in ethanol at reflux temperature. [b]Isolated yields.

4. CONCLUSION

In conclusion, this paper describes a convenient and efficient process for the synthesis of 2,4,5-Triaryl-1*H*-Imidazole derivatives by use of Tannic acid as catalyst at reflux temperature. Present

methodology offers very attractive features such as simple experimental procedure, higher yields and economic viability, when compared with conventional method.

Table 3: Tannic acid catalyzed synthesis of 2,4, 5, triaryl substituted imidazoles.

Compound	Ar-	Time (h)		Yield (%)[b]		M.P. (°C)
		Benzil	Benzoin	Benzil	Benzoin	
4a	C_6H_5	4	6	90	89	274-276
4b	2-ClC_6H_4	4.5	6.5	91	88	195-196
4c	4-ClC_6H_4	5	6	93	90	258-260
4d	4-$CH_3C_6H_4$	5.5	7	91	87	230-232
4e	4-$OCH_3C_6H_4$	4.5	6	89	85	227-228
4f	4-OH,3-$OCH_3C_6H_4$	5	5.5	91	90	220-221
4g	4-$NO_2C_6H_4$	5.5	7.5	92	88	230-232
4h	4$(CH_3)_2NC_6H_4$	4.5	5	91	89	257-258
4i	4-OHC_6H_4	5	6.5	90	92	268-269
4j	4-FC_6H_4	3.5	4.5	92	90	190-191
4k	C_4H_3O	5	6.5	92	90	199-200
4l	C_4H_3S	5.5	7.5	90	87	259-260

[a]Reaction conditions: **1** (4-$NO_2C_6H_4$ 1 mmol), **2a-l** (1 mmol), **3** (2 mmol), tannic acid (7.5 mol%) in ethanol at reflux temperature. [b]Isolated yields.

5. ACKNOWLEDGMENTS

We are grateful to the Head Department of Chemistry, Dr Babasaheb Ambedkar Marathwada University, Aurangabad-431 004 (MS), India for providing the laboratory facility.

6. REFERENCES AND NOTES

[1] Lambardino, J. G.; Wiseman, E. H. *J. Med.Chem.* **1974**, *17*, 1182. [CrossRef]

[2] Brimblecombe, R. W.; Duncan, W. A. M.; Durant, G. J.; Emmett, J. C.; Ganellin, C. R.; Parons, M. E. *J. Int. Med. Res*. **1975**, *3*, 86.

[3] Tanigawara, Y.; Aoyama, N.; Kita, T.; Shirakawa, K.; Komada, F.; Kasuga, M. K. *Clin. Pharmacol. Ther*. **1999**, *66*, 528. [CrossRef]

[4] Hunkeler, W.; Mohler, H.; Pieri, L.; Polc, P.; Bonetti, E. P.; Cumin, R.; Schaffner, R.; Haefely, W. *Nature* **1981**, *290*, 514. [CrossRef]

[5] Wasserscheid, P.; Keim, W. *Angew. Chem. Int. Ed. Eng*. **2000**, *39*, 37872. [CrossRef]

[6] Bourissou, D., Guerret, O., Ggabbai, F. T., Bertrand, G. *Chem. Rev*. **2000**, 100.

[7] Satoru, I.; Jap. Pat. **1989**, 01117, 867, *Chem. Abstr*. **1989**, *111*, 214482.

[8] Radziszewski, B. *Chem. Ber*. **1882**, *15*, 1493. [CrossRef]

[9] Japp, F. R.; Robinson, H. H. *Chem. Ber*. **1882**, *15*, 1268. [CrossRef]

[10] Grimmett, M. R.; Katritzky, A. R.; Rees, C. W.; Scriven, E. F. V. Pergamon: NewYork, 1996.

[11] Balalaie, S.; Arabanian, A.; Hashtroudi, M. S.; *Mont. Fur. Chem*. **2000**, *131*, 945. [CrossRef]

[12] Usyatinsky, A. Y., Khmelnitsky, Y. L. *Tetrahedron Lett*. **2000**, *41*, 5031. [CrossRef]

[13] Wolkenberg, S. E.; Winoski, D. D.; Leister, W. H.; Wang, Y.; Zhao, Z.; Lindsley, C. W. *Org. Lett*. **2004**, *61*, 453.

[14] Sharma, G. V. M.; Jyothi, Y.; Lakshmi, P. S. *Syn. Commun*. **2006**, *36*, 2991. [CrossRef]

[15] Siddiqui, S. A.; Narkhede, U. C.; Palimkar, S. S.;

Daniel, T.; Lahoti, R. J.; Srinivasan, K. V. *Tetrahedron* **2005**, *61*, 3539. [CrossRef]

[16] Kidwai, M.; Mothsra, P.; Bansal, V.; Goyal, R. *Mont. Fur. Chem*. **2006**, *137*, 1189. [CrossRef]

[17] Kidwai, M.; Saxena, S.; Ruby, Rastogi, S. *Bull. Korean Chem. Soc*. **2005**, *26*, 2051.

[18] Wang, L. M.; Wang, Y. H.; Tian, H.; Yao, Y. F.; Shao, J. H.; Liu, B. *J. Fluorine Chem*. **2006**, *127*, 1570. [CrossRef]

[19] Heravi, M. M.; Bakhtiari, K.; Oskooie, H. A.; Taheri, S. J. Mol. Cata. A: Chem. **2007**, *263*, 279. [CrossRef]

[20] Sangshetti, J. N.; Kokare, N. D.; Kothakar, S. A.; Shinde, D. B.; *Mont. Fur. Chem.* **2008**, *139*, 125. [CrossRef]

[21] Wang, X. C.; Gong, H. P.; Quan, Z. J.; Li, L.; Ye, H. L. *Chin. Chem. Lett*. **2009**, *20*, 44. [CrossRef]

[22] Shelke, K. F.; Sapakal, S. B.; Sonar, S. S.; Madje, B. R.; Shingate, B. B.; Shingare, M. S. *Bull Korean Chem. Soc*. **2009**, *30*, 1057. [CrossRef]

[23] Sangshetti, J. N., Kakare, N. D.; Kotharkar, S. A.; Shinde, D. B. *J. Chem. Sci*. **2008**, *120*, 463. [CrossRef]

[24] Karami, B.; Eskandari, K.; Ghasemi, A. *Turk. J. Chem*. **2012**, *36*, 601.

[25] Mohammadi, A.; Keshvri, H.; Sandaroos, R.; Roushi, H.; Sepehr, Z. *J. Chem. Sci*. **2012**, *124*, 717. [CrossRef]

[26] Mizuno, N.; Misono, M. *Chem. Rev*. **1998**, *98*, 199. [CrossRef]

[27] Sturmer, J. W.; Pharmaceutical Toxicity." The Pharmaceutical Era. Vol 21. New York: D.O. Haynes & Co., 1899.

[28] Halkens, S. B. A. "The use of tannic acid in the local treatment of burn wounds: intriguing old and new perspectives." *Wounds* **2001**, *13*, 144.

[29] Hangarge, R. V.; Jarikote, D. V.; Shingare, M. S. *Green Chem*. **2002**, *4*, 266. [CrossRef]; (b) Madje, B. R.; Shindalkar, S. S.; Ware, M. N.; Shingare, M. S. *Arkivoc* **2005**, *14*, 82. [CrossRef]; (c) Sadaphal, S. A.; Shelke, K. F.; S. S. Sonar,; Shingare, M. S. *Central. Euro. J. Chem*. **2008**, *6*, 622; (d) Diwakar, S. D.; Bhagwat, S. S.; Shingare, M. S.; Gill, C. H. *Bioorg. Med. Chem. Lett*. **2008**, *18*, 4678. [CrossRef][PubMed]; (e) Sapkal, S. B.; Shelke, K. F.; Shingare, M. S.; *Tetrahedron Lett*. **2009,** *50*, 1754. [CrossRef]

Orbital: The Electronic Journal of Chemistry
journal homepage: www.orbital.ufms.br
ISSN 1984-6428

| Vol 5 | | No. 1 | | January-March 2013 |

Full Paper

Desenvolvimento de Metodologia Eletroquímica para Degradação da Ciprofloxacina por Agentes Oxidantes Gerados *in situ*

Jaime Rodrigues da Silva[a], Renê H. Tavares dos Santos[a], Luciano E. Fraga[a], Carmem L. de Paiva e Silva Zanta[b], Carlos Alexandre B. Garcia[a], Maria de Lara P. M. Arguelho*[a]

[a]*Departamento de Química, Universidade Federal de Sergipe, São Cristóvão – SE – Brasil.*
[b]*Departamento de Química, Universidade Federal de Alagoas, Maceió – AL – Brasil.*

Article history: Received: 23 December 2012; revised: 13 March 2013; accepted: 18 March 2013. Available online: 17 April 2013.

Abstract: Ciprofloxacin is second generation quinolones flour, which is very soluble in water. This drug can be found in Sewage Treatment Plants (STPs) and natural waters at concentrations of μg L^{-1} and ng L^{-1}. Electrolysis was carried out using Ag/AgCl as reference electrode and as cathode and anode plates of Ti/TiO_2 were used. To study the role of supporting electrolyte were used H_2SO_4, HCl, NaCl, $NaNO_3$, KCl, and Na_2SO_4. Were applied current densities (DC) between 20 and 160 $mA.cm^{-2}$. The electrodic process indicates be dependent on pH and ionic strength. Through electrolysis, the degradation /mineralization occurs more easily in the presence of Cl^-.

Keywords: electrodegradation; ciprofloxacin; dimensionally stable anodes

1. INTRODUÇÃO

A ciprofloxacina é um fármaco classificado quimicamente como uma fluorquinolona (Figura 1), sendo bastante solúvel em água e praticamente insolúvel em acetona [1-5]. A aprovação de sua comercialização foi concedida pela Agência de Regulamentação de Drogas e Alimentos dos EUA (FDA - U. S. Food and Drug Administration) no final da década de 80. Sintetizada em 1983 pela Bayer alemã, foi introduzida com o nome de "BAY 09867" mostrando-se ser de 4 a 8 vezes mais ativa que demais antibióticos, principalmente contra enterobactérias e pseudômonas. É considerada um antibiótico de amplo espectro de ação, agindo rapidamente tanto nas fases proliferativas quanto nas fases germinativas, contra patógenos gram-positivos e gram-negativos, através de um mecanismo de ação fundamentado na inibição das enzimas topoisomerase IV e DNA-girase, sendo esta última essencial na replicação, transcrição e reparação do DNA bacteriano [6-9].

Inicialmente utilizada apenas para fins veterinários, a ciprofloxacina tem sido estrategicamente utilizada no combate a ataque terrorista sendo, atualmente, a única droga aprovada pela FDA para tratamento após exposição ao antraz inalado. Além disso, tem sido recomendada como fármaco de primeira linha na quimioterapia da tuberculose, no tratamento de infecções do trato urinário e de doenças sexualmente transmissíveis (DSTs) [10-12].

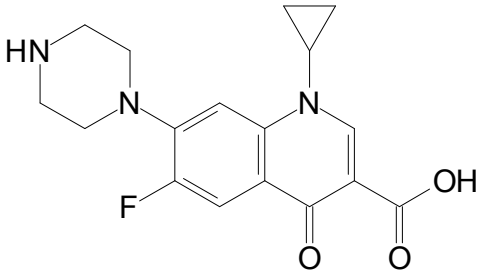

Figura 1. Estrutura da Ciprofloxacina.

Devido a essas razões, a ciprofloxacina é um dos fármacos mais amplamente prescrito no mundo. O monitoramento ambiental de sua forma original e de seus metabólitos despertou o interesse da comunidade científica, visto que, uma parte significativa da dosagem ingerida é excretada pelo organismo humano sem alteração, aportada para o

* Corresponding author. E-mail: larapalm@yahoo.com

meio ambiente através do esgoto in natura, podendo ser encontrada em Estações de Tratamento de Esgoto (ETEs) e águas naturais em concentrações da ordem do μg L^{-1} e do ng L^{-1}. Além disso, os processos convencionais de tratamento de água realizados nas estações de tratamento de água do Brasil não são suficientemente eficazes para a sua completa remoção por tratar-se de um poluente orgânico polar e de baixo peso molecular [13-17].

No Brasil, as leis que estabelecem os parâmetros físico-químicos para o padrão de potabilidade da água não contemplam poluentes emergentes, tais como fármacos e produtos de higiene pessoal. Atualmente, a resolução RDC 44, de 26/10/2010, da Agência Nacional de Vigilância Sanitária (ANVISA), apenas restringiu a prescrição e venda de antibióticos, com a exigência de retenção e validade nas receitas no âmbito nacional [18-20]. Entretanto, números indiretos, como por exemplo, a importação da China e da Índia de 71 milhões de dólares em medicamentos entre 2002 e 2007, fortalece a hipótese da contaminação emergente [21-22]. A falta de legislação específica e o descarte de efluente doméstico in natura podem resultar em alta toxicidade para o meio ambiente [23], sendo uma das consequências da contaminação a longo prazo, o aumento gradual da resistência bacteriana em função da seleção de cepas resistentes. Apesar disso, existem poucas informações sobre o destino dos fármacos no meio ambiente e sua interação com o meio [24-27].

A ciprofloxacina é uma quinolona, um composto polar e não volátil que no meio ambiente reage através de mecanismos pouco conhecidos. Possui estrutura química complexa, onde os grupos funcionais ácido carboxílico, amina (secundária e terciária), cetona e haleto orgânico estão envolvidos na elevada atividade química e biológica. Com valores de pKa iguais a 6,2 e 8,8 é encontrada permeando o solo, podendo ser carreada para águas subterrâneas até atingir os rios [28, 29], o que mesmo em níveis baixos, podem causar mudanças genéticas com impactos negativos sobre a fauna e a flora [30-33].

A degradação química como mecanismo de remediação ambiental tem sido amplamente empregada no estudo da remoção de corantes, por exemplo, via ação de agentes oxidantes (reações de Fenton) ou via eletrodegradação. Na oxidação eletroquímica de forma direta, o substrato é oxidado na superfície do eletrodo necessitando de um alto sobrepotencial para o desprendimento de oxigênio. A primeira etapa envolve a oxidação de moléculas de água sobre a superfície do eletrodo (MOx) [34-35].

$$MOx + H_2O \rightarrow MOx[\bullet OH] + H^+ + e^- \quad (1)$$

Posteriormente, os radicais hidroxila (•OH) interagem com o oxigênio presente no ânodo formando um óxido superior de acordo com a equação 2:

$$MOx[\bullet OH] \rightarrow MOx[O] + H^+ + e^- \quad (2)$$

Então, o óxido superior formado oxida os compostos orgânicos (R) sem promover a sua total mineralização (equação 3):

$$MOx[O] + R \rightarrow RO + MOx \quad (3)$$

Além disso, também é possível que os radicais hidroxila eletrogerados oxidem os compostos orgânicos a dióxido de carbono e água, como indicado na equação 4:

$$MOx[\bullet OH] + R \rightarrow MOx + mCO_2 + nH_2O + H^+ \quad (4)$$

Na oxidação eletroquímica indireta, espécies catalíticas de elevado poder oxidante são geradas *in situ*. O cloreto de sódio (NaCl) é um sal usado frequentemente no tratamento de efluentes aquosos como eletrólito suporte, devido a formação de gás cloro (Cl_2) e consequentemente, das espécies como OCl^- e/ou $HOCl^-$ [31]. A formação do cloro (Cl_2), pela eletrólise do NaCl aquoso, pode ser indicado nas equações 5 e 6:

$$\text{ânodo: } 2Cl^- \rightarrow Cl_2 + 2e^- \quad (5)$$

$$\text{cátodo: } 2H_2O + 2e^- \rightarrow H_2 + 2OH^- \quad (6)$$

Na produção do ânion hipoclorito (ClO^-), o Cl_2 gerado no ânodo reage com o hidróxido formado no cátodo (equação 7):

$$Cl_2 + 2OH^- \rightarrow H_2O + ClO^- + Cl^- \quad (7)$$

Eletrodos onde ocorre oxidação de compostos orgânicos, sem a completa mineralização, são chamados de eletrodos ativos para o desprendimento de oxigênio, como por exemplo, o eletrodo $Ti/TiRuO_2$. Esses ânodos dimensionalmente estáveis (ADE) são constituídos de um suporte metálico, como o titânio, onde por decomposição térmica, deposita-se uma mistura de óxidos formados por metais nobres, como o rutênio. Os óxidos industriais mais comuns são formados por RuO_2 e TiO_2 ($Ti/Ru_{0,3}Ti_{0,7}O_2$), onde o rutênio é o agente catalítico e o titânio permite a estabilidade mecânica. Apresentam alta estabilidade eletroquímica, forte poder catalítico, boa seletividade e resistência mecânica a altos valores de sobrepotencial.

Pela oxidação eletroquímica de compostos orgânicos, a reação anódica, que ocorre através de vários mecanismos diferentes, tende a formar produtos menos tóxicos à saúde humana e menos agressivos ao meio ambiente e com maior grau de biodegradabilidade. A técnica eletroquímica apresenta como vantagens a versatilidade, onde o mesmo reator pode ser usado para diferentes reações químicas; a compatibilidade, pelo fato do elétron ser um reagente de liberação controlada, bem como a possibilidade de automação de todo o processo, no qual, os poluentes de baixa massa molar, como a maioria dos fármacos, são rapidamente degradados [36].

A eletrodegradação de fármacos presentes em águas de abastecimento público representa um passo importante para o aprimoramento dos métodos de tratamento de água. Neste sentido, este estudo visa desenvolver uma metodologia eletroquímica para degradação da ciprofloxacina em água de abastecimento público através da produção *in situ* de agentes oxidantes.

2. MATERIAL E MÉTODOS

2.1. Reagentes e soluções

As soluções tampão empregadas no estudo do efeito do pH foram preparadas segundo Britton & Robinson, pelo uso de uma solução ácida contendo 0,04 mol L^{-1} de CH_3CO_2H, 0,04 mol L^{-1} de H_3BO_3 e 0,04 mol L^{-1} de H_3PO_4 e de volumes apropriados de uma solução básica contendo 0,2 mol L^{-1} de NaOH. O pH final de cada mistura, no intervalo de 2 a 12, foi medido com pHmetro Analion, modelo PM 608, calibrado com tampão universal nos valores de pH iguais a 4, 7 e 10. Todos os reagentes empregados foram de grau analítico. As soluções aquosas de cloridrato de ciprofloxacina (Biofarma; MM = 331,35 g mol^{-1}) foram preparadas diariamente na concentração de 1 10^{-4} mol L^{-1}.

2.2. Instrumentação

As eletrólises a corrente constante foram realizadas pelo uso de um potenciostato/galvanostato AutoLab PGTSTAT-30 (Ecochemie), conectado a um microcomputador e controlado pelo software GPES versão 4.8. Uma célula eletroquímica com capacidade para 250 mL de solução foi adaptada para inserção dos eletrodos. Um eletrodo de Ag/AgCl foi utilizado como eletrodo de referência e dois eletrodos de rede de titânio recobertos com óxidos ($Ti/Ru_{0,34}$ e $Ti_{0,66}O_2$), nas dimensões de 4,0 x 4,0 cm foram empregados como cátodo e ânodo.

Nas medidas espectrofotométricas realizadas durante as eletrólises foi empregado um espectrofotômetro da marca Biochrom, modelo Libra S12 e uma célula de quartzo com comprimento de caminho ótico de 1,0 cm.

2.3. Metodologia

Nos estudos de otimização do processo eletrolítico foram realizadas eletrólises na presença de diferentes eletrólitos suporte (H_2SO_4, HCl, NaCl, $NaNO_3$, KCl e Na_2SO_4), no intuito de reconhecer a influência positiva de cátions e ânions na eletrodegradação da ciprofloxacina, mantendo-se constante a intensidade de corrente e a concentração do fármaco, em todos os experimentos. Avaliou-se também o efeito da força iônica pela variação da concentração do eletrólito suporte entre 0,1 e 0,0001 mol L^{-1}. A influência do pH foi avaliada pelo uso de soluções tamponadas na escala de valores entre 2 e 12 em intensidade de corrente constante.

Depois de estabelecidas as condições do meio reacional foi realizada a otimização da corrente aplicada. Os eletrodos de Ânodos Dimensionalmente Estáveis foram submetidos a correntes entre 20 e 160 mA. O monitoramento das amostras tratadas, através de alíquotas retiradas da célula eletroquímica em tempos controlados de 5 minutos, foi realizado através de medidas espectrofotométricas na faixa de 0 a 800 nm.

Para quantificação espectrofotmétrica da ciprofloxacina, uma curva analítica foi obtida através do método de adição de padrão, sendo que cada medida foi realizada em triplicata e as curvas analíticas obtidas a partir de 6 adições. As medidas foram realizadas seguindo procedimento analítico sugerido pelo INMETRO [30].

As amostras de água do rio Poxim, um dos rios que compõe a malha hídrica de Aracaju-SE, foram coletadas na estação de captação próxima a Universidade Federal de Sergipe. Ao todo, três amostras foram utilizadas. Devido à baixa condutividade das amostras de água de rio, adicionou-se ao volume de 250 mL quantidades adequadas de sais ou ácidos, conforme valores estabelecidos no estudo da influência da força iônica.

3. RESULTADOS E DISCUSSÃO

3.1. Espectrofotometria

Para identificar e monitorar a variação da concentração da ciprofloxacina foi obtido um espectro de absorção na região do UV-Vis (200-800 nm), possibilitando identificar suas bandas de máxima absorção. Recentemente, foram descritos dois métodos espectrofotométricos, o primeiro utilizando sistema FIA (análise por injeção em fluxo) e o segundo a espectrofotometria em fase sólida para a determinação da ciprofloxacina [45, 46].

A ciprofloxacina em solução aquosa apresenta dois picos de absorção em bandas completamente distintas e com máximos em 270 nm e 315 nm. De acordo com a literatura, a absorção da radiação eletromagnética na região do ultravioleta e visível (UV-Vis) é característica de moléculas que sofrem transições eletrônicas nos orbitais de baixa energia [37, 38]. O espectro no UV-vis da ciprofloxacina (Figura 2) apresenta duas bandas de absorção referentes aos grupos cromóforos presentes na molécula, uma amina e um grupo carboxílico [11, 16, 20].

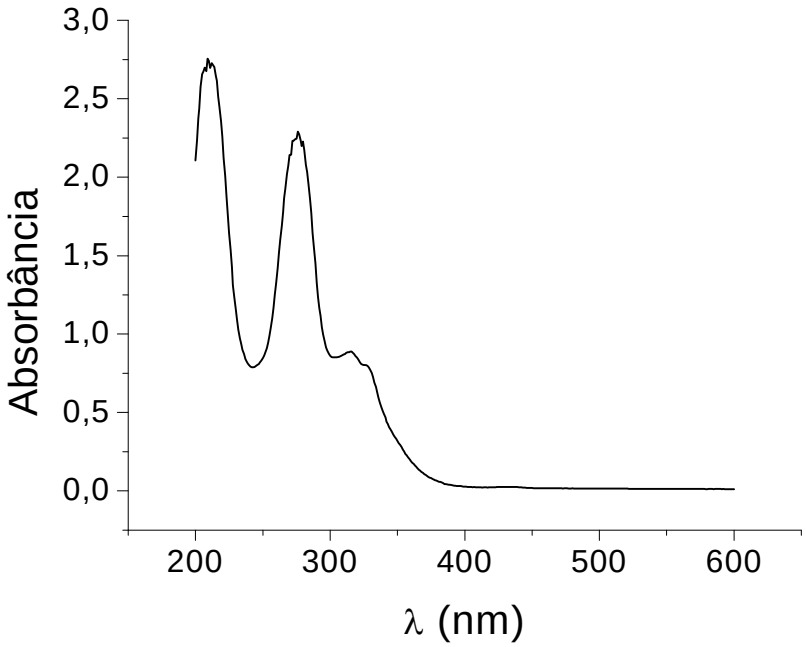

Figura 2. Espectro de absorção molecular da ciprofloxacina em tampão pH 2,0 a 10^{-1} mol L^{-1}.

3.2. Estudo analítico

A curva analítica resultante do comportamento do sinal analítico da ciprofloxacina em função da concentração pode ser representada pela equação i = 7,4 10^{-2} + 9,2 10^{4}[cipro], sendo que o valor de correlação linear indica forte associação entre as variáveis com r = 0,9928 (n=7).

O desvio padrão encontrado foi de 0,09 e a faixa linear esteve entre 3,0 10^{-6} e 2,0 10^{-5} mol L^{-1}. O limite de detecção foi de 3,0 10^{-6} mol L^{-1}, que corresponde a menor quantidade de ciprofloxacina presente em uma amostra e que pode ser detectada, porém não necessariamente quantificada, sob as condições experimentais estabelecidas (INMETRO, 2010). Para o limite de quantificação, obteve-se um valor de 9,6 10^{-6} mol L^{-1}, o qual corresponde ao menor nível determinável com precisão e exatidão aceitáveis.

3.3. Comportamento eletródico

A Figura 3 apresenta o voltamograma cíclico típico da ciprofloxacina, no qual é possível observar a presença de um processo de oxidação irreversível em 0,8 V vs Ag/AgCl em eletrodo de carbono vítreo. Assim como em outros sistemas eletroquímicos, o processo eletródico é dependente da natureza química da espécie eletroativa, do meio reacional e da composição da superfície do eletrodo. Estas variáveis são as principais responsáveis pelas diferenças de comportamento eletródico.

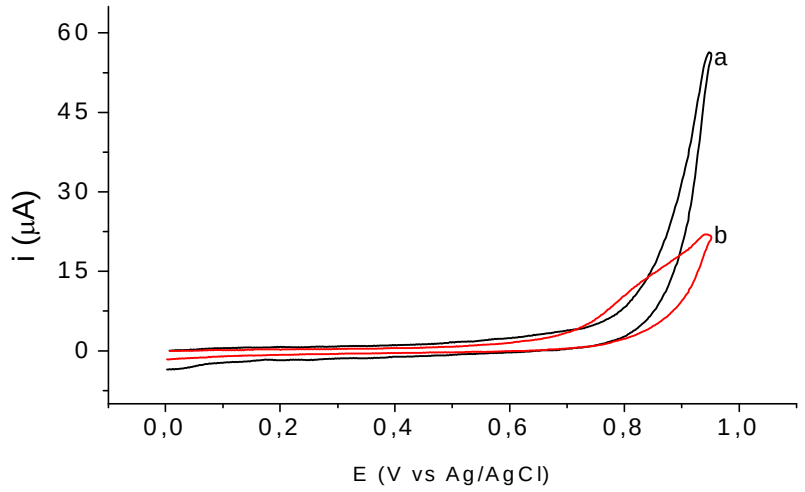

Figura 3. Voltamogramas cíclicos em eletrodo de carbono vítreo. a) somente HCl 0,1 mol L^{-1}, b) ciprofloxacina 1,0 10^{-4} mol L^{-1}. pH = 2,0 e ν = 80 mVs^{-1}.

3.3. Tipo de eletrólito

Um eletrólito é um composto que ao ser dissolvido num dado solvente, produz uma solução com uma condutividade elétrica maior que a do solvente puro. A escolha do eletrólito adequada a um sistema eletroquímico tem sido considerada uma etapa fundamental na otimização da cinética eletroquímica e das propriedades elétricas da solução. Apesar de serem escassas as informações a respeito, algumas abordagens termodinâmicas podem ser deduzidas através do estudo do tipo de eletrólito. Considerando a água como solvente, os eletrólitos suporte testados foram os sais: NaCl, KCl, $NaNO_3$ e Na_2SO_4 e os ácidos HCl e H_2SO_4. Nos sistemas eletroquímicos o eletrólito suporte é adicionado em altas concentrações onde confere à solução e à interface metal-solução uma série de propriedades, como por exemplo, a força iônica.

A ciprofloxacina em solução de Na_2SO_4 apresentou baixa solubilidade, não tendo sido analisado o seu comportamento eletródico neste meio. Já nos estudos com HCl, NaCl e KCl foi observado 100% de remoção da cor amarelada, característica da reação da ciprofloxacina com o Cl^- e da posterior formação de íons hipoclorito (ClO^-) gerados eletroquimicamente. Segundo a literatura, o cloro pode ser representado nas três formas (cloro/Cl_2, ácido hipocloroso/HClO e íons hipoclorito/ClO^-). O comportamento de eletrólitos contendo cloreto, nos processos de oxidação, é bem conhecido, sendo que sua eficácia, se deve em parte a adsorção do íon cloreto na superfície do eletrodo, este fenômeno afeta a cinética do processo e as características dos produtos de oxidação.

O efeito do eletrólito suporte sobre a reação H^+/H_2 vem sendo estudado por diversos autores [39, 40], sendo o equilíbrio entre as formas, dependente do pH do meio e da temperatura. Em temperaturas ambientes e para 1,0 10^{-3} mol L^{-1} de cloro/$Cl_{2(aq)}$, o ácido hipocloroso/HClO tem importante contribuição em condições muito ácidas sendo a espécie predominante nesse meio. Os eletrólitos de HCl e NaCl apresentaram o melhor desempenho em valores de pH 2 e 4 (Figura 4), o que pode ser observado pela maior variação da absorbância indicando maior degradação da ciprofloxacina.

3.4. Efeito de pH

A natureza do eletrólito e o pH apresentam grande influência na velocidade do processo de degradação. O controle de pH tem sido um dos fatores determinantes do grau de desinfecção quando associado a concentração de cloro livre. Isto se deve a capacidade de desinfecção do ácido hipocloroso/HClO que costuma ser 80 a 100 vezes maior do que a do íon hipoclorito/ClO^- [41, 42].

Em meio a Cl^- ocorre uma maior eficiência na degradação, que pode ser caracterizada pela acentuada supressão dos picos nas curvas de absorbância em UV-Vis. Entretanto, o pH é um dos fatores limitantes deste processo, sendo que a reação acontece de maneira mais eficiente em valores de pH na faixa

ácida (pH < 4,0).

É sabido que o espectro no UV-Vis da ciprofloxacina é composto de duas bandas de absorção. Para diferentes valores de pH há uma mudança no espectro referente a cada banda e, a medida que o pH da solução aumenta ocorre o favorecimento do processo de protonação/desprotonação, que corresponde aos grupos amina e ácido carboxílico, respectivamente.

O efeito do pH na absorção da ciprofloxacina pode ser notado pela mudança nos valores de absorbância cujo comportamento adequa-se a uma curva sigmoidal típica de equilíbrio ácido-base. A intersecção entre as faixas lineares I-II e as faixas II e III (Figura 5) correspondem aos valores de pH de 6,0 e 7,9, respectivamente. Estes valores são atribuídos ao pKa_1 e pKa_2 da ciprofloxacina que de acordo com a literatura encontram-se próximos a 6,2 e 8,8.

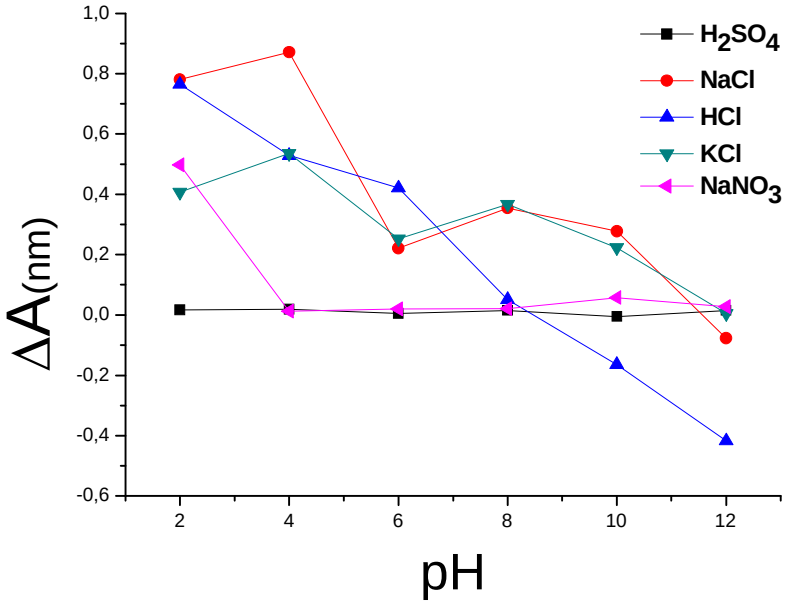

Figura 4. Variação da absorbância da ciprofloxacina (270 nm) em diferentes eletrólitos em função do pH. Condições: Ic: 80 mA; concentração de ciprofloxacina de 1,0 10^{-4} mol L^{-1}.

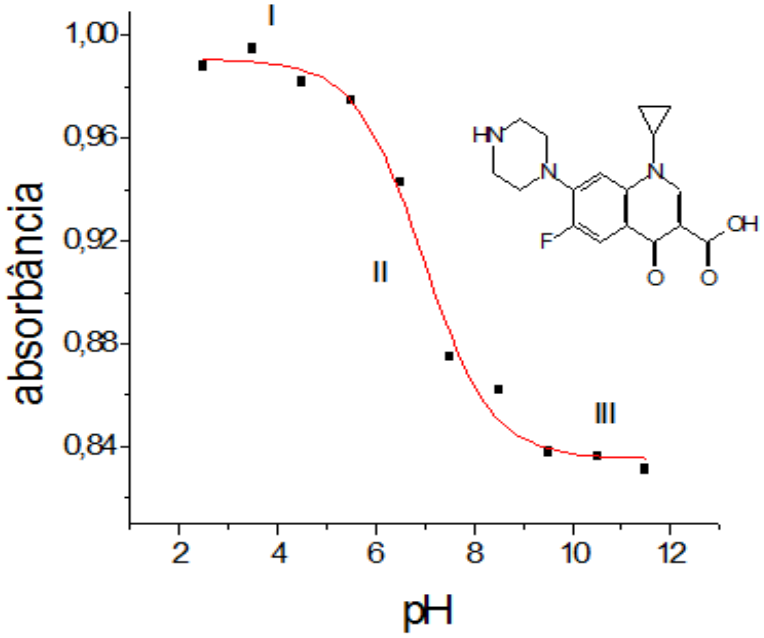

Figura 5. Espectro de absorção da ciprofloxacina, 1,0 10^{-4} mol L^{-1}, em diferentes valores de pH (λ= 270 nm).

Na medida em que se diminui a acidez do meio, o equilíbrio ácido-base tende a deslocar-se no sentido da desprotonação da molécula. O primeiro equilíbrio corresponde a desprotonação do grupo amina e o segundo a desprotonação do grupo carboxílico. Consequentemente, pode-se encontrar em solução quatro espécies: a espécie mais protonada (1), a espécie neutra (2), a espécie anfotérica (3) e a espécie com carga negativa (4). A alteração do pH promove alteração desse equilíbrio, favorecendo a formação de uma ou duas dessas formas representados no esquema 1.

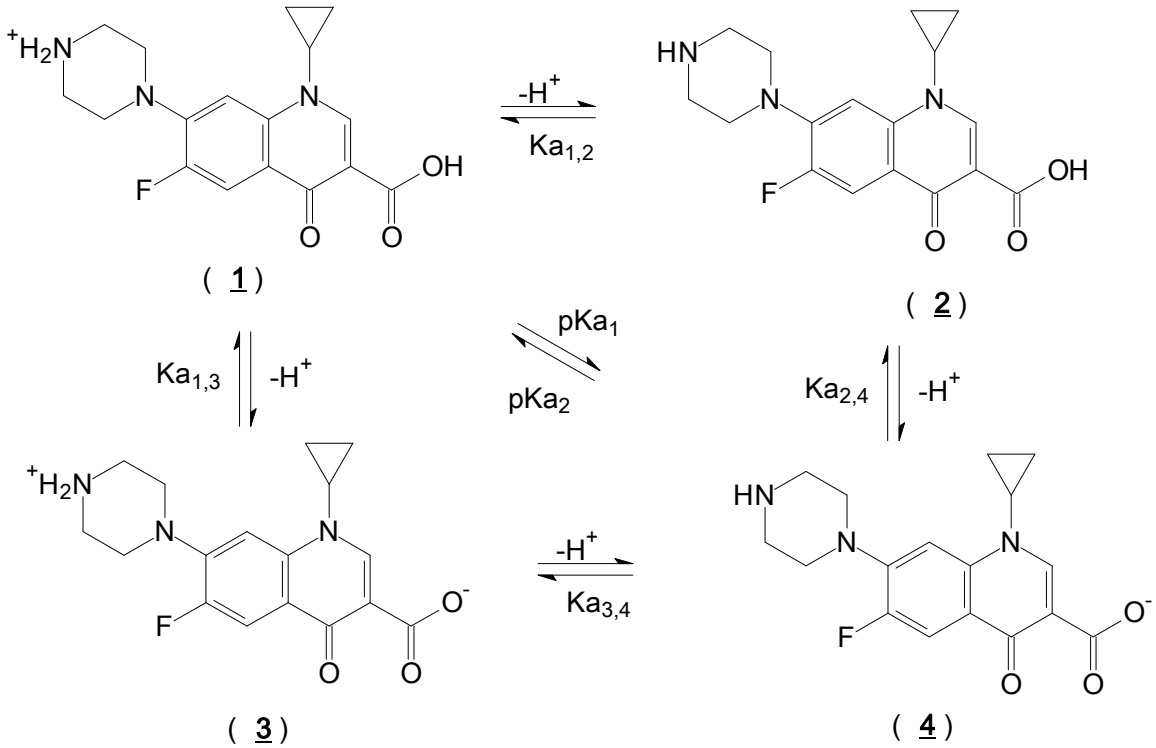

Esquema 1. Equilíbrio de protonação da ciprofloxacina.

3.5. Efeito da Força Iônica

De acordo com a teoria de Debye-Hückel, em soluções de eletrólitos fortes como o HCl, os íons estão sujeitos a ação da Lei de Coulomb. Portanto, quanto maior a carga desses íons e maior a concentração da solução, maior será à força de atração interiônica. Para soluções diluídas a probabilidade de formação de aglomerados iônicos é muito pequena ou quase nula, nesse caso a atividade se aproxima ou até se iguala à concentração analítica. Já a intensidade do campo elétrico gerado pela presença de íons em solução é quantificada através do parâmetro força iônica, introduzida por Lewis em 1921.

Para avaliar o efeito da força iônica foram realizados experimentos em diferentes concentrações do eletrólito suporte na faixa de 0,1 a 1,0 10^{-4} mol L^{-1}. Em soluções diluídas houve pouca variação no comportamento de eletrodegradação da ciprofloxacina. A Figura 6 mostra a influência da força iônica no processo de eletrólise da ciprofloxacina, soluções com força iônica abaixo de 1,0 10^{-2} mol L^{-1} não apresentaram boa eficácia no processo de degradação.

Com o estudo da força iônica foi possível perceber que o aumento na concentração do eletrólito interfere diretamente na taxa de degradação da ciprofloxacina. Nos experimentos com HCl foi observado que, para uma mesma intensidade de corrente e em concentrações maiores, ocorre uma maior velocidade de remoção da cor. Com o HCl, provavelmente ocorreu a eletrólise indireta, ou seja, a oxidação da ciprofloxacina devido a formação do ácido hipocloroso. Não obstante, o excesso de H^+ no meio pode interferir na reação de protonação/desprotonação da ciprofloxacina, onde o excesso desta espécie estabiliza a molécula orgânica encobrindo possíveis sinais de reações redox que possam vir a ocorrer.

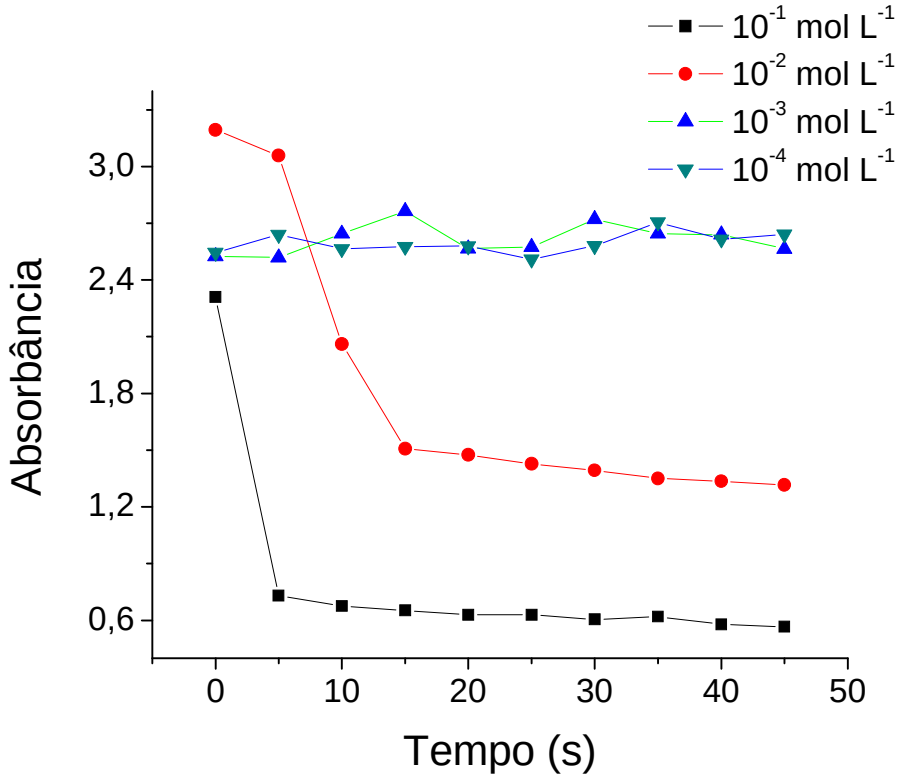

Figura 6. Estudo da Força iônica em HCl, pH=2,0 e Ic: 80 mA.

3.6. Efeito da intensidade de corrente

O consumo de energia em processos eletroquímicos é de suma importância para verificar a sua viabilidade. A eficiência da corrente aplicada é maior para menores intensidades de corrente. Aumentando-se a corrente, diminui-se a eficiência do processo, uma vez que altos valores favorecem a reação de desprendimento de oxigênio. Além disso, em menores intensidades de corrente, o consumo de energia é menor. Esse comportamento é explicado pelo fato de que em menores correntes a reação de desprendimento de oxigênio não interfere na oxidação do composto orgânico, assim a maior parte da corrente aplicada se concentra na oxidação da ciprofloxacina. Correntes maiores apresentam maior consumo de energia, uma vez que uma parte da corrente aplicada não é utilizada para a reação de interesse que é a oxidação do fármaco.

O consumo de energia por volume de água tratada foi calculado em kWh m^{-3} e pode ser calculado por $E\ i\ t\ /\ 1000\ V$, onde E é o potencial médio da célula durante a eletrólise (V), i é a corrente aplicada em ampére (A), t é o tempo da eletrólise em horas e V é o volume do efluente em m^3. O resultado indicou um consumo de 0,035 kWh m^{-3} para uma aplicação de corrente de 80 mA a 25 ^{o}C. Este valor indica um baixo consumo para remoção de traços de poluente orgânico, sendo coerente com a baixa concentração da ciprofloxacina presente. Sistemas mais contaminados chegam a consumir 2 a 10 kWh m^{-3}, a exemplo do tratamento eletroquímico do chorume que consome 4,06 kWh m^{-3}.

Para verificar a influência das intensidades de corrente na eletrodegradação da ciprofloxacina foram testados as correntes de 20, 40, 80 120 e 160 mA (Figura 7), que estima-se corresponder a potenciais entre 0,8 e 2,6 V. Foram retiradas e analisadas amostras da solução por espectrofotometria no intuito de monitorar o clareamento da solução de ciprofloxacina. Observou-se uma diminuição na intensidade da cor a partir de corrente de 40 mA. O aumento da eficiência da oxidação eletroquímica da ciprofloxacina, com o aumento da intensidade de corrente, é atribuído ao acréscimo de transporte iônico que provoca um aumento na velocidade das reações no eletrodo. De acordo com o acompanhamento da cinética reacional, em cerca de 2 minutos, todas as intensidades de corrente foram eficientes na degradação da molécula de ciprofloxacina, visto que os radicais $OH^{\bullet}$ produzidos nos processos eletroquímicos reagem rapidamente, de 1,8 a 16,9 mol^{-1} L min^{-1}, com compostos orgânicos que contém

anéis aromáticos, como a ciprofloxacina.

Utilizando-se correntes entre 20 e 40 mA foi possível notar que o processo de oxidação se completa em torno de 25 minutos, sendo que em intensidade de corrente acima desse valor o percentual de remoção alcança aproximadamente 100% em apenas 5 minutos de tratamento. Além disso, em correntes superiores a 120 mA e na ausência de compostos orgânicos oxidáveis, os radicais oxigênio ativos e dissolvidos formam o gás oxigênio de forma mais rápida que a oxidação eletroquímica da ciprofloxacina, diminuindo a eficácia do processo. Na Figura 7, observa-se o comportamento do sistema quando da aplicação de diferentes valores de corrente (i). A corrente ótima está abaixo de 120 mA, sendo o melhor resultado obtido em 80 mA. Acima deste valor a energia disponível tende a ser consumida em reações paralelas, como pode ser observado pelo aumento da corrente após um tempo de 17 minutos. Por sua vez, valores de corrente muito baixos como 20 mA não permitem que a reação se propague na velocidade ideal como numa reação homogênea em regime de pseudo-primeira ordem.

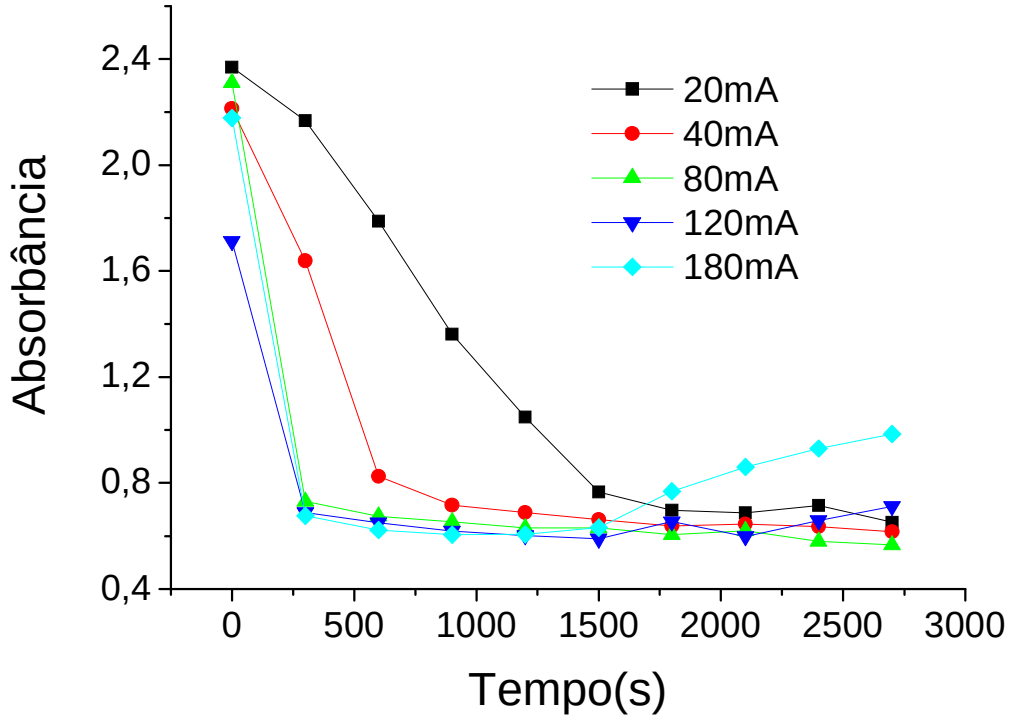

Figura 5. Comportamento da absorbância em 270 nm em função do tempo de oxidação da ciprofloxacina em eletrodo de Ti/TiO_2. Condições: 2,5 10^{-5} mol L^{-1} de ciprofloxacina, pH = 2,0; HCl 0,1 mol L^{-1} e Ic: 80 mA.

3.7. Aplicação da eletrodegradação da ciprofloxacina em água de abastecimento

A eletrodegradação da ciprofloxacina foi acompanhada por espectrofotometria, escolhida pela sua versatilidade em fornecer informações qualitativas no estudo dos processos eletroquímicos, permitindo o monitoramento da oxidação da ciprofloxacina [43, 44].

Os resultados da aplicação da eletrodegradação da ciprofloxacina em água de rio utilizando HCl como eletrólito suporte em meio reacional de pH 2,0 estão ilustrados no gráfico da Figura 8. A cada 5 minutos de aplicação de uma intensidade de corrente de 80 mA foi possível perceber a viabilidade do método. O teor de carbono orgânico total (COT) tem sido usado com frequência no monitoramento das oxidações eletroquímicas, no entanto, para este sistema, não obtivemos resultados satisfatórios [45-48], em função da quantidade de ciprofloxacina estar em nível abaixo do limite de detecção e da faixa de trabalho usual da técnica, que seria da ordem de 50 mg L^{-1} a 10 g L^{-1}. Para a ciprofloxacina o limite de detecção estaria em torno de 43 mg L^{-1} (1,3 10^{-4} mol L^{-1}), sendo que as

análises tem como valor inicial 1,0 10^{-5} mol L^{-1}.

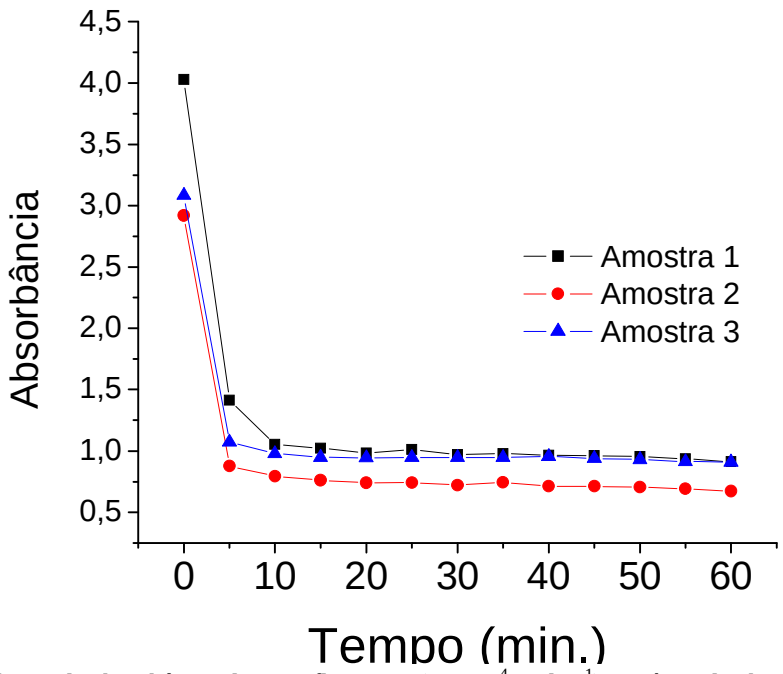

Figura 8. Redução da absorbância da ciprofloxacina (1,0 10^{-4} mol L^{-1}) em água de abastecimento acrescida de eletrólito suporte (HCl a 0,1 mol L^{-1}) em função do tempo de eletrólise. (λ = 270 nm).

4. CONCLUSION

A eficiência da eletrodegradação da ciprofloxacina em Ânodos Dimensionalmente Estáveis foi avaliada através da eletroatividade da ciprofloxacina em meio a diferentes condições experimentais. Na otimização do processo de eletrodegradação, a intensidade de corrente de 80 mA foi considerada adequada para um bom desempenho do sistema eletroquímico. Aliado a isto, observou-se que o uso de HCl ou NaCl como eletrólito suporte favoreceram o processo de eletrodegradação. Em estudos na presença de cloreto houve a remoção de 100% da cor amarela, característica da degradação da solução aquosa de ciprofloxacina após 5 minutos. Em ambos os eletrólitos a presença do ânion Cl^- propiciou a formação do ácido hipocloroso que apresentou uma melhor eficiência na eletrodegradação do fármaco. Nos estudos com variação de pH, foi possível perceber que este é um fator limitante, uma vez que a reação acontece com maior eficácia em pH abaixo de 4,0. Por espectrofotometria foi possível determinar as formas presentes em cada ambiente protônico na presença de dois valores de pKa, o primeiro em 6,0 atribuído ao equilíbrio de protonação do grupo amina e o segundo atribuído ao equilíbrio de grupo carboxílico. A molécula de ciprofloxacina foi degradada após aproximadamente 5 minutos. Por outro lado, a degradação de ciprofloxacina em meio a água de abastecimento ocorreu em um tempo maior, aproximadamente 8 minutos. Esse fato demonstra que o tratamento com eletrodos ADE são efetivos para a degradação de baixas concentrações de ciprofloxacina em ambiente aquático e que o tipo de eletrólito, a força iônica e o pH do meio são fatores determinantes na eficácia do processo de eletrodegradação.

5. AGRADECIMENTOS

Ao CNPq pelo suporte financeiro, processo 157123/2010-3.

6. REFERENCIAS E NOTAS

[1] Farmacopeia Portuguesa. 8ª ed. Lisboa: Infarmed, 2005.

[2] United States Pharmacopeia (USP). 31th ed. United States Pharmacopoeia Convention: Rockville, 2008.

[3] Reynolds, J. E. F. (Ed); Martindale the extra pharmacopoeia, 35ª ed. London: Pharmaceutical

Press, 2007.

[4] Sousa, J. C.; Manual de antibióticos antibacterianos, 2ª ed. Porto: Edições Universidade Fernando Pessoa, 2006.

[5] Sungpyo, L.; Aga, A.S. *Journal of Toxicology and Environmental Health, Part B*, **2007,** *10*, Issue 8, 559.

[6] Silva, P.; Farmacologia. 6ª ed. Rio de Janeiro: Guanabara Koogan, 2002.

[7] Andreu, V.; Blasco, C.; Pico, Y. *Trends Anal. Chem.* **2007**, *26*, 534. [CrossRef]

[8] Blondeau, J. M. Fluoroquinolones: mechanism of action, classification, and development of resistance. Survey of Ophthalmology, **2004**, 49.

[9] Evstigneev; Rybakova, K. A; Davies D. B. *Biophy. Chem*. **2006**, *121*, 84. [PubMed]

[10] Wang, J; Liu, Z; Liu, J; Liu, S; Shen, W. *Spectroch. Acta Part A*, **2008**, *699*, 956. [CrossRef][PubMed]

[11] Souza, M. V. N; Almeida, V; Silva, A. D.; Couri, M. R. C. *Rev. Bras. Farmac*. **2004**, *85*, 13.

[12] Vade-Mecum de Medicamentos, 12ª ed. Sao Paulo: Soriak, 2006/2007.

[13] Hirsch, R.; Ternes, T.; Haberer, K.; Kratzb, K. L. **199**, *225*, 109.

[14] Kummerer, K. *Part I, Chemosp.* **2009**, *75*, 417. [PubMed]

[15] Kummerer, K. *J. Environ. Manag*. **2009**, *90*, 2354. [CrossRef][PubMed]

[16] García-Galán, M. J., Díaz-Cruz, M. S., Barceló, D. *Tren. Anal. Chem*. **2008**, *27*, 1008. [CrossRef]

[17] Sanderson, H; Thomsen, M. *Toxic. Lett*. **2009**, *187*, 84. [CrossRef][PubMed]

[18] Bolong, N.; Ismaila, A. F.; Salimb, M. R.; Matsuura, T. Desalination **2009**, *239*, 229. [CrossRef]

[19] Suchara, E. A. et al. *Anal. Chim. Acta* **2008**, *613*, 169. [CrossRef][PubMed]

[20] ANVISA, Agência Nacional de Vigilância Sanitária. Available from: http://portal.anvisa.gov.br/. Access January, 2012.

[21] Ministério de Desenvolvimento, Indústria e Comércio. Available from: http://www.aliceweb.gov.br/. Access January, 2012.

[22] Marques, D. A. V. Produção e extração de ácido clavulânico de Streptomyces spp. por fermentação extrativa utilizando sistemas de duas fases aquosas. [Tese de Doutorado.] São Paulo, Brasil: Faculdade de Ciências Farmacêuticas, Universidade de São Paulo, 2010. [Link]

[23] Palmeira Filho, P. L.; Pan, S. S. K.; BNDES Setorial, Rio de Janeiro, n. 18, p. 3-22, 2003.

[24] Mascolo, G.; Balest, L.; Cassano, D.; Laera, G.; Lopez, A.; Pollice, A.; Salermo, C. *Biores. Tech.* **2010**, *101*, 2585. [CrossRef][PubMed]

[25] Farré, M. L.; Pérez, S.; Kantiani, L.; Barceló, D. *Tren. Anal. Chem.* **2008**, *27*, 991.[CrossRef]

[26] Fent, K.; Weston, A. A.; Caminada, D. *Aqua. Toxic.* **2006**, *76*, 122. [CrossRef][PubMed]

[27] Coelho, A. D. Degradação dos Antiinflamatórios Diclofenaco, Ibuprofeno e Naproxeno por Ozonização. [Tese de Doutorado.] Engenharia Química, Universidade Federal do Rio de Janeiro, Rio de Janeiro, 2008. [Link]

[28] Castiglioni, S.; Fanelli, R.; Calamari, D.; Bagnati, R. *Reg. Toxic. Pharm.* **2004**, *39*, 25. [CrossRef][PubMed]

[29] Onesios, K. M.; Yu, J. T.; Bouwer, E. *J. Biodeg.*, **2009**, *20*, 441. [CrossRef][PubMed]

[30] INMETRO. Orientação sobre validação de métodos de ensaios químicos, DOQ-CGCRE-008, Revisão 02. Available from: http://www.inmetro.gov.br/Sidoq/Arquivos/CGCRE/DOQ/DOQ-CGCRE-8_02.pdf. Access June, 2010

[31] Richardson, S. D. *Anal. Chem.* **2007**, *79*, 4295. [CrossRef][PubMed]

[32] Malpass, G. R. P.; Miwa, D. W.; Machado, S. A. S.; Olivi, P.; Motheo, A. J. **2006**, *137*, 565.

[33] Malpass, G. R. P.; Neves, R. S.; Motheo, A. *J. Electroc. Acta* **2006**, *52*, 936. [CrossRef]

[34] Silva, R. C.; *Dissertação de Mestrado*, Instituto de Quimica, Universidade de Sao Paulo, Sao Carlos, 2006.

[35] Harris, D. C.; Análise Química Quantitativa, 6ª ed. Rio de Janeiro: LTC, 2005.

[36] Skoog, D. A.; West, D. M.; Holler, F. J. Fundamentos da Química Analítica, 1ª ed., São Paulo: Thomson Learning, 2005.

[37] Ticianelli, E. A.; Gonzalez, E. R.*; Eletroquímica*, 2ª ed., São Paulo: Editora da Universidade de São Paulo, 2005.

[38] Park, H-R., Chung, K-Y., Lee, H-C., Lee, J-K, Bark, K-M.; *Bull. Kor. Chem. Soc.*, **2000**, *21*, 849.

[39] Arguelho, M. L. P. M.; Zanoni, M. V. B.; Stradiotto, N. R.; *Anal. Lett.* **2005**, *38* 1415. [CrossRef]

[40] Calza, P.; Medana, C.; Carbone, F; Giancotti, V.; Baiochi, C.; *Rap. Comm. Mass Spectrom.* **2008**, *22*, 1533. [CrossRef][PubMed]

[41] Snoeyink, V. L.; Jenkins, D. Water Chemistry, New

York: John Wiley & Sons, 1980.

[42] Stum, W.; Morgan, J. J. *Aqua. Chem.*, 3ª ed., New York: John Wiley & Sons, 1996.

[43] Li, B.; Zhang, T. *Environ. Scie.Tech.* **2010**, *44*, 3468.

[44] Melo, S. A. S.; Trovó, A. G.; Bautitz, I. R.; Nogueira, R. F. P. *Quím. Nova* **2009**, *32*, 188.

[45] Rufino, É. C. G.; Faria, L. A.; Silva, L. M. *Quím. Nova* **2011**, *34*, 200.

[46] Guimarães, D. O.; Momesso, L. S.; Pupo, M. T. *Quím. Nova* **2010**, *33*, 667.

[47] Psomas, G. *J. Inorg. Niochem.* **2008**, *102*, 1798. [CrossRef][PubMed]

[48] Locatelli, M. A. F.; Sodré, F. F.; Jardim, W. F. *Environ. Contam. Toxic.* **2011**, *60*, 385. [CrossRef][PubMed]

Orbital: The Electronic Journal of Chemistry
journal homepage: www.orbital.ufms.br
ISSN 1984-6428

| Vol 5 | | No. 1 | | January-March 2013 |

Full Paper

Synthesis and Characterization of Cobaltite Spinels Using Infrared, Thermogravimetric Analyses and X-Ray Crystallography

R. Manimekalai*, K. Kalpanadevi and R. Sinduja

Department of Chemistry, Kongunadu Arts and Science College, Coimbatore, Tamilnadu, India.

Article history: Received: 28 December 2012; revised: 07 February 2013; accepted: 13 March 2013. Available online: 17 April 2013.

Abstract: This paper presents the synthesis of cobaltites of the nominal composition of $NiCo_2O_4$ and $CdCo_2O_4$ from the precursors $NiCo_2(N_2H_4)1.5(crot)_2.H_2O$ and $CdCo_2(N_2H4)(crot)_2.H_2O$ respectively. The precursor complexes have been synthesized by simple chemical technique and characterized by their elemental composition, FT-IR spectroscopy and TG-DTA. Thermograms of both the complexes indicated their facile decomposition at relatively low temperature range 141 ºC-398 ºC to give the corresponding stable mixed metal oxides. The Infrared analysis of the residue shows two absorption bands in the region 662 cm^{-1} and 560 cm^{-1} corresponding to the metal-oxygen stretching from tetrahedral and octahedral sites respectively, which are characteristics of cobaltites. Formation of cobaltite has been confirmed by thermogravimetry (TG) weight loss and X-ray diffraction. Combustion of the precursor in air yields fine powder of cobaltites with large surface area which has been confirmed by XRD patterns.

Keywords: cobaltites; FT-IR spectroscopy; TG-DTA; XRD

1. INTRODUCTION

Spinels are an important class of material due to their catalytic and magnetic properties. Cobaltites show significant catalytic activity [1]. Spinels are also used as a basis for the conceptual development and application of crystal field theory, particularly, through the calculation of site preference energies in determination of inverse or normal spinel structures which has also been demonstrated through the use of ping-pong ball models to aid the understanding of structure development [2, 3]. Various methods for the synthesis of spinels have been studied, such as co-precipitation of the hydroxides and oxylates, complexometric (sol-gel) synthesis through glycolate, ethylenediaminetetraacetate (EDTA), fumarate and citrate intermediates, organometallic synthesis in a polymer matrices, mechanochemical methods using binary oxides and synthesis within silica ampoules[4, 5].

Researchers have given a considerable attention in synthesizing cobaltite system by exploring the precursors used, preparation methods, processing control and firing temperatures. Among the binary cobaltites of transition metals with the general formula MCo_2O_4, where M is a divalent cation of a d element, Ni, Cu and Zn cobaltites are of definite interest due to their diverse applications as oxide electrode materials, magnetic materials, thermistors and catalysts [6-11]. Cobaltites have attracted much attention of the chemists due to their application as low cost fuel cell electrodes.

A wide option of preparative methods can be employed to obtain the desired novel products. Some of the methods applied are traditional ceramic preparation or better known as solid-state route and chemical techniques such as sol-gel, electrochemical, solvothermal, hydrothermal, combustion and co-precipitation. Thermal treatment of co-precipitated precursors is proven to be the most promising method in preparing cobaltite spinels [12-15].

The possibility of synthesis of cobaltites as high-dispersity material using the respective metal cobalt crotonate hydrazinate as precursors is studied in the present paper.

* Corresponding author. E-mail: manimekalair@ymail.com

2. MATERIAL AND METHODS

2.1. Preparation of nickel cobalt crotonate hydrazinate

The nickel cobalt crotonate hydrazinate is prepared by heating aqueous suspension of the corresponding metal carbonates ($NiCO_3.2Ni(OH)_2.4H_2O$, 1 g, 0.002 mol; $CoCO_3$, 1 g, 0.008 mol) and crotonic acid (3.44 g, 0.03 mol) in 50 mL of water. It is filtered and cooled. To this resulting clear solution, aqueous solution (50 mL) of hydrazine hydrate (2.5 mL, 0.05 mol) is added. The complex is formed after a few minutes. It is kept for an hour for digestion, then filtered and washed with water, alcohol followed by diethylether and air dried.

2.2. Preparation of cadmium cobalt crotonate hydrazinate

This complex is also prepared by the same procedure as above with molar ratio of $CdCO_3$, 1 g, 0.006 mol: crotonic acid, 3.44 g, 0.04 mol: hydrazine hydrate, 2.5 mL, 0.05 mol. The colourless spongy crystals of the complex are formed slowly.

Both the precursor complexes are obtained as polycrystalline powders which are insoluble in water, alcohol, diethyl ether and other organic solvents. All the complexes are stable in air and insensitive to light.

2.3. Preparation of cobaltites

The cobaltites MCo_2O_4 where M = Ni or Cd have been obtained as residues by heating respective precursors at 400 ˚C in pre-heated silica crucible for about 15 minutes. While heating, the precursors should be added in small portions to the crucible in order to avoid explosions, since they decompose violently.

2.4. Quantitative methods

The hydrazine content in the sample was determined by titration using KIO_3 as the titrant [16]. The percentage of nickel or cadmium and cobalt in the precursor was estimated by the standard methods given in the Vogel's textbook [16].

2.5. Physico-chemical techniques

2.5.1. Infrared spectrum

The infrared spectra of the solid samples were recorded by the KBr disc technique using a Perkin Elmer 597/1650 spectrophotometer.

2.5.2. Thermal analysis

The simultaneous TG-DTA experiments were carried out in Shimadzu DT40, Stanton 781 and STA 1500 thermal analyzers. Thermal analyses were carried out in air at the heating rate of 10 °C per minute using 5-10 mg of the samples. Platinum cups were used as sample holders and alumina as reference. The temperature range was ambient to 700 °C.

2.5.3. X-ray powder diffraction

The X-ray powder diffraction patterns of the samples were obtained using a Philips X-ray Diffractometer with vertical goniometry model PW 1050/70 using Cu Kα/Co Kα /Mo Kα radiation with nickel / iron / tantalum filters.

3. RESULTS AND DISCUSSION

3.1. Chemical formula determination of nickel cobalt crotonate hydrazinate

From the IR spectrum of this complex, it is observed that the N-N stretching frequeny is seen at 964 cm^{-1}, which unambiguously proves the bidentate bridging nature of the hydrazine ligand [17]. The asymmetric and symmetric stretching frequencies of the carboxylate ions are seen at 1613 and 1410 cm^{-1}, respectively with the Δυ (υasymm- υsym) separation of 203 cm^{-1}, which indicate the monodentate linkage of both carboxylate groups in the dianion. The N-H stretching is observed at 3029 cm^{-1}. The IR data thus confirms the formation of nickel cobalt crotonate hydrazinate complex. The chemical formula $NiCo_2(N_2H_4)1.5(crot)_2.H_2O$ has been assigned to the complex, nickel cobalt cinnamate hydrazinate based on the observed percentage of hydrazine (16.19), nickel (6.58) and cobalt (13.23) which are found to match closely with the calculated values 17.07, 6.50 and 12.13 for hydrazine, nickel and cobalt respectively.

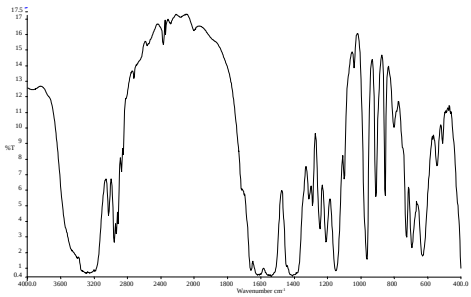

Figure 1. IR Spectrum of $NiCo_2(N_2H_4)1.5(crot)_2.H_2O$.

3.2. Chemical formula determination of cadmium cobalt crotonate hydrazinate

The IR spectrum of this complex shows that the N-N stretching frequency is at 960 cm^{-1}, which clearly proves the bidentate bridging nature of the hydrazine ligand [17]. The asymmetric and symmetric stretching frequencies of the carboxylate ions are seen at 1560 and 1413 cm^{-1}, respectively with the Δυ (υasymm-υsym) separation of 147 cm^{-1}, which indicate the unidentate linkage of both carboxylate groups in the dianion. The N-H stretching is observed at 3259 cm^{-1}. The chemical formula $CdCo_2(N_2H_4)(crot)_2.H_2O$ has been assigned to the complex, cadmium cobalt cinnamate hydrazinate based on the observed percentage of hydrazine (6.00), cadmium (12.38) and cobalt (13.16) which are found to match closely with the calculated values 5.28, 11.38 and 12.00 for hydrazine, cadmium and cobalt, respectively.

3.3. Thermal analysis of the precursor

From the thermal decomposition data of the prepared complexes, it is observed that the compounds decompose exothermically to yield the corresponding oxides, $NiCo_2O_4$ and $CdCo_2O_4$ as the final products. The observed weight losses match very well with the expected values. The major weight losses of 76.43% and 69.24% on the TG curve from 141-385 °C and 233-398 °C respectively are attributed to the decarboxylation of dehydrazinated complexes.

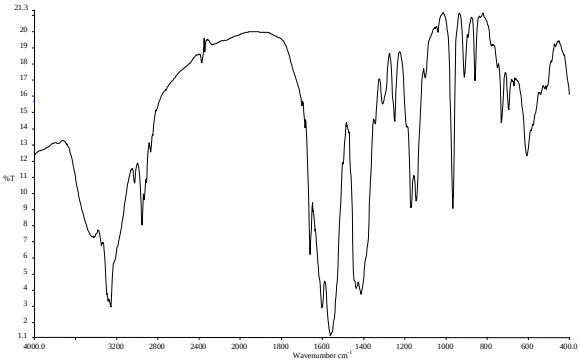

Figure 2. IR Spectrum of $CdCo_2(N_2H_4)1.5(crot)_2.H_2O$.

Table 1. Thermal analysis.

S. No	Compound	TG Temp range °C	% Weight loss		DTA peak temp (°C)	Decomposition product
			Cald	Obsd		
1	$NiCo_2(N_2H_4)_{1.5}(crot)_2.H_2O$ Mol.Wt.: 297.17	141 - 385	73.13	76.43	375 (-)	$NiCo_2O_4$
2	$CdCo_2(N_2H_4)_{1.5}(crot)_2.H_2O$ Mol.Wt.: 298.64	233 - 398	67.30	69.24	383 (-)	$CdCo_2O_4$

3.4. Cobaltites

The chemical analysis of the cobaltites prepared from the precursors show that the metal and cobalt in these residues are present in 2:1 ratios. Formation of cobaltites by the thermal decomposition of the mixed metal complexes was confirmed by thermogravimetry (TG) weight loss and XRD patterns. The Infrared Spectra of the residues show two absorption bands in the region 660-665 and 555-562 cm^{-1} corresponding to the metal-oxygen stretching from tetrahedral and octahedral sites respectively, which are characteristics of cobaltites [13]. Further investigation has been carried out by obtaining X–ray powder diffraction pattern of the residues. The 'a' value of cobaltites with cubic symmetry calculated from the pattern match very well with the reported values [18]. The crystalline sizes of the nickel and cadmium cobaltites are calculated using Scherrer formula, $T = K\lambda / \beta\cos\theta$, which are found to be 8.0833nm and 8.1050 nm respectively. The cobaltites thus obtained prepared by thermal decomposition of hydrazine mixed metal crotonates are in finely powdered form with large surface area. Hence this can be used in the catalytic reactions. The X-ray pattern of $NiCo_2O_4$ is shown in Figure 3 as a representative example.

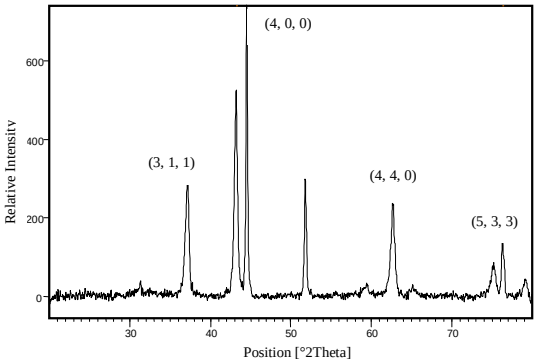

Figure 3. XRD pattern of $NiCo_2O_4$.

4. CONCLUSION

The synthesis of transition metal oxides via the metal–crotonate hydrazinate precursor is a convenient synthetic route to prepare nanosized mixed metal oxides. In this method hydrazine complexes exhibit an autocatalytic behaviour after ignition in air. The precursors decompose autocatalytically on ignition forming nanosized $NiCo_2O_4$ and $CdCo_2O_4$.

The chemical analysis, total weight loss and infrared spectral analysis of the complex confirm the formation of the complexes $NiCo_2(crot)_2(N_2H_4)_2$ and $CdCo_2(crot)_2(N_2H_4)_2$. The TG-DTA analysis shows that the complexes have good thermal stability with initial decompose temperature at above 250 °C.

The TG studies of the complex show the formation of single phase $NiCo_2O_4$ and $CdCo_2O_4$ nanoparticles, which are also confirmed by XRD studies.

5. REFERENCES AND NOTES

[1] Paike, V. V.; Niphadkar, P. S.; Bokade, V. V.; Joshi, P. N. *J. Am. Ceram. Soc*. **2007**, *90*, 3009. [CrossRef]

[2] Suchow, L. *J. Chem. Educ*. **1967**, *53*, 560. [CrossRef]

[3] Weller, M. T. ; Inorganic materials chemistry. Oxford: Oxford University Press, 1994.

[4] Turkin, A. I; Drebushchak, V.A. *J. Cryst. Growth*. **2004**, *265*, 165. [CrossRef]

[5] Turkin, A. I.; Drebushchak, V. A.; Kovalevskaya, Y. A ; Paukov, I. E. *J. Therm. Anal. Calorim*. **2008**, 92, 717. [CrossRef]

[6] Kikukawa, N.; Takemori, M.; Nagano, Y.; Sugasawa, M. and Kobayashi, S. *J. Magn. Magn. Mater*. **2004**, *284*, 206. [CrossRef]

[7] Prakash, A. S.; Khadar, A. M. A.; Patil K. C.; Hegde, M. S. *J. Mater. Synth. Process*. **2002**, *10*, 2002.

[8] Vaidyanathan, G.; Sendhilnathan, S. Arulmurugan, R. *J. Magn. Magn. Mater*. **2007,** *313*, 293. [CrossRef]

[9] Azadmanjiri, J.; Salehani, H. K.; Barati, M. R.; Farzan, F. *Mater. Lett*., **2007**, *61*,84. [CrossRef]

[10] Ahmed, M. A.; El-Sayed, M. M. *J. Magn. Magn. Mater*. **2007**, *308*,40. [CrossRef]

[11] Kim, C. K.; Lee, L. H.; Katoh, S.; Murakami, R.; Yoshimura, M. *Mater. Res. Bull*. **2001**, *36*, 2241. [CrossRef]

[12] Klissurski, D.; Uzunova, E. *J. Mat. Sci*. **1994**, *29*, 285. [CrossRef]

[13] Patil, K. C. *Bull. Mat. Sci*. **1993**, *16*, 533. [CrossRef]

[14] Ravindranathan, P.; Patil, K. C. *Amer. Ceram. Soc. Bull*. **1987**, *66*, 688.

[15] Sivasankar, B. N.; Govindarajan, S. *Ind. J. Chem*. **1994**, *33 A*, 329.

[16] Vogel, I. A Textbook of Quantitative Inorganic Analysis, 4th ed., Longman, UK, 1985.

[17] Braibanti, A.; Dallavalle, F.; Pellinghelli, M. A.; Laporati, E. *Inorg. Chem*. **1968**, *7*, 1430. [CrossRef]

[18] Powder Diffraction File, Inorganic volume, pp. 1S – 5iRB, Joint Committee on Diffraction Standards, Pennsylvania, 1967.

Orbital: The Electronic Journal of Chemistry
journal homepage: www.orbital.ufms.br
ISSN 1984-6428

| Vol 5 | | No. 1 | | January-March 2013 |

Full Paper

Efficient Asymmetric Synthesis of *S,S*-2-methylsulfanyl-2-methylsulfinyl-1-indanone

Derisvaldo R. Paiva*[a] and Roberto S. Gomes*[b]

[a]*Federal University of São Paulo, Rua Prof. Artur Riedel, 275, Jd. Eldorado, postal code: 09972-270, Diadema, SP, Brazil.*
[b]*SINTMOL laboratory, Institute of Chemistry, Federal University of Mato Grosso do Sul, Avenida Senador Filinto Muller, 1555, Postal Code 79074-460, Campo Grande/MS, Brazil.*

Article history: Received: 01 December 2012; revised: 25 March 2013; accepted: 30 March 2013. Available online: 17 April 2013.

Abstract: Diastereoselective synthesis of *SS*-2-methylsulfanyl-2-methylsulfinyl-1-indanol by reduction of SS-2-methylsulfanyl-2-methylsulfinyl-1-indanone optically enriched demonstrating to be highly efficiency using the sulfanyl group as asymmetric induction control agent during an addition reaction to carbonyl group.The 2-methylsulfinyl-1-indanone was obtained for the first time in one unique step without further oxidation steps. The synthesis of *SR*, *SS* of 2-methylsulphinyl-1-indanone optically enriched in good yield and good enantiomeric excess determined by nuclear magnetic resonance technique employing the Kagan reagent as chiral shift agent.

Keywords: asymmetric synthesis; indanone; indanol; phase-transfer catalysis

1. INTRODUCTION

The term "phase-transfer catalysis" (PTC) was first used by Starks [1] in 1971 and can be defined as "a synthetic method that accelerates or causes reactions between substances that are placed in contact via one transfer agent or catalyst." [2] The transfer agent or catalyst is often an ammonium salt or quaternary phosphonium, usually called "quat" and symbolized by Q^+ (Q^+X^-). An example of such salts are tetrabutyl ammonium bromide $(C_4H_9)_4N^+Br^-$.

The first mechanistic proposal for the process of phase-transfer catalysis was formulated by Starks [1, 3] for a liquid-liquid system (LL-PTC) using a nucleophilic substitution reaction (Scheme 1).

This type of catalysis has wide range of applications, especially in nucleophilic substitution reactions and reactions involving deprotonation of weak organic acids [4].

It is estimated that, nowadays, the PTC is used in over 500 industrial processes, for example, in the production of pharmaceuticals, agrochemicals, polymers etc [5].

Other systems in addition to the (LL-PTC) [3] are used, such as solid-liquid (SL-PTC) [6] and gas-liquid (GL-PTC) [7] wherein the catalytic cycle occurs with the transfer between the two phases, analogous to that proposed for the liquid-liquid system.

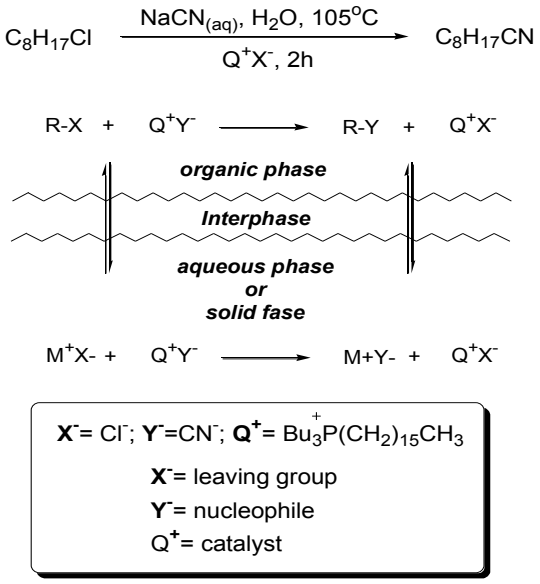

Scheme 1. Mechanistic proposal for a nucleophilic substitution reaction via phase-transfer catalysis.

Among these types of catalysis is the asymmetric phase-transfer catalysis (APTC) which has used quaternary ammonium salts with defined

*Corresponding author. E-mail: paivaman007@gmail.com or roberto.gomes@ufms.br

stereogenic centers of asymmetric induction in organic compounds, for example, the salts (**1**) and (**2**) of alkaloids ephedra and (**3**) and (**4**) of the Cinchona [8] (Figure 1) have been used frequently and conducted at good results in terms of stereoselectivity, especially when the substituents in the quaternary nitrogen are bulky.

Although chiral ethers-crown are more resistant to decomposition and have been used successfully, for example, in asymmetric Michael addition reactions, their high cost makes impracticable their use in industrial scale [8].

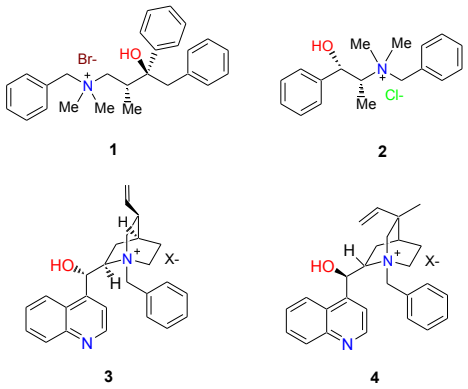

Figure 1. Salts derivated of the ephedra alcaloids: (**1**) and (**2**) and salts derivated of the cinchona (**3**) and (**4**).

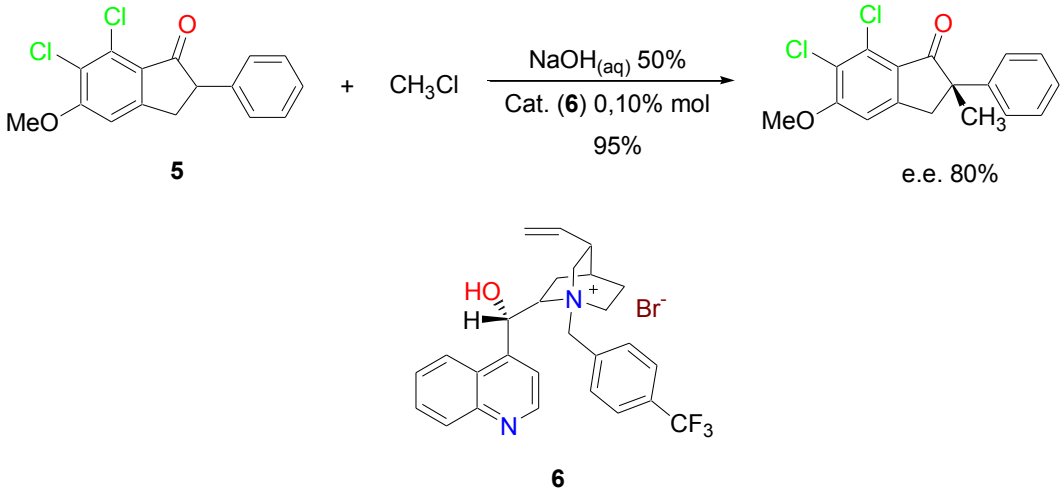

Scheme 2. Methylation of 6,7-dichloro-5-methoxy-2-phenyl-1-indanone by asymmetric phase-transfer catalysis.

One of the best results in APTC reactions were obtained by Dolling [9] on the asymmetric methylation of 6,7-dichloro-5-methoxy- 2-phenyl-1-indanone (**5**) using as catalyst *N*-[(4-trifluoromethyl) benzyl] cinchoninium bromide (**6**) (Scheme 2).

The enantioselection mechanism proposed in this case is based on the formation of a chiral enolate of indanone (**5**) by the association of three points with the catalyst. In this mechanistic model, the formation of an intimate ionic-pair is guaranteed by a hydrogen bond between the hydroxyl group of the catalyst and the oxygen of the enolate by an interaction type π-π (aromatic ring of the enolate with the quinoline ring of the catalyst) and also other π-π interaction (benzyl ring of the catalyst with the phenyl group of the enolate) (Figure 2).

The association between the enolate and the catalyst must block one face of the enolate for the approximation of the electrophile, explaining the high values of enantiomeric excess. It is noteworthy that the mechanistic model proposed is supported by the stereochemistry of the obtained adducts.

The asymmetric phase-transfer catalysis proved to be a versatile method for inducing asymmetry in organic compounds; the literature contains several examples of the use of APTC in organic synthesis as sowed in the Table 1.

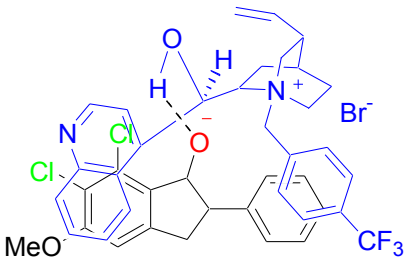

Figure 2. Methylation of 6,7-dichloro-5-methoxy-2-phenyl-1-indanone by asymmetric phase-transfer catalysis.

Among the synthetic reactions using APTC, the sulfanylation of β-sulfoxides have shown to be important because the obtained sulfoxides can be used

as chiral auxiliary in asymmetric synthesis [14, 15] and may be efficient as stereoselective inductors in reduction reactions, Diels-Alder reactions and the formation of C-C reactions [16-20]

Table 1. Some example of reactions catalyzed by APTC.

Reaction	Catalyst	Ref.
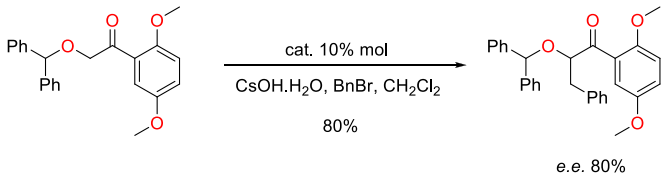	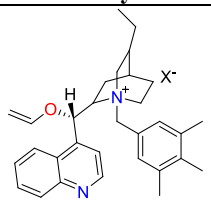	[10]
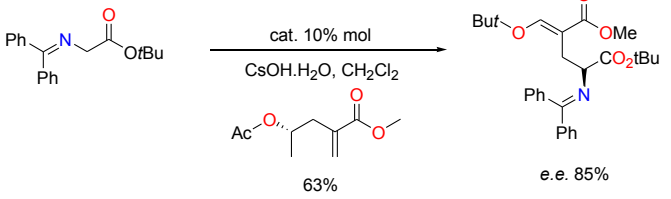	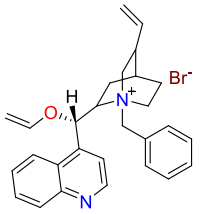	[11]
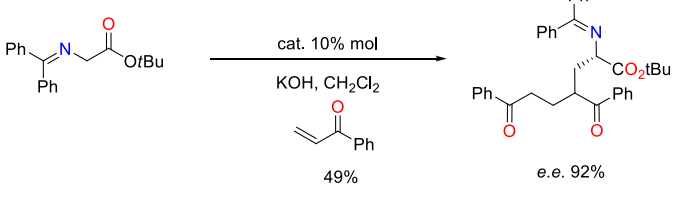	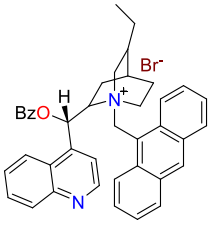	[12]
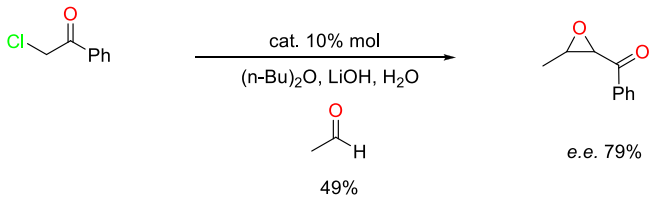	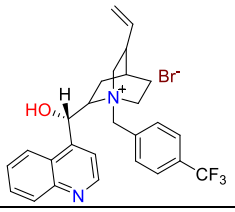	[13]

The efficiency of asymmetric induction is directly related to steric and electronic factors [17-20] between the groups attached in the sulfur atom. Thus, new methods for obtaining optically active sulfoxides are required for the synthesis of enantiomerically enriched compounds.

The α-hydroxy aldehydes and ketones proved to be very important precursors for the synthesis of biologically active compounds such as pheromones, ionophores and carbohydrates [21-23]. In this paper we present a synthetic study of *S,S*-2-methylsulfinyl-2- methylthio-1-indanol (**7**) enantiomerically enriched (Figure 3).

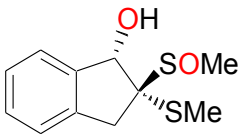

(**7**)

Figure 3. Structure of *S,*S-2-methylsulfinyl-2-methylthio-1-indanol.

2. MATERIAL AND METHODS

2.1. Materials

All reagents were purchased from Sigma-Aldrich and used without further purifications. ^{1}H-NMR and ^{13}C-NMR spectra were recorded on a Varian Inova 300 spectrometer (10% in $CDCl_3$ solutions) operating at 299.956 MHz and 75.418 MHz, respectively. Data processing was carried out on a Solaris workstation.

^{1}H and ^{13}C chemical shifts are given on the δ scale (ppm) and coupling constants (*J*) are reported in Hz. The following abbreviations were used: s, d, q and m, for singlet, doublet, quartet and multiplet, respectively.

Thin layer chromatography was performed on glass-backed silica plates and visualized in UV-detection. The GC analysis were carried on Varian GC 431, equipped with CP 8944 column associated with Varian MS, model 210, using He as carrier gas.

The diastereomeric excess was obtained by

using of Kagan reagent.

2.2. Synthetic Procedures

2.2.1 (±)-2-methylsulfinyl-1-indanone (**8**): A mixture of *n*-butyllithium (5 mL, 10.0 mmol), THF (60 mL) and lithium diisopropylamide (LDA) (1.0 g, 10.0 mmol) were stirred at 200 rpm for 5 min, after this time the reaction mixture was cooled until -78 ºC and added 1-indanone (1.32 g, 10.0 mmol) and stirred for 15 min, then, methanesulfinyl chloride (0.98 g, 10.0 mmol) was added. The mixture was stirred at 200 rpm for 2 hours and after this time, a saturated solution of sodium chloride (60 mL) was added and stirred at 200 rpm for 2 min. All of procedure occurred at room temperature. The organic phase was extracted with CH_2Cl_2 (3X 60 mL), dried over $MgSO_4$ and concentrated under reduced pressure. The concentrate was purified by flash chromatography (silica, hexane/ether, 1:1, respectively) [24].

2.2.2 (±)-2-methylsulfanyl-2-methylsulfinyl-1-indanone (9): A mixture of (±)-2-Methylsulfinyl-1-indanone (0.19 g, 1.0 mmol), $CH_3SSO_2CH_3$ (0.126 g, 1.0 mmol), solid K_2CO_3 (0.27 g, 2,0 mmol), a solution of CH_2Cl_2/C_6H_6 1:1 (10 mL) and benzyltriethylamonium chloride (TEBAC) (0.022 g, 0.1 mmol) or *N*-benzylquininium chloride (QUIBEC) (0.090 g, 0.2 mmol) was stirred for 3 hours at room temperature. The reaction mixture was filtered concentrated under reduced pressure. The concentrate was purified by flash chromatography (silica, hexane/ether, 1:1, respectively) [25].

2.2.3 *S*,*S*-2-methylsulfanyl-2-methylsulfinyl-1-indanol (7): A mixture of methanol (15 mL), a solution of $NaBH_4$ (0.076 g, 2.0 mmol) in 3 mL of methanol and a diastereomeric mixture 17:1 of (±)-2-methylsulfanyl-2-methylsulfinyl-1-indanone (**9**) (0.242 g, 1.0 mmol) was stirred at 200 rpm during 1 hour at -78 ºC. After this time, was added a saturated solution of ammonium chloride (10 mL). The organic phase was extracted with CH_2Cl_2 (3 X 60 mL), dried over $MgSO_4$ and concentrated under reduced pressure. The concentrate was purified by lixiviation using acetone [26].

3. RESULTS AND DISCUSSION

The keto sufoxide (**8**) was obtained adapting a synthetic method used for (±)-2-methylsulfinyl-1-tetralone [27] (Scheme 3).

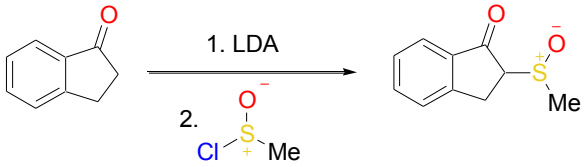

Scheme 3. Synthesis of the keto sulfoxide (**8**).

The enolate from 1-indanone (generated in homogeneous phase, using LDA as the base) reacted with the methylsulfinyl chloride to form the keto sulfoxide in one step [28]. Is noteworthy that this is the first time that this reaction without the oxidation step [29] is reported in the literature. This method avoided the formation of disulfanilated product in the first step and conducted to the product (**8**) in 65% yield and 59% of diastereomeric excess, calculated from the integration of the ^{1}H-NMR signals corresponding to methylsulfinyl group in 2.88 and 2.59 ppm.

Initially, the sulfanylation reaction of the sulfinylated derivative (**8**) was tested in APTC conditions using TEBAC as catalyst, K_2CO_3 as base, *S*-methylmethanethiolsulfonate as the sulfanylating agent and a CH_2Cl_2/C_6H_6 1:1 as solvent (Scheme 4) [29]. The sulfanylation of racemic mixture of 2-methylsulfinyl-1-indanone in these conditions was monitored by TLC and after 3 hours the reaction finished.

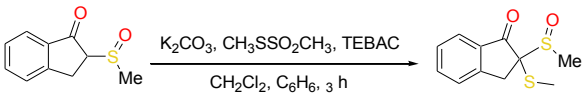

Scheme 4. Sulfanylation reaction of 2-methylsulfinyl-1-indanone (**8**).

After purification, the 2-methylsulfanyl-2-methylsulfinyl-1-indanone was obtained in 84% yield and 73% of diastereomeric excess. The majority diastereoisomer was isolated by TLC in 55 % yield. The ^{1}H-NMR spectra for the majority diastereoisomer showed 2 siglets in 2.82 and 2.34 ppm that corresponds to methylsulfinyl and methylsulfanyl groups respectively [30]. The X-ray to the same compound obtained under scalemic form demonstrated to be the *CS*, *SS* diastereoisomer (Figure 4).

Aiming to improve the yield of the reaction we tested the same APTC conditions replacing TEBAC by QUIBEC as catalyst. In this case, the obtained yield was 93% and 73% of diastereomeric excess. It is noteworthy that the majority diastereoisomer formed was the same in the case of the reaction catalyzed by TEBAC.

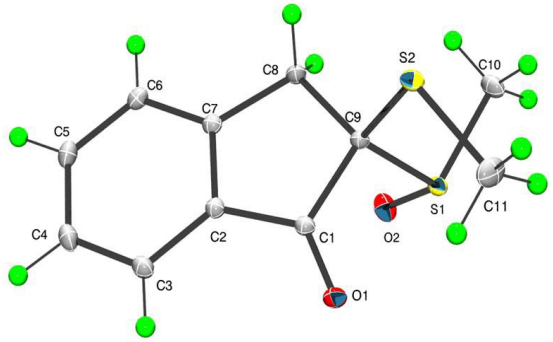

Figure 4. X-ray projection of (CS, SS) component of the pair of the 2-methylsulfanyl-2-methylsulfinyl-1-indanone racemic compound.

For comparison with homogeneous conditions, we establish the sulfanylation reaction of (**8**) using LiOH as base, CH_2Cl_2 as solvent and *S*-methylmethanethiolsulfonate as the sulfanylating agent. In this case, the reaction occurred faster than the first condition, and it was finished in 1 hour. The yields obtained were 93% and 90% diastereomeric excess.

The reduction of *S,S*-2-methylsulfanyl-2-methylsulfinyl-1-indanone (diastereoisomer mixture 10:0.8) using $NaBH_4$ was performed in metanol as solvent, isolating a unique diastereoisomer (**10**) in 70% yield and 90% of diastereomeric excess (Scheme 5).

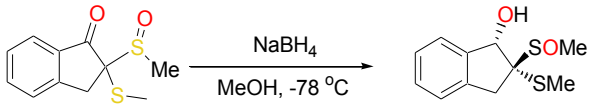

(**9**) (**7**)

Scheme 5. Reduction reaction of (±)-2-methylsulfanyl-2-methylsulfinyl-1-indanone (**9**).

The hydrogen bonded to C-1 was observed in the ^{1}H-NMR spectra, in the form of doublet at 5.58 ppm (*J*=12 Hz).

4. CONCLUSION

In this paper we demonstrated the asymmetric synthesis *SR* or *SS* of 2-methylsulfanyl-2-methylsulfinyl -1-indanone (**9**) optically enriched in good yield, but in excellent diastereomeric excess determined by nuclear magnetic resonance technique employing the Kagan reagent as chiral shift reagent.

Therefore, we showed the diastereoselective synthesis of *S,S*-2-methylsulfanyl-2-methylsulfinyl-1-indanol (**7**) by reduction reaction using 2-methylsulfanyl-2-methylsulfinyl-1-indanone (**9**) optically enriched demonstrating the high efficiency of the sulfoxide group on the control of asymmetric induction in the carbonyl addition reaction.

5. ACKNOWLEDGMENTS

The authors thank to the Fundação de Apoio ao Desenvolvimento de Ensino, Ciência e Tecnologia do Estado do Mato Grosso do Sul (Fundect), to the Coordenação de Aperfeiçoamento de Pessoal de Nível Superior (CAPES) and to the Conselho Nacional de Desenvolvimento Científico e Tecnológico (CNPq) for the financial support and fellowships offered for this research.

6. REFERENCES AND NOTES

[1] Starks, C. M. *J. Am. Chem. Soc*. **1971**, *93*, 195. [CrossRef]
[2] Lucchese, M.A. Marzorati, L. *Quim. Nova* **2000**, *5*, 23. [Link]
[3] Starks, C. M.; Liotta, C. L.; Halpern, M. *Phase-Transfer Catalysis*, Chapman & Hall, New York, **1994**. [CrossRef]
[4] Makosza, M. *Pure Appl. Chem.* **1975**, *43*, 439. [CrossRef]
[5] Pereira, M. M. *Div. Cat. Mat. Porosos* **2006**, *100*, 27.
[6] Liotta, C.; Burgess, E. M.; Ray, C. C.; Black, E. D.; Fair, B. E. *ACS Symp. Ser.* **1987**, *326*, 15. [CrossRef]
[7] Zini, C. A.; Von Holleben, M. L. A. *Quim. Nova* **1992**, *15*, 40. [Link]
[8] Dijkstra, G. D. H.; Kellogg, R. M. Wynberg, H. *Rec. Trav. Chim. Pays-Bas* **1989**, *108*, 195.
[9] Dolling, U-H.; Davis, P.; Grabowski, J.J. *J. Am. Chem. Soc.* **1984**, *106*, 446. [CrossRef]
[10] Merritt, B. A.; Erik, J.H.; Jeffrey C. S.; Karl D.B. *J. Org. Chem.* **2005**, *70*, *23*, 9470. [CrossRef]
[11] Veeraraghavan, P. R.; Sateesh M.; Laylka B.; Venkat R. R.; O`Donnel J. *J. Am. Chem. Soc.* **2005**, *127*, 13450. [CrossRef]
[12] Lygo, B.; Beynon, C.; Mcleod, M.C.; Roy, C.; Wade, C.E. *Tetrahedron* **2010**, *66*, 8832. [CrossRef]
[13] Shigeru, A.; Takayuki, S. *Tetrahedron* **1998**, *39*, 2148. [CrossRef]
[14] Solladié, G; Huser, N. *Tetrahedron Lett.*, **1994**, *35*, 5297. [CrossRef]
[15] Carreño, M. C. ; Garcia Ruano, J. L. *J. Org. Chem.* **1993**, *58*, 4529. [CrossRef]
[16] Carreño, M. C, *Chem Rev.* **1995**, *95*, 1717. [CrossRef]
[17] Andersen, K. K.; Patai, S. ; Rappoport, Z.; Stirling, C.J.M. *In The chemistry of Sulfones and Sulfoxides*, John Wiley &Sons; New York. **1988**.
[18] Ouazzani, H.E.; Khiar, N.; Fernandes, J.; Alcudia, F. Y. *J. Org. Chem.* **1997**, *62*, 287. [CrossRef]
[19] Pitchen, P.; Kagan, H. B. *Tetrahedron Lett.* **1984**, *25*, 1049. [CrossRef]
[20] Solladié, G.; Lohse. O. *J. Org. Chem.* **1993**, *58*, 4555. [CrossRef]
[21] Ogura, K.; Tsuruda,T.; Takahashi, K.; Hirotada, I. H.; *Tetrahedron Lett.* **1986**, *7*, *31*, 3665. [CrossRef]
[22] Fernandez, I.; Khiar, N.; Llera, J. M.; Alcudia, F. *J. Org.*

Chem. **1992**, *57*, 6789. [CrossRef]

[23] Carreño, M.C.; Ruano, G.J.L.; Rubio A. *Tetrahedron Lett.* **1987**, *28*, 4861. [CrossRef]

[24] *SS*-2-methylsulfinyl-1-indanone (**8a**): [α] 25D -73 (c = 1, CH_2Cl_2), m.p. 137-138 ºC, ^{1}H NMR (200 MHz, CDCl 3) (ppm): 2.88 (s, 3H, CH_3), 3.49 (dd, 1H, J=18, J=7.8), 3.79 (dd, 1H, J=18, J=3.0), 3.86 (dd, 1H, J=7.8, J=3.0), 7.43(dt, 1H, Ar, J=7.3), 7.56 (dd, 1H, Ar, J=7.3), 7.67 (dt, 1H, Ar, J=7.3 and 1.2), 7.78 (dd, 1H, Ar, J= 7.3) TOF MS ES$^+$ M/z calc.: 195.05, found: 195.03. *SR*-2-methylsulfinyl-1-indanone (**8b**): [α]25D +57 (c = 1, CH_2Cl_2) m.p. 136-138 ºC, ^{1}H NMR (200 MHz, $CDCl_3$) 2.88 (s, 3H, CH_3), 3.49 (dd, 1H, J=18, J=7.8), 3.79 (dd, 1H, J=18, J=3.0), 3.86 (dd, 1H, J=7.8, J=3.0), 7.43(dt, 1H, Ar, J=7.3), 7.56 (dd, 1H, Ar, J=7.3), 7.67 (dt, 1H, Ar, J=7.3 e 1.2), 7.78 (bd, 1H, Ar, J= 7.3), TOF MS ES$^+$ M/z calc.: 195.05, found: 195.03.

[25] *CS*,*SS*-2-methylsulfanyl-2-methylsulfinyl-1-indanone (**9a**): colorless solid, m.p. 96-98 °C, [α]25D + 78 (c = 1, CH_2Cl_2), ^{1}H NMR (200 MHz, $CDCl_3$) (ppm): 2.34 (3H, s), 2.82 (3H, s), 3.02 (1H, d, J = 18 Hz), 4.11 (1H, d, J = 18 Hz), 7.39 (dt, 1H, Ar, J=7.6), 7.49 (dd, 1H, Ar, J= 7.6), 7.64 (dt, 1H, Ar, J= 7.6), 7.80 (dd, 1H, Ar, J=7.6) ^{13}C NMR (ppm): 12.1, 32.1, 33.8, 70.0, 125.0, 126.3, 128.2, 134.2, 135.6, 150.4, 196.1. TOF MS ES$^+$ M/z calc.: 241, 03 found: 241,0385. *CR*,*SR*-2-methylsulfanyl-2-metilsulfinyl-1-indanone (**9b**); colorless solid, [α]25D -86 (c = 1, CH_2Cl_2), m.p. 95- 98 °C, ^{1}H NMR (200 MHz, $CDCl_3$) (ppm): 2.34 (3H, s), 2.82 (3H, s), 3.02 (1H, d, J = 18 Hz), 4.11 (1H, d, J = 18 Hz), 7.39 (dt, 1H, Ar, J=7.6), 7.64 (dt, 1H, Ar, J=7.6), 7.80 (dd, 1H, Ar, J=7.6)) ^{13}C NMR (ppm): 12.1, 32.1, 33.8, 70.0, 125.0, 126.3, 128.2, 134.2, 135.6, 150.4, 196.1. TOF MS ES+ M/z calc.: 241, 03 found: 241,03.

[26] *Ss*-2-methylsulfanyl-2-metilsulfinyl-1-indanol: colorless liquid, [α]25D + 7 (c = 1, D_2O) ^{1}H NMR (200 MHz, $CDCl_3$) (ppm): 2.74 (3H, s), 2.21 (3H, s), 5.59 (1H, s), 5.87 (1H, wide singlet, change with D_2O), 2.85 (1H, d , J = 14 Hz), 3.07 (1H, d, J = 14 Hz), 7.17-7.41 (4H, m, Ar). ^{13}C NMR (50 MHz, D_2O) (ppm): 13.01, 34.08, 33.77, 76.42, 78.18, 124.37, 124.54, 127.83, 128.76, 136.62, 141.80. E. A. calc.: C = 54.51 % H= 5.82%, found: C = 54.59 % H= 6.21%.

[27] Scholtz, D. *Synthesis* **1983**, 944.

[28] Douglass, I. B.; Norton, R.V. *J. Org. Chem.* **1968**, *33*, 210. [CrossRef]

[29] Wladislaw, B.; Bueno, M. A.; Marzorati, L.; Di Vitta, C.; Zukerman-Schepector, J. *J. Org. Chem.* **2004**, *69*, 9296. [CrossRef]

Orbital: The Electronic Journal of Chemistry
journal homepage: www.orbital.ufms.br
ISSN 1984-6428

| Vol 5 | | No. 1 | | January-March 2013 |

Review

A Review of the Synthetic Strategies for the Development of BODIPY Dyes for Conjugation with Proteins

Lucas C. D. de Rezende and Flavio da Silva Emery*

Faculdade de Ciências Farmacêuticas de Ribeirão Preto - Universidade de São Paulo. Av. do Café s/n, Ribeirão Preto-SP, 14040-903, Brazil.

Article history: Received: 12 March 2013; revised: 28 March 2013; accepted: 02 April 2013. Available online: 17 April 2013.

Abstract: Conjugation of fluorophores to proteins is fundamental to several biotechnological applications and in the last decades boron-dipyrromethene (BODIPY) dyes started to be used in this field. BODIPYs are dipyrrin derivatives complexed to difluoroboryl that possesses several attractive photophysical properties. Herein we reviewed the synthetic methodologies published by academic and non-academic research groups aiming the obtainment of reactive BODIPY derivatives for conjugation with proteins.

Keywords: BODIPY; fluorophore; synthesis; protein; bioconjugation

1. INTRODUCTION

Fluorescence was discovered in the 16th century and is the non-thermal emission of light by molecules in a singlet excited state [1]. With the development of fluorescence spectroscopy, flow cytometry and fluorescent-based image techniques in the last few decades of the 20th century, fluorescent chemicals (fluorophores or fluorochromes) have become suitable research tools [2, 3]. In this context, interest in the synthesis of fluorescent compounds has grown dramatically, and there are several fluorescent dyes with variable photophysical properties that can be obtained commercially (e.g. BODIPY FL, BODIPY TMR, BODIPY TR, BODIPY R6G).

4,4-difluoro-4-bora-3a,4a-diaza-s-indacene, also known as boron-dipyrromethene and BODIPY (which will be used hereafter), consists of a group of fluorescent dyes first synthesized by Treibs and Kreuzer in 1968 [4]. This class of fluorophores exhibits interesting properties, such as high stability, sharp fluorescence peaks, tunable emission and high quantum yields. Although BODIPYs have been known for a long time, only after the publication of a patent [5] in 1988 by Molecular Probes®, which is a company founded by Professor Richard Haugland and later incorporated by Life Technologies™, did the technological applications of BODIPY as a biomolecule label begin to increase. This patent was a turning point in the application and study of BODIPYs, and some of its synthetic approaches will be discussed in this review. No commercial interests involving the authors and this, or any other, company exists, and the discussions within the text are only for academic purposes.

Symmetric BODIPYs can be obtained from the condensation of two identical pyrrolic units and a carbonyl compound (aldehyde or acyl chloride) in a reaction catalyzed by a strong acid, which is commonly hydrobromic acid (HBr) or trifluoroacetic acid (TFA) (Figure 1). This reaction yields a dipyrromethane substituted by the structure previously linked to the carbonyl reagent at the central position (meso position). The dipyrromethane is aromatized (chloranil or DDQ are commonly used) resulting in a dipyrromethene (or dipyrrin) that is ultimately converted to the BODIPY by complexation with a difluoroboryl unit in a base-catalyzed reaction with trifluoroboryl etherate ($BF_3.OEt_2$), classically using triethylamine (TEA). Non-meso-substituted BODIPYs can be obtained using two different pyrrolic units where one of them contains a carboxyaldehyde group at C2 position of the pyrrolic ring. The reaction is catalyzed by phosphoryl chloride and directly yields the dipyrrin, which is subsequently converted to BODIPY by the same method discussed earlier (Figure 1).

In the last 20 years, thousands of structurally diverse BODIPYs have been synthesized

* Corresponding author. E-mail: flavioemery@fcfrp.usp.br

and applied in several studies [6]. BODIPYs have a widely range of application in biochemistry, biophysics and biotechnology with protein labeling being one of the most common uses. Because of the lack of available organized literature in the synthesis of reactive BODIPY dyes for protein labeling, we will review the state of the art synthetic methods for obtaining reactive BODIPY dyes described in the literature and the applicability of such compounds as protein labels. The subjects are organized by the reactive chemical functionalities and their specific target in the field of protein labeling (Table 1). Through the text academic and commercial syntheses of BODIPYs are shown, which reflects the importance of the subject for both basic and applied sciences.

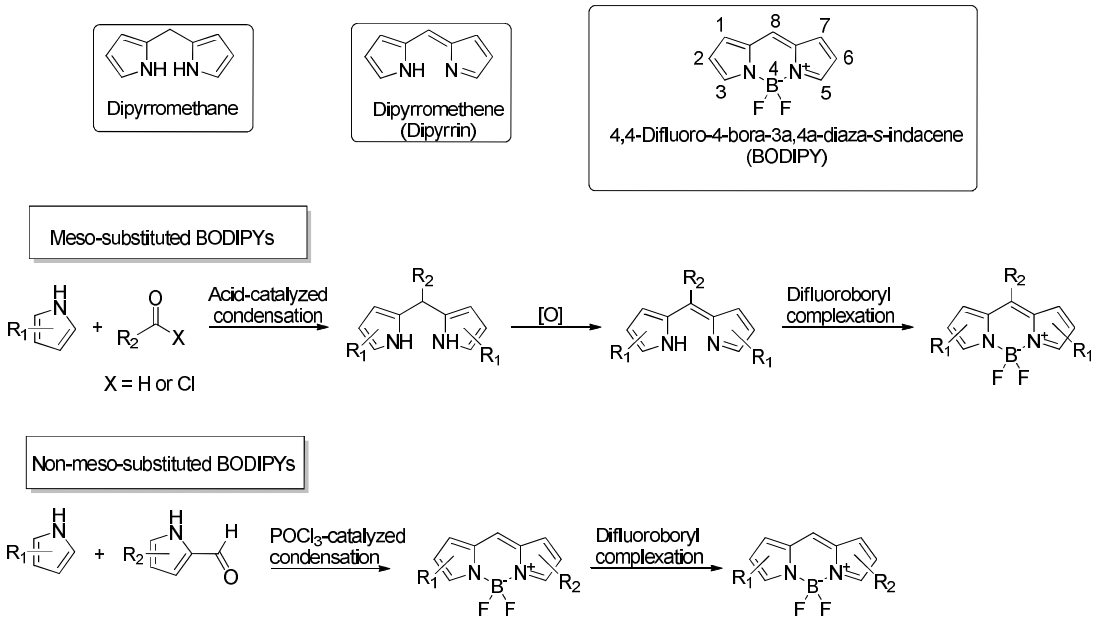

Figure 1. Chemical structures of dipyrromethane, dipyrromethene and BODIPYs, and the general approaches for the synthesis of BODIPYs.

Table 1. Overview of the functionalities addressed in this review.

Reactive Functionality	Main protein target	Linkage type
Succinimidyl Ester	Amine group (Lysines)	Amide
Isothiocyanate	Amine group (Lysines)	Thiourea
Iodoacetamide	Sulfhydryl group (Cysteine)	2-mercaptoacetate
Maleimide	Sulfhydryl group (Cysteine)	Mercaptopyrrolidinone
Thiosulfate/Thiosulfonate	Sulfhydryl group (Cysteine)	Disulfide Bond
Hydrazine/Hydrazide	Ketone/Aldehydes (Bioorthogonal coupling)	Hydrazone
Hydroxylamine	Ketone/Aldehydes (Bioorthogonal coupling)	Oxime
Azide	Alkynes (Bioorthogonal coupling)	1,2,3-triazole
Alkyne	Azides (Bioorthogonal coupling)	1,2,3-triazole
Imidazole	Phosphate (Phosphorylated amino acids)	Phosphoroimidazolide
Diacrylate	Arg-Cys-X-X-Cys-Arg (RC peptide tag)	Michael adduct/ Hydrogen Bond

2. SUCCINIMIDYL ESTER BODIPY DYES

Succinimidyl ester is undoubtedly the most used motif for conjugation of BODIPYs to amine-containing structures including proteins. Its use in protein manipulation began during the early 1960s, when results from the use of succinimidyl ester in the elongation of peptide chains were published [7]. For many years, N-hydroxysuccinimide and its ester derivatives were applied in the synthesis of several peptides acting as a carboxy-activating group. The

reactivity of succinimidyl ester toward amines in the lateral chains of amino acid residues (specifically lysines) was also explored for the acylation of proteins [8], and the high reactivity of succinimidyl ester toward protein amines boosted its application in protein labeling. Early application of this methodology involved the labeling of proteins with acyl chains containing heavy metals, such as mercury, for x-ray crystallographic investigations [9], radioactive isotopes, such as iodine-125 [10], tritium [11], and Carbon-14 [12], for radioactive-based assays and fluorescent molecules, such as fluorescein [13].

Classically, succinimidyl ester reacts with amines forming an amide bond and releasing N-hydroxysuccinimide as a leaving group (Figure 2). The acylation of sulfhydryl or hydroxy containing compounds that form thioester bonds and ester, respectively, does not yield stable compounds due to their rapid hydrolysis or exchange with amines, which explains the selectivity of the method. An extensive list of succinimidyl ester BODIPY applications would be tedious and beyond the scope of this review, but we find it interesting to exemplify its uses throughout the text. In general, the simple stirring of a protein solution with the ester in DMSO at room temperature for 30 minutes to 4 hours is enough for the conjugation to occur. Purification with HPLC or dialysis against deionized water yields the pure fluorescent protein.

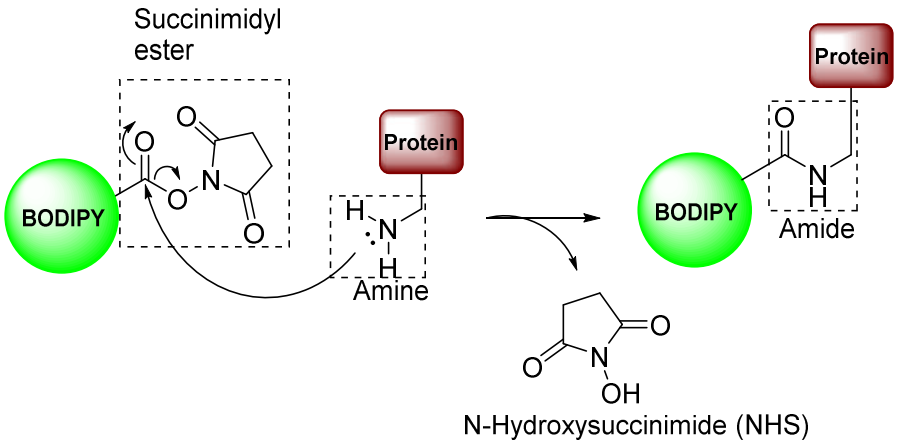

Figure 2. Mechanism of amine labeling with succinimidyl ester derivatives.

Several BODIPY compounds containing a succinimidyl ester reactive group have been synthesized by academic and industrial research groups. The first synthesis of a BODIPY-succinimidyl ester was published in a 1988 patent by Molecular Probes® [5], which reported the synthesis of three BODIPY derivatives. The approach involved the coupling of an ester-substituted pyrrole with a pyrrole carboxyaldehyde unit yielding a dipyrromethene, which, after complexation with $BF_3.OEt_2$, generated the BODIPY linked to the ethyl ester. The hydrolysis of this product with an aqueous solution of K_2CO_3 released the carboxyl group that was then coupled with N-hydroxysuccinimide (NHS) (Figure 3). Currently, dozens of succinimidyl ester BODIPY derivatives with various spectral characteristics are commercially available.

An example of the application of commercially available succinimidyl ester BODIPY dyes is the labeling of casein, which is a simple protein that serves as a substrate to several endoproteases. Due to the release of the fluorophore, initially linked to the protein, the fluorescent signal is enhanced after protein cleavage. Therefore, the conjugated protein was successfully applied as novel substrates for protease assays via fluorescence spectroscopy [14, 15]. Surfactant protein B (SP-B), which is a pulmonary surfactant protein, was another fluorescent protein conjugated to a commercially available succinimidyl ester BODIPY. This protein is important for preventing the alveoli from collapsing, and its fluorescent derivative was developed to monitor distribution of surfactants administered to patients with respiratory problems related to pulmonary surfactant production [16].

The synthesis and application of asymmetric BODIPY derivatives bearing succinimidyl ester using similar methods have also been reported by various

research groups. Meltola et al. synthesized a small library of BODIPY compounds with the succinimidyl ester group, also using carboxylic substituted BODIPY and NHS/CCD [17]. The compounds synthesized in this work showed variable emission characteristics due to extension of the conjugated system resulting from the substitution of one pyrrole unit with aryl-, heteroaryl-, and arylethenyl substituents. To raise the hydrophilicity of these compounds, they were modified by insertion of a hydrophilising dipeptide linker followed by addition of NHS/DCC (Figure 4). The performance of these molecules for the biolabeling of mouse monoclonal IgG antibodies was studied under various conditions and showed good reactivity. Similar synthetic strategies using NHS and DCC for the coupling of carboxyl-functionalized BODIPYs have been used for applications beyond biolabeling. However, we will not review all of the synthetic routes in detail.

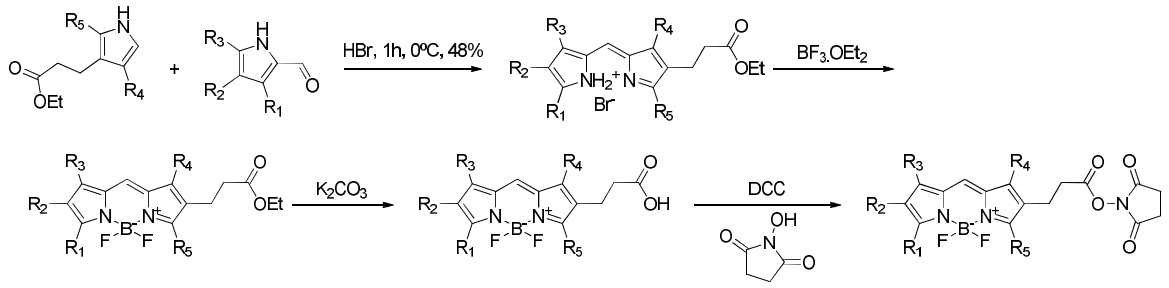

Figure 3. Synthetic route to a BODIPY derivative functionalized with a succinimidyl ester reactive group, which was first published in a patent by molecular probes[5].

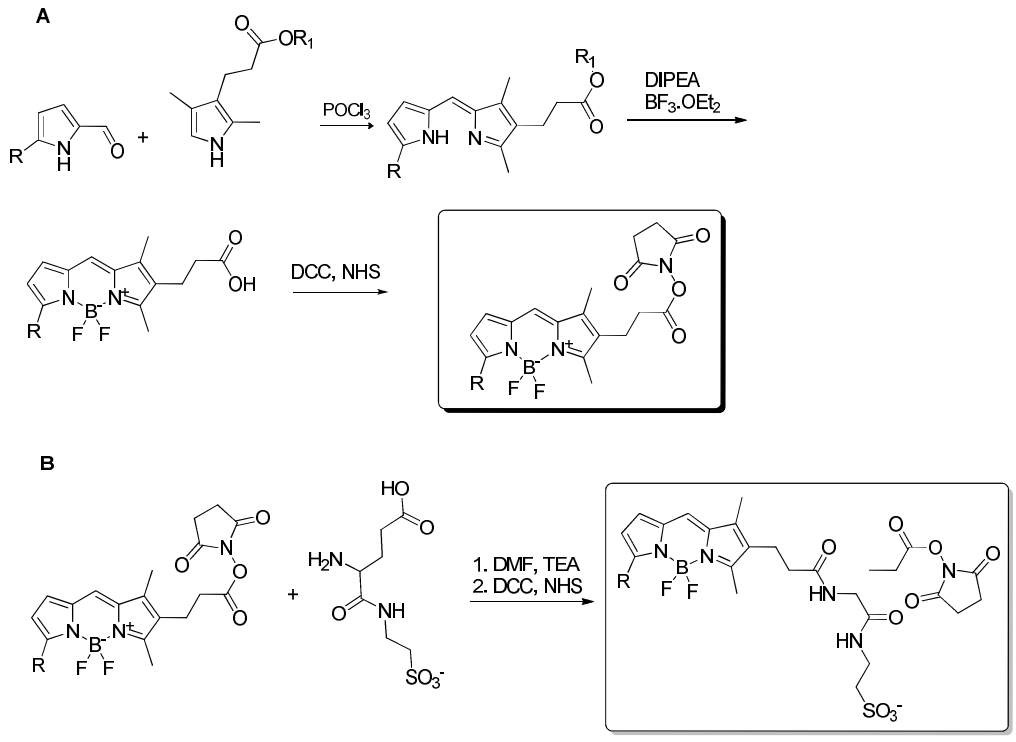

Figure 4. **A**: Synthetic approaches for obtaining a small library of BODIPYs functionalized with N-succinimidyl ester [17]. **B**: Insertion of a hydrophilising dipeptide linker [17].

The synthesis of symmetric BODIPY using ester-substituted benzaldehyde [18] or cyclic anhydride [19] has also been applied to the synthesis of succinimidyl ester functionalized BODIPY derivatives (Figure 5). These compounds were functionalized with an amino reactive moiety using NHS/DCC or N,N'-disuccinimidyl carbonate (DSC). No applications of these compounds for protein

labeling have been reported. Because this reactive moiety is widely used in protein manipulation, its application in this field may allow for the desired coupling.

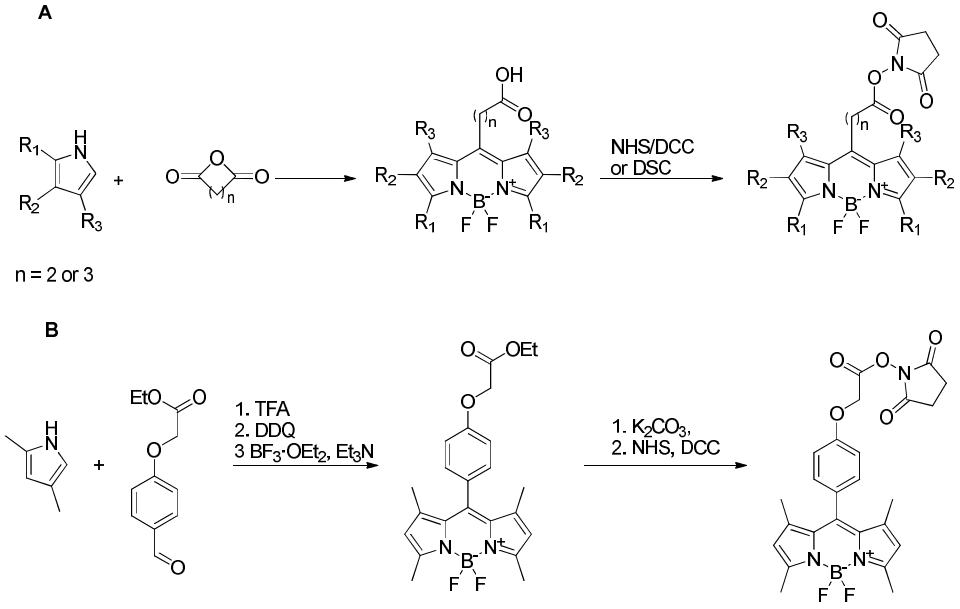

Figure 5. **A**: Synthesis of a symmetric BODIPY from bicarboxylic anhydrides and functionalization with succinimidyl ester [19]. **B**: Synthesis of a symmetric meso-aromatic-substituted BODIPY derivative and functionalization with succinimidyl ester.

3. ISOTHIOCYANATE BODIPY DYES

The electrophilic character of the central carbon in isothiocyanate is usually explored as a reactive group for biologic nucleophiles. This group is reactive toward nucleophilic attack of amines, resulting in the formation of a thiourea linkage (Figure 6). Compounds bearing this group were discovered at the beginning of the 20th century, and their application in biolabeling was first proposed in 1958 as a substituent for isocyanate, which was commonly used for the conjugation of rhodamine and fluorescein to antibodies [20].

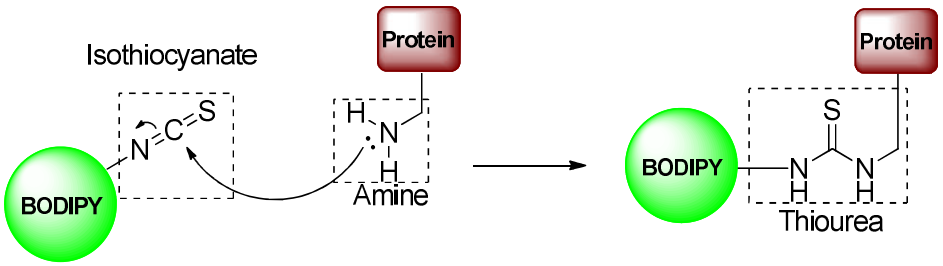

Figure 6. Mechanism of amine labeling with isothiocyanate derivatives.

For BODIPY derivatives, the first published BODIPY isothiocyanate synthesis was reported in a molecular probes patent from 1988 [5]. Although this company does not commercialize any isothiocyanate, claiming they have poor stability, it is commercially available from other companies. The synthetic route reported in this 1988 patent uses the succinimidyl ester derivative, which was previously discussed, as the starting material [5]. The reaction of the succinimidyl ester BODIPY with ethylenediamine yielded an amino-amido-BODIPY, which was converted to the isothiocyanate using thiophosgene [5] (Figure 7).

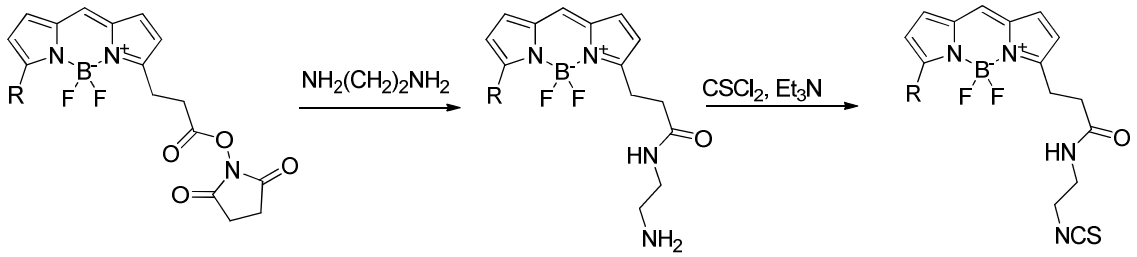

Figure 7. BODIPY dye functionalized with an isothiocyanate, which was first published in a patent by molecular probes [5].

A similar approach was applied by Meltola et al. in an article published in 2004 [21]. A BODIPY containing two propionic acids appended to its core was synthesized from a tetra-substituted pyrrole. Initially, HBr and formic acid were used to obtain the dipyrrin that was complexed with $BF_3.OEt_2$. The free carboxylic function was coupled to N-hydroxy succinimide using only DCC as the catalyst. Then, the active carboxylic function was coupled with 4-(2-aminoethyl)-aniline to yield a BODIPY dye with a free amine group, which was converted to isothiocyanate with thiophosgene in a basic medium (Figure 8). A 10-fold excess of the synthesized fluorophore was incubated for 2 hours with an IgG antibody in basic pH followed by size-exclusion chromatography to obtain the pure product. Particularly, in this study, more efficient conjugation to the antibody was observed for the succinimidyl ester BODIPY dye compared to that observed with the isothiocyanate derivative.

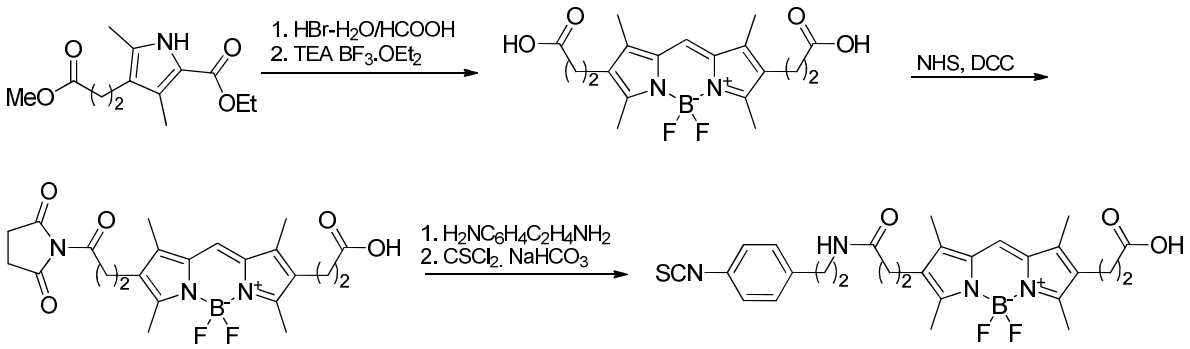

Figure 8. Another approach for the synthesis of isothiocyanate BODIPY dye from a succinimidyl ester BODIPY dye [21].

Another approach for the synthesis of isothiocyanate derivatives involves the production of nitro substituted BODIPY followed by the reduction of the nitro compound to the respective amine, which can be modified to generate the isothiocyanate. This methodology is often used in the literature, and the conversion of symmetric anilino-BODIPYs to the respective isothiocyanate is widely reported. The proposed syntheses in these studies can be grouped into three paths, which will be referred to paths A, B and C (Figure 9). Paths B and C starts with the coupling of nitrobenzaldehyde with pyrrole, resulting in a dipyrromethane. In approach C, the nitro group in the dipyrromethane is reduced to an amine that is then protected with Fmoc [22]. Next, the dipyrromethane is oxidized to the respective dipyrromethene, followed by boron complexation and amine deprotection. In approach B, the dipyrromethane is readily oxidized to the dipyrromethene and complexed with boron fluoride to generate the nitro-BODIPY [23]. Then, this compound is reduced to the respective amine. In approach A, the dipyrromethene is directly synthesized using nitrobenzoyl chloride as the carbonyl compound in the reaction with pyrrole [24]. Similar to the previous discussion, after the reaction with $BF_3.OEt_2$, a nitro BODIPY is obtained and then reduced to the respective amine. Instead of using thiophosgene, which involves several safety issues, 1,1'-thiocarbonyldi-2(1H)-pyridone (TDP) is used in the preparation of isothiocyanate BODIPYs.

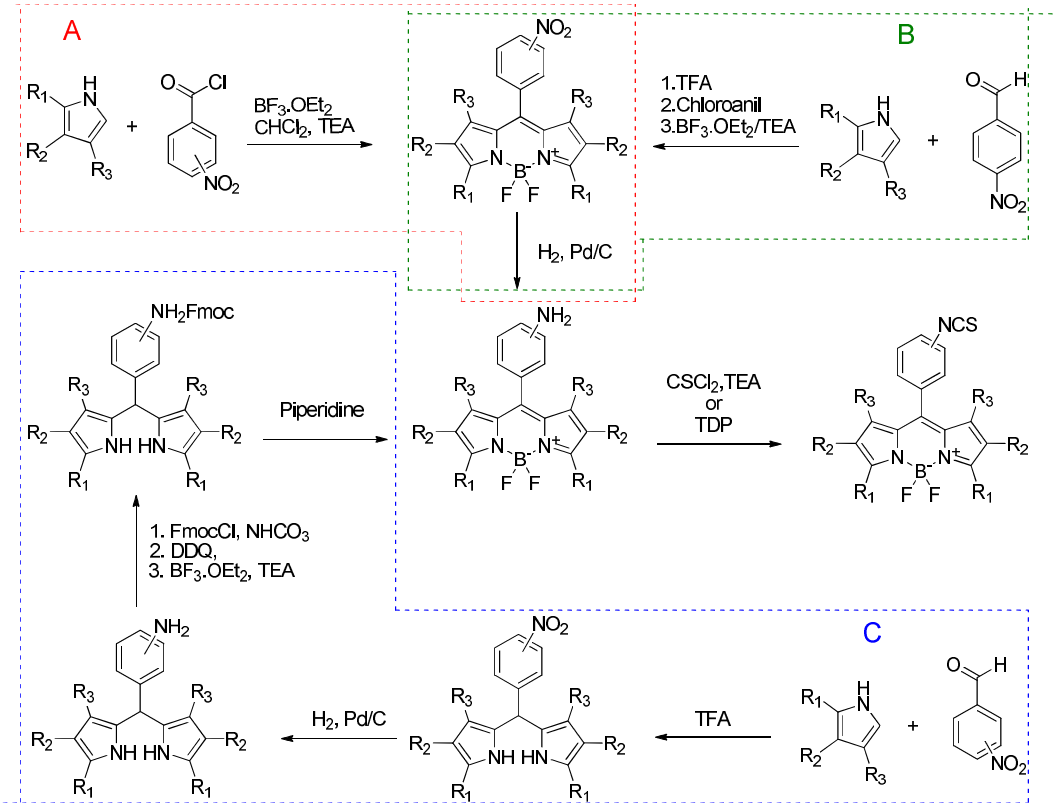

Figure 9. Synthesis of symmetric isothiocyanate BODIPY dyes from nitro-aromatic aldehydes.

4. IODOACETAMIDE BODIPY DYES

Iodoacetamides are member of the haloacetamide group, and is recognized for decades to be very reactive toward sulfhydryl groups [25]. Regarding protein reactivity, this chemical motif can react with several amino acid side chains, resulting in alkylated amino acids with a terminal primary amide. The direct linkage to an amide and a halogen makes the alpha carbon very electrophilic and very susceptible to attack by the nucleophiles present in protein functionalities. In particular, this moiety is reactive toward the sulfhydryl groups of cysteines, however, it can react with other nucleophiles in amino acids, in the following order of decreasing reactivity: imidazolyl of histidines, thioether of methionines and amines from lysines (Figure 10). Among the haloacetamides, iodoacetamides are the more reactive compounds, followed by bromoacetamides, chloroacetamides and fluoroacetamides (almost unreactive). This reactivity accounts for the widespread use of iodoacetamides for bioconjugations [26]. In practice, the specificity for sulfhydryl alkylation can be enhanced by using a limiting amount of haloacetamide and a slightly alkaline pH.

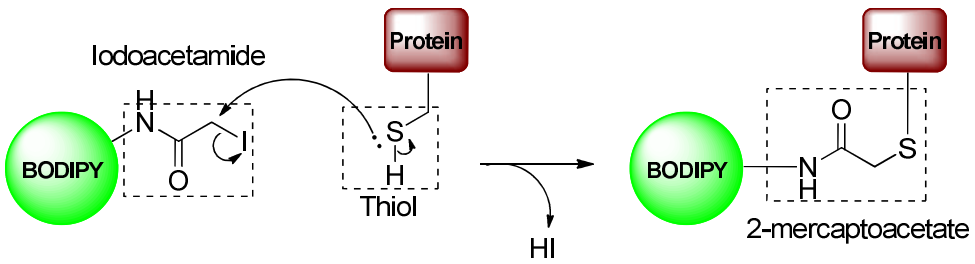

Figure 10. Mechanism of sulfhydryl labeling with iodoacetamide derivatives.

In the patent filed by molecular probes in 1988, the synthesis of a BODIPY dye functionalized with iodoacetamide was reported[5]. Similar to the isothiocyanate BODIPY that was discussed earlier, the synthetic approach for generating the thio-reactive fluorochrome involves the use of a BODIPY functionalized with a succinimidyl ester precursor. The coupling of the free amine from cadaverine monotrifluoroacetamide with an activated carboxylic group yielded a BODIPY containing a trifluoroacetamide function at the end of the five-carbon chain, which was linked to the BODIPY core via an amide linkage. The hydrolysis yielded the deprotected amine. Finally, the iodoacetamide function was added to the compound with *para*-nitrophenyl iodoacetate, which is a suitable iodoacetamide donor due to the electron-withdrawing effect of the *para*-nitro group. In this reaction, the amine attacks the carbonyl, resulting in the formation of BODIPY iodoacetamide and a *para*-nitrophenol as a byproduct (Figure 11).

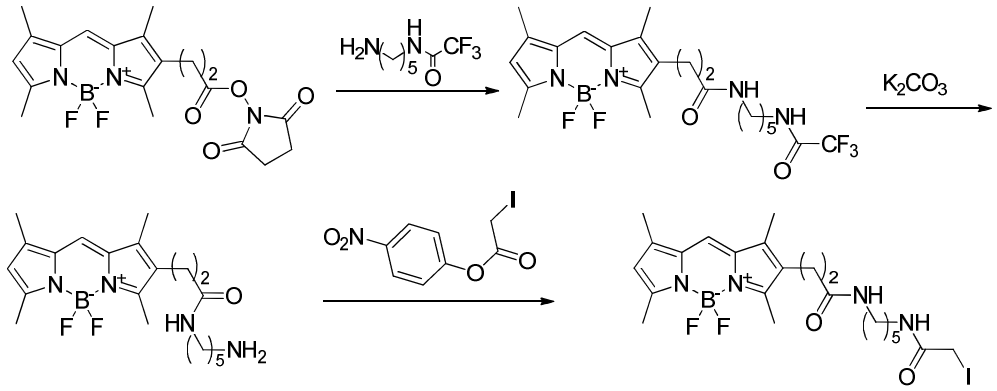

Figure 11. Synthesis of the first BODIPY dye functionalized with iodoacetamide, which was patented by molecular probes[5].

Molecular probes currently produces two iodoacetamide-BODIPY derivatives (i.e., BODIPY 507/545 IA and BODIPY FL C1-IA). Some studies applied BODIPY iodoacetamide compounds produced by this company that are now discontinued (i.e., BODIPY® 530/550 IA, BODIPY® FL IA and BODIPY® TMR CADAVERINE IA). To study the effect of fluorophores on protein dynamics, bovine serum albumin (BSA) was modified at Cys34 using a commercially available iodoacetamide BODIPY by simply stirring equimolar quantities of BODIPY and BSA in DMSO for 8 hours at 4ºC [27]. Using similar conditions, plasminogen activator inhibitor I, which is a protein that modulates fibrinolytic activity in human blood, was also labeled with a commercial BODIPY carrying an iodoacetamide to study the important interaction sites responsible for inhibition in the protein [28].

Another iodoacetamide-BODIPY has also been described in the literature. Using a different methodology from the described above, the compound was synthesized to couple the fluorophore to sulfhydryl groups, in the side-chain of two cysteine residues in a heptapeptide designed to target peroxisomes. The synthetic procedure is not fully described in the manuscript, but the approach involved the use of 2-iodoacetamide and a BODIPY dye with a carboxyl group activated by a succinimidyl ester to obtain the thioreactive BODIPY with an N-iodoacetylacetamide group [29] (Figure 12).

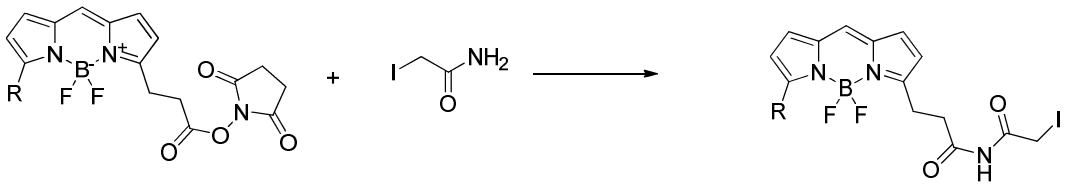

Figure 12. Use of 2-iodoacetamide for the functionalization of a succinimidyl ester-containing BODIPY to obtain an iodoacetylacetamide functionality [29].

It is interesting to note that, in addition to the synthesis of BODIPY derivatives containing the iodoacetamide functionality for sulfhydryl coupling, the synthesis of a chloroacetamide BODIPY has been reported. In general, this functionality is under-explored in bioconjugation reactions, moreover in this case it was applied in the study of polyamine transport [30]. The synthetic procedure involved the use of an aniline-substituted BODIPY obtained from the catalytic hydrogenation of a *para*-nitrophenyl BODIPY, which is similar to the above described methodology for preparation of isothiocyanate BODIPY. 3-Ethyl-2,4-dimethylpyrrole and 4-nitrobenzaldehyde were coupled with catalytic quantities of TFA followed by aromatization with DDQ to yield the respective dipyrrin, which was used to obtain the respective BODIPY after complexation with $BF_3.OEt_2$. The aniline-substituted BODIPY was coupled with chloroacetyl chloride to yield a reactive chloroacetamide BODIPY (Figure 13).

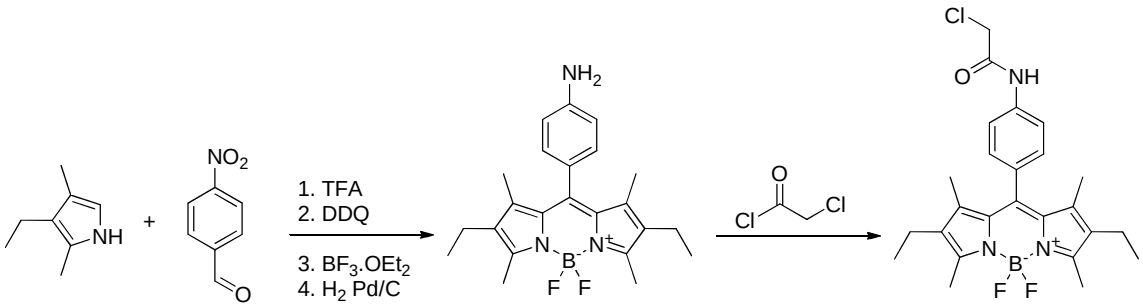

Figure 13. Synthesis of a BODIPY dye functionalized with chloroacetamide from aniline-substituted BODIPY and chloroacetyl chloride [30].

5. MALEIMIDE BODIPY DYES

Maleimide is a 2,5-pyrroledione known since mid-twentieth century to react rapidly and specifically with sulfhydryls [31]. At a pH near 7, maleimide tends to form Michael adducts specifically with sulfhydryl groups in spite of amine or hydroxyls, which would only happen in higher values of pH (Figure 14). Therefore, maleimide derivatives have been extensively applied for the manipulation and analysis of proteins with cysteine [32].

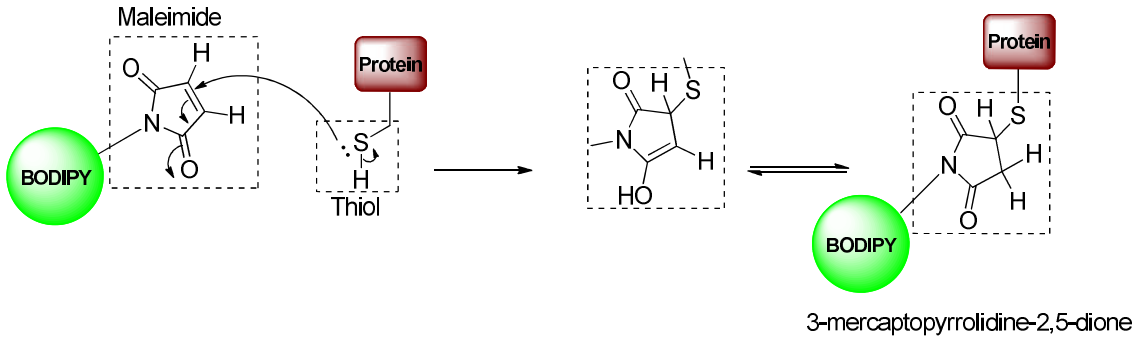

Figure 14. Mechanism of sulfhydryl labeling with maleimide derivatives.

In another molecular probes patent filed in 1993, the synthesis of a BODIPY dye functionalized with maleimide was reported [33]. Again, the synthetic route reported in the patent started with a succinimidyl ester-BODIPY. This amino-reactive BODIPY was employed in a reaction with ethylenediamine resulting in a BODIPY with a free amine group, which reacted with N-succinimidyl maleimidoacetate, a crosslinking reagent that inserts a maleimide group into the molecule via an amide

linkage (Figure 15).

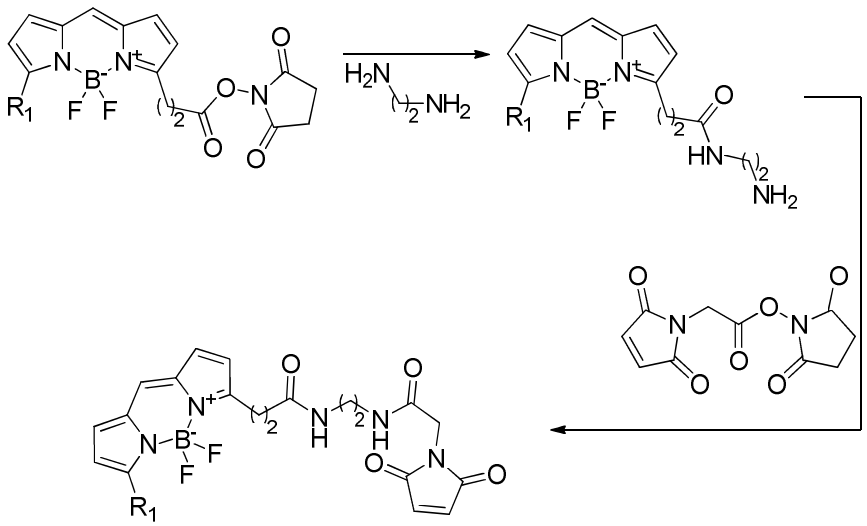

Figure 15. Synthesis of the first BODIPY dye functionalized with maleimide, which was patented by molecular probes [33].

Commercially available BODIPYs with the maleimide group have been employed in the conjugation of proteins (e.g., glyceraldehyde-3-phosphate dehydrogenase (GAPDH)). Equimolar quantities of the maleimido-BODIPY and GAPDH were incubated for 4 hours in an ice bath with a phosphate buffer solution followed by dialysis against the same buffer. The conjugation was developed to standardize a novel fluorimetric assay to quantify reactive thiols in biological samples [34]. Fluorescence quantification of the fluorophore followed by protein quantification provided a rough estimative of the thiol groups in the sample.

A Japanese group in 2007 reported the synthesis of another maleimide BODIPY dye. Again, BODIPYs containing an aniline group were employed in the synthesis of a thio-reactive fluorophore. Three isomeric compounds were synthesized by this approach. 2,4-Dimethyl pyrrole was coupled with nitro-benzaldehyde in the presence of TFA, followed by aromatization with DDQ, classic complexation with $BF_3.OEt_2$ and catalytic hydrogenation. To obtain the desired compound, the amino-BODIPY reacted with maleic anhydride to form a maleic acid appended to the BODIPY core by an amide linkage. The maleimide motif is achieved after dehydrative cyclization catalyzed by acetic anhydride and sodium acetate [35] (Figure 16).

Starting from different nitro-benzaldehydes, three isomers differing only in the position of the maleimide in the ring were obtained in the above described methodology. The ortho compound was found to have low fluorescence, which is most likely due to a photoinduced electron transfer phenomenon [35]. Interestingly, the reaction with free thiol prevented the electron transfer due to the extinction of the double bound resulting in the restoration of the BODIPY fluorescence. The authors propose that this probe would most likely exhibit a high signal-to-noise ratio due to these characteristics. The conjugation with BSA was realized in phosphate buffer at 37ºC, and the obtained product exhibited high fluorescence intensity and low rates of non-specific fluorescence [35].

The synthesis of a BODIPY dye bearing a maleimide group using a hydrazide-BODIPY as the starting material was also reported. This approach resulted in a BODIPY with an acyl hydrazone bridge between the fluorescent core and the maleimide group [36]. This synthesis was part of an interesting strategy to study the lability of the acyl hydrazone linker to the pH of endosomes containing folate-receptors (FR). A commercially available hydrazido-BODIPY was employed in a reaction with 4-maleimidophenylacetic acid resulting in the desired BODIPY. This BODIPY was linked to the sulfhydryl group of a cysteine that was already linked to a dark quencher and folic acid. If the acyl hydrazone linker was labile to the pH inside this endosomes, this probe was designed to

fluoresce only inside of FR-containing endosomes (Figure 17).

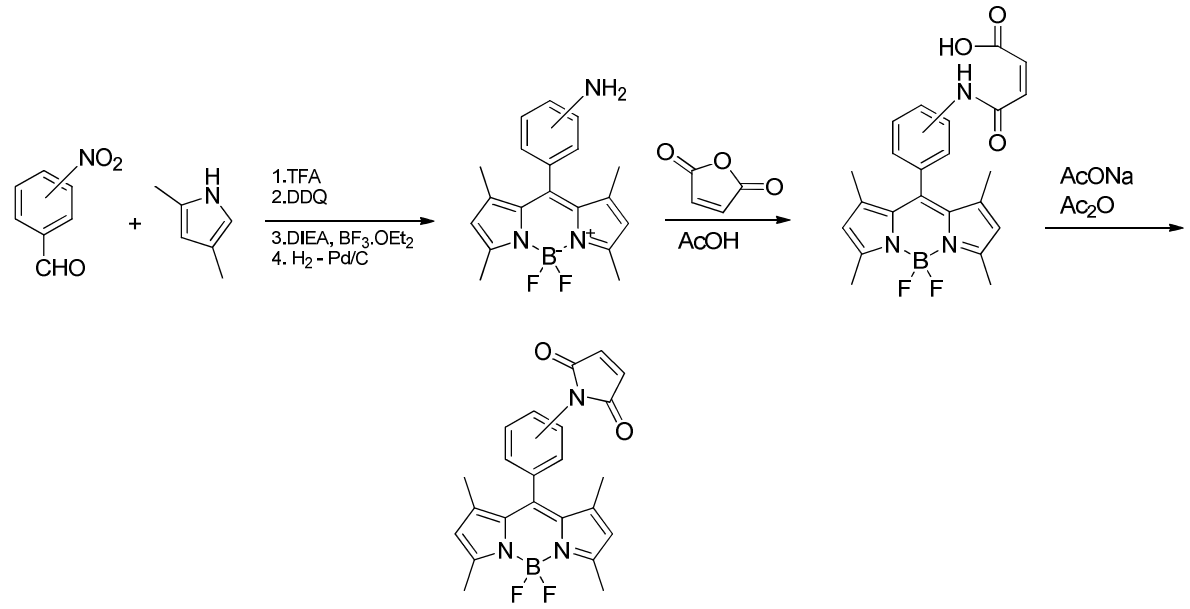

Figure 16. Synthesis of three isomeric BODIPY dyes containing the maleimide moiety using a meso-aniline-substituted precursor [35].

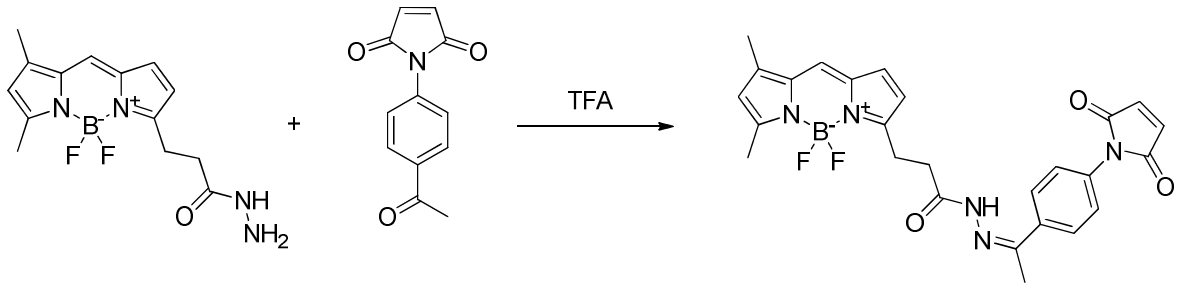

Figure 17. Synthetic procedure for obtaining a maleimide BODIPY dye from a commercially available hydrazide BODIPY [36].

6. THIOSULFATE AND THIOSULFONATE BODIPY DYES

Thiosulfate and thiosulfonate are derived from thiosulfuric and thiosulfonic acids, respectively, by alkylation at a sulfur atom. They differ from sulfonate and sulfate functions due to the exchange of an oxygen atom for a sulfur atom. The linkage between the two sulfur atoms is quite labile and tends to exchange with free thiols to generate a disulfide bond leaving sulfite or sulfinate. An interesting feature of these reactive groups is the reversibility of the disulfide bond they generate, which is different from the highly stable thioether bond. Common reducing reagents, such as dithiothreitol (DTT) and tris(2-carboxyethyl)phosphine (TCEP), can be used to break the disulfide bond (Figure 18).

Applications of thiosulfates and thiosulfonates date back to the 1970s with methyl methanethiosulfonate (MTS), which is a reagent known for its capacity to modify cysteine by inserting a methyl group at the sulfur atom [37]. These moieties were widely used to conjugate compounds as site-directed spin-labels [38], markers for electron microscopy [39] and fluorescent probes [40].

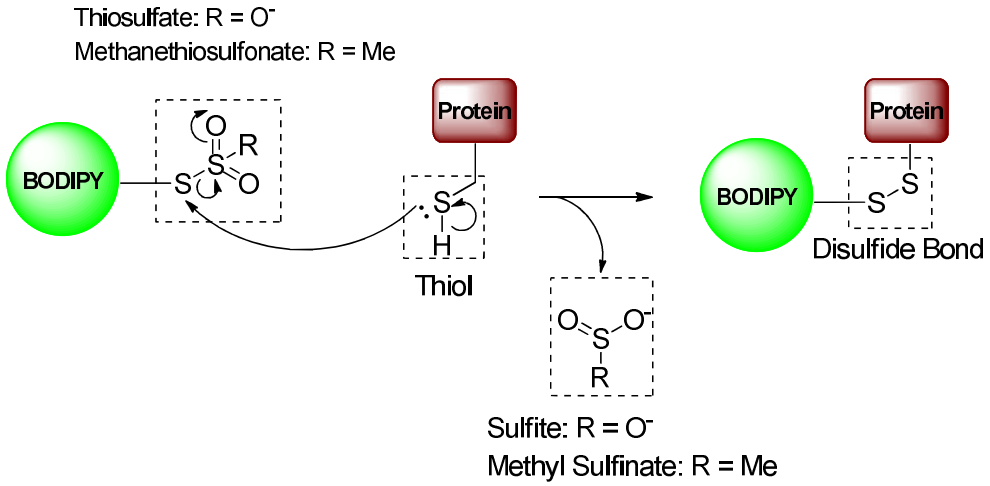

Figure 18. Mechanism of sulfhydryl labeling with thiosulfate and methanethiosulfinate derivatives.

Recently, a patent by molecular probes [41] exclusively addressed compounds containing the thiosulfate moiety and reported the preparation of BODIPY dyes bearing this funcionality. The applied approach involved the use of a reactive compound (i.e., 1,2,4,5-tetrafluorophenoxycarbonylmethyl thiosulfate), whose synthesis was also reported in the patent. From the reaction between sodium thiosulfate and alpha-bromoacetic acid, a carboxylic acid containing the thiosulfate functionality was obtained. This compound was coupled via an ester bond to 1,2,4,5 tetrafluorophenyl in a base-catalyzed reaction using tetrafluorophenyl trifluoroacetate as the initial reagent (Figure 19). The reactive compound obtained was employed in a reaction to transfer its thiosulfateacetyl group to an aminated BODIPY, which was described earlier in this review.

Thiosulfate BODIPY dyes were commercially available from molecular probes but have been discontinued. A commercial thiosulfate BODIPY dye [42] has been used for labeling a cysteine residue at the C-terminal end of the peptide pHLIP. Unfortunately, the conjugation methodology was not presented in detail, but the rationale behind the choice of conjugation method can be elucidated. pHLIP is known to exhibit pH-controlled insertion in cell membranes, and the authors were interested in assaying for peptide insertion. If the peptide is inserted through the membrane, the labeled cysteine would be in the cytoplasm. Once the disulfide bond was cleaved by the cytoplasm environment, the retention of the fluorophore would provide insight into peptide insertion.

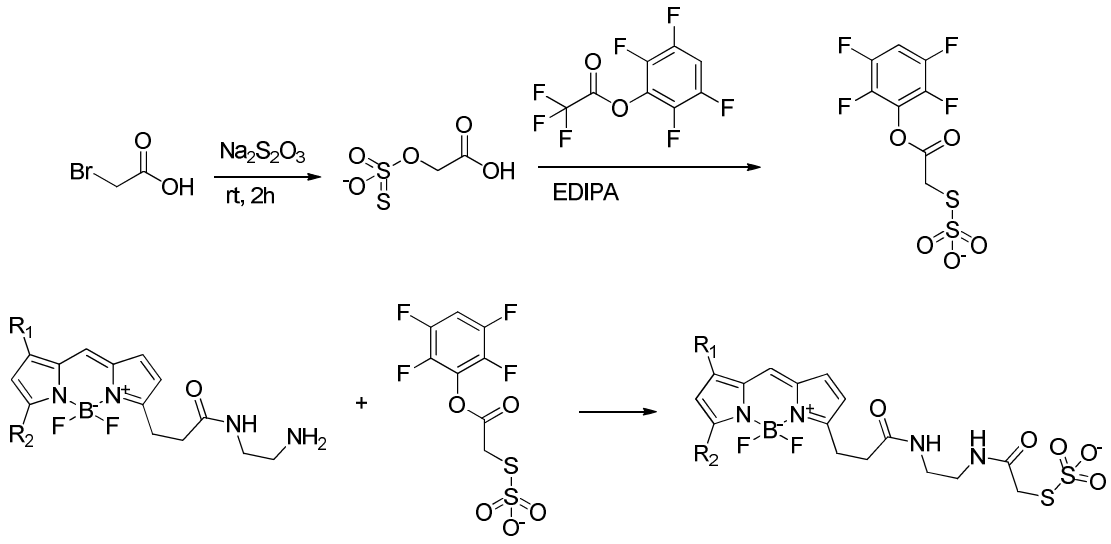

Figure 19. Synthetic procedure for obtaining a thiosulfate BODIPY dye, which was presented in the molecular probes patent filed in 2005 [41].

Several companies commercially produce BODIPY dyes functionalized with MTS, and their applications in protein labeling can be found in the literature. One of these compounds was employed to study the structural properties of the N-terminal domain in photosynthetic complex CP29 using Förster resonance electron transfer (FRET) [43]. Each amino acid in this domain was separately substituted with a cysteine residue, resulting in several singly mutated proteins that were subsequently labeled with the BODIPY dye at the cysteine residue. The application of the FRET studies allowed the authors to determine how each amino acid position interact with the other protein motifs, resulting in the elucidation of the structural properties of the protein.

Two procedures for the synthesis of MTS BODIPYs have been published. One synthetic method conjugated the pyrrolic unit with chloroacetyl chloride generating a chlorinated dipyrrin that was converted to the respective BODIPY using TEA and $BF_3.OEt_2$ [44]. The chlorine was displaced by iodine in a reaction with sodium iodide followed by formation of a thiosulfonate moiety via reaction with sodium thiosulfonate (Figure 20). Although the authors propose the use of the obtained BODIPY for biolabeling, it is not tested.

The other synthetic approach involved the use of a commercially available BODIPY bearing a succinimidyl ester reactive group [45]. The reaction of the commercial BODIPY and 3-aminopropyl methanethiosulfonate hydrobromide catalyzed by diisopropylethylamine (DIPEA) yielded a BODIPY derivative with a free MTS group (Figure 20). The conjugation of the BODIPY with the muscle nicotinic acetylcholine receptor was not successful, despite the success achieved with other MTS fluorophores [44].

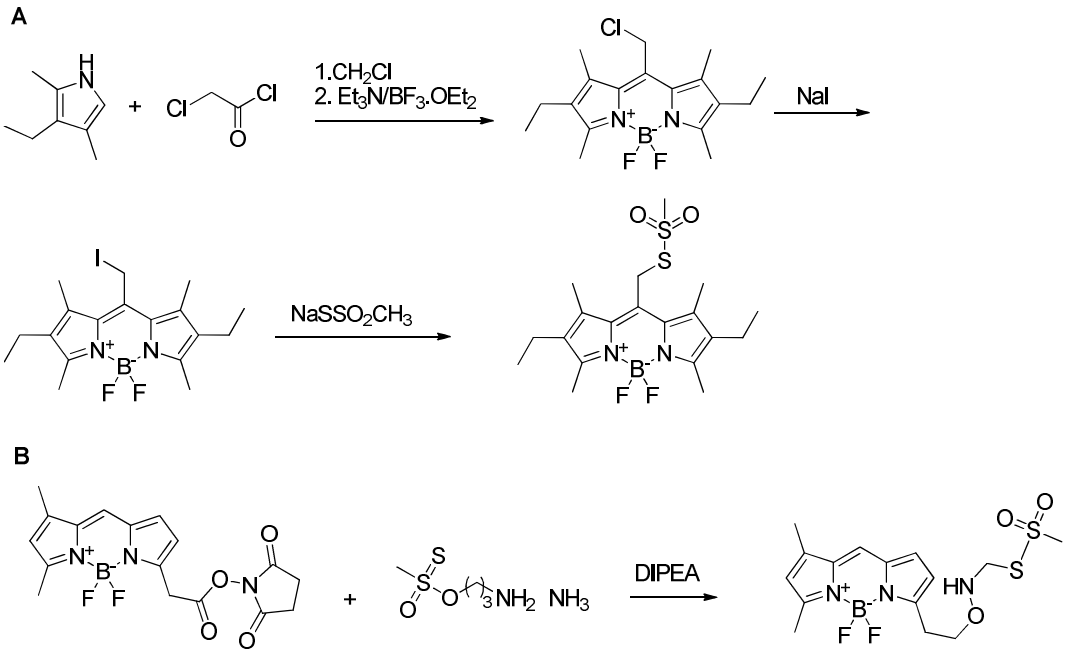

Figure 20. Two synthetic procedures for the preparation of MTS-BODIPY.

7. BODIPYS FOR BIOORTHOGONAL LABELING

In addition to classic protein bioconjugation targeting functionalities present in the side chains of natural amino acids, bioorthogonal labeling arose as a valuable approach for protein modification. In this approach, specific chemical modifications are realized in the protein allowing its specifc protein labeling by targeting non-natural functional groups [46].

The nucleophilic attack by a nitrogen nucleophile, such as hydrazine, hydrazide and hydroxylamine, in carbonyl-containing functionalities, such as an aldehyde or ketone, has been an extensively explored orthogonal approach for protein labeling. These functionalities can be introduced into proteins via chemical or genetic strategies, such as the insertion of the unnatural amino acid *para*-acetyl-phenylalanine, post-translational enzymatic modification of glycine to

formylglycine and chemical insertion of aminooxy at the C-terminus [46, 47]. After reaction with the carbonyl compounds, hydrazine and hydrazide form a hydrazone linkage while hydroxylamine forms an oxime linkage (Figure 21).

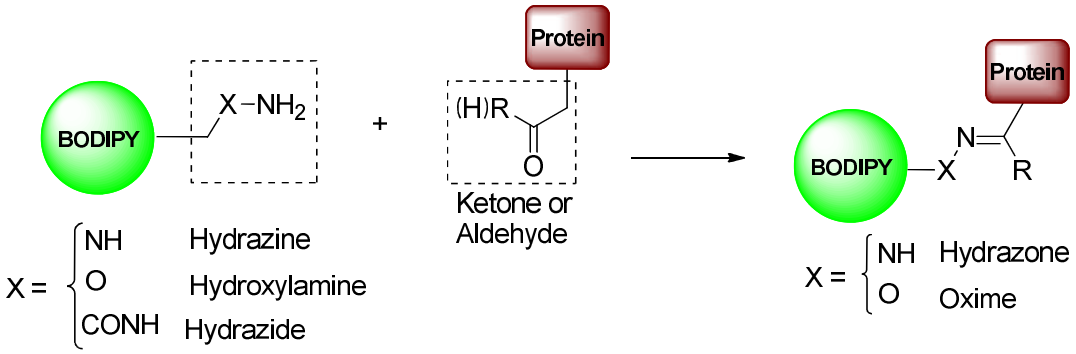

Figure 21. Mechanism of ketone and aldehyde labeling using hydrazine, hydrazide or aminooxy compounds.

The 1988 molecular probes patent [5] reported the synthesis of BODIPY dyes tagged with hydrazide and sulfonyl hydrazide moieties. The hydrazide derivative was obtained from a BODIPY precursor containing an ethyl ester, which was obtained from the reaction of a 2-pyrrole carbaldehyde and another pyrrolic unit with an ethyl ester functionality. These units were condensed in a reaction catalyzed by hydrobromic acid to yield the respective dipyrrin, which was then complexed with the difluoroboryl unit. The ester is converted to a hydrazide via reaction with hydrazine hydrate (Figure 22).

The synthetic procedure to obtain the sulfonyl hydrazide employed a sodium sulfonate BODIPY, which we speculate was generated from the reaction of BODIPY and chlorosulfuric acid. The sulfonate BODIPY is converted to a sulfonyl chloride derivative through the reaction with thionyl chloride followed by conversion to sulfonyl hydrazide using hydrazine hydrate as the reagent (Figure 22).

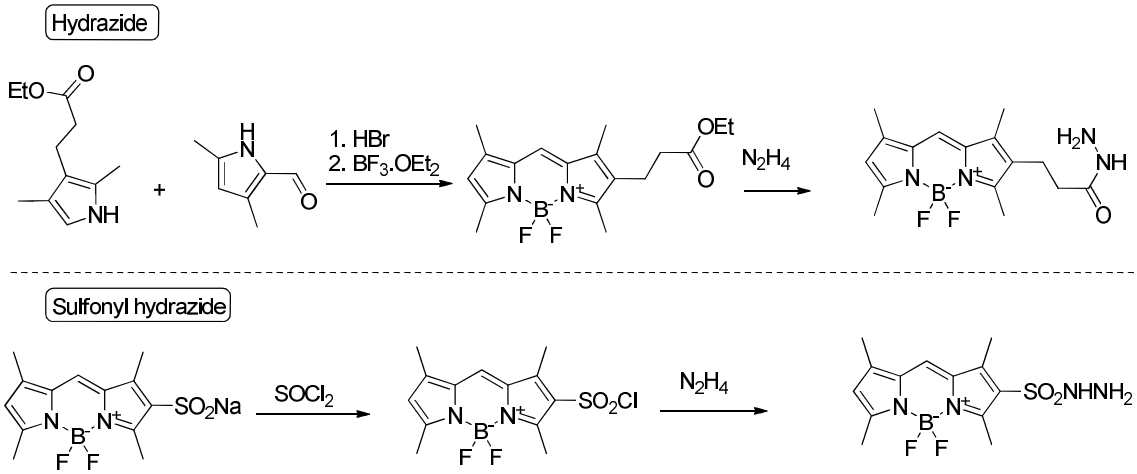

Figure 22. Synthetic methods for obtaining hydrazide and sulfonyl hydrazide BODIPY derivatives described in the molecular probes patent [5].

Two additional papers describe synthetic procedures for generating hydrazine and hydrazide BODIPYs. One procedure involved the use of dichloro-BODIPY, which was obtained from the chlorination of dipyrromethane with N-chlorosuccinimide (NCS) followed by aromatization and complexation to obtain the respective BODIPY [48]. By manipulation of the stoichiometric

relationship between this compound and hydrazine, it was possible to obtain either the monohydrazine or the dihydrazine BODIPYs. The displacement of the remaining chloride atom with various electrophiles generated a small library of monohydrazine BODIPYs (Figure 23). The application of the compounds in bioorthogonal labeling was proposed, and their reactivity against simple aldehydes was successfully shown. However, no assays with proteins are reported.

The hydrazide-BODIPY was synthesized for application as a marker for quantification of serum aldehyde via chromatographic methods. The procedure employed a meso-substituted BODIPY with a carboxylic moiety synthesized using a cyclic anhydride precursor [49]. The carboxyl group was activated with a succinimidyl ester functionality in a reaction with NHS catalyzed by DCC and subsequently reacted with hydrazine to yield the hydrazide functionality (Figure 23).

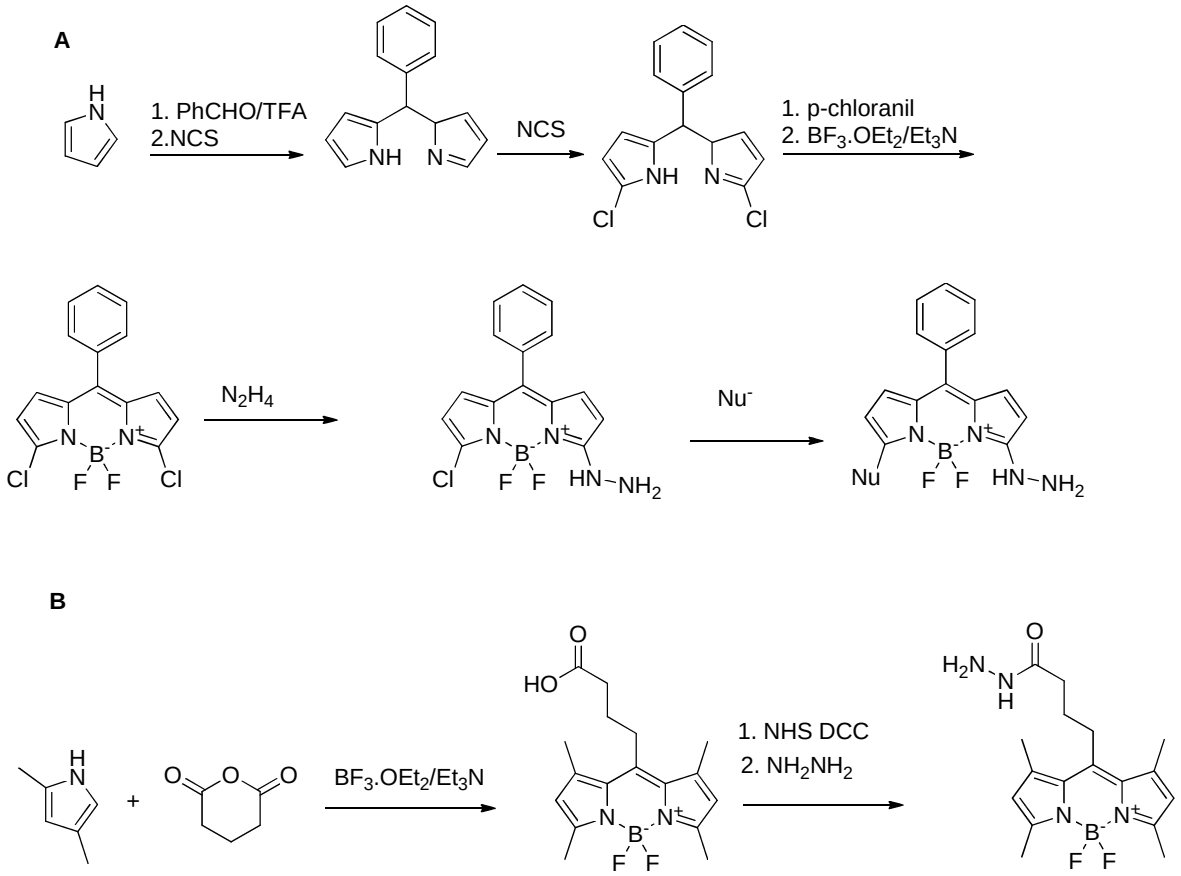

Figure 23. **A**: Method for synthesizing the hydrazine-BODIPY **B**: Method for synthesizing the hydrazide-BODIPY reported in the literature.

In 2011, a synthetic procedure described the preparation of a BODIPY bearing an aminooxy reactive group. The aim of the study was to synthesize a fluorescent probe to mark a quorum sensing chemical (i.e., 3-oxododecanoyl homoserine lactone) bound to a proteic transcriptional modulator present in some bacteria, which would allow for the bioorthogonal labeling of this protein [50]. The initial steps of the synthetic procedure were addressed earlier in this review and involved the synthesis of a BODIPY with an aniline moiety. In this particular case, the fluorophore precursor was obtained by the reduction of the nitro-containing BODIPY using sodium borohydride and nickel chloride. Phthalimido-aminooxyacetic acid (obtained from the sodium hydride-catalyzed reaction of N-hydroxyphthalimide and bromoacetic acid) was linked to the BODIPY by an amide linkage catalyzed by DCC. The phthalimido-protected BODIPY was converted to the hydroxylamine derivative using hydrazine with phthalimide as the leaving group (Figure 24). The hydroxylamine BODIPY was successfully attached to the keto group present in the transcriptional activator. When catalyzed by aniline, better results were obtained from the *in vitro* coupling at pH 4 compared to that at neutral pH.

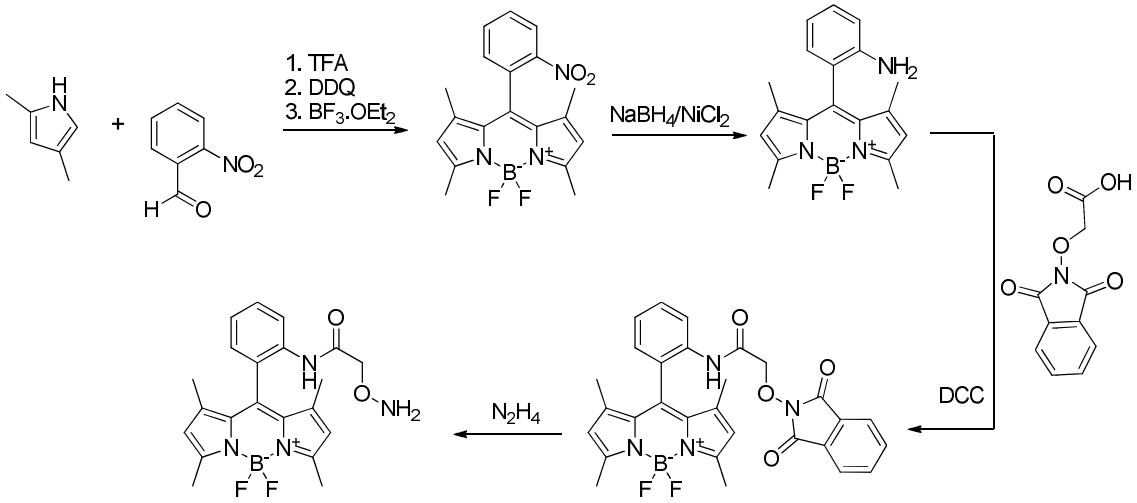

Figure 24. Successful synthetic approach for generation of hydroxylamine-BODIPY.

The cycloaddition of azides and alkynes is another important strategy for orthogonal protein labeling. This reaction occurs via a concerted mechanism, which has been known for a long time. However, only recently the copper-catalyzed azide-alkyne cycloaddition reaction (CuAAC), known as Huisgen cycloaddition, was applied to the field of biomolecule labeling. More recently, the use of cyclooctynes is being employed as the reagent to avoid the use of a metal catalyst [46]. The coupling of substances using this method results in a 1,2,3-triazole linkage, which is the most popular reaction in "click chemistry" (Figure 25). Currently, several azide and alkyne tags are available for protein modification for their labeling with click chemistry-based conjugation.

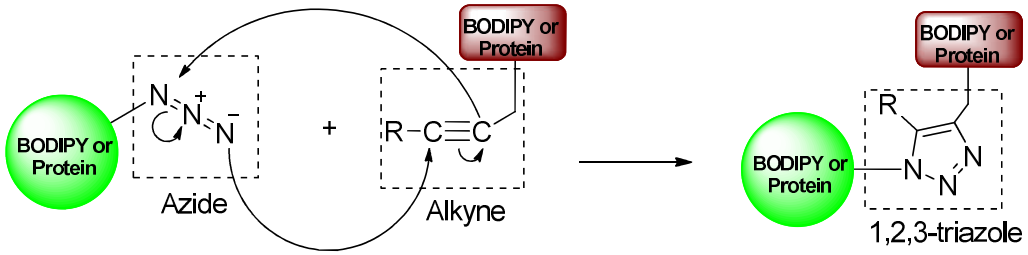

Figure 25. Mechanism of coupling between an alkyne and an azide yielding the 1,2,3-triazole as the connecting linker.

Since its development, the click azide-alkyne reaction has been widely employed for conjugations in several areas of chemistry, we were not surprised to find several methods to obtain alkyne-BODIPY and azide-BODIPYs in the literature. Interestingly, to the best of our knowledge, none of the synthesized azido-BODIPYs were employed in the orthogonal labeling of proteins. However, due to their potential application in this field, we will review the synthetic approaches for preparing these molecules. The 1988 Molecular Probes patent reports an azide-BODIPY synthesized from the addition of sodium nitrite and hydrochloric acid to form hydrazide-BODIPY, whose synthesis was shown above (Figure 26).

An approach employed in other studies involved the use of bromohexyl benzaldehyde in a reaction with a pyrrolic derivative. After aromatization and complexation, the respective meso-substituted BODIPY was obtained, yielding an azido-BODIPY after reaction with sodium azide [51, 52] (Figure 26). A similar approach involves the conversion of the halogen in a haloalkyl benzaldehyde to the azido functionality, followed by the direct application of the azido-appended benzaldehyde in

the synthesis of a meso-substituted BODIPY (Figure 26). This method was successfully employed for the synthesis of azido-BODIPY dyes [53, 54]. The use of alkyne-substituted benzaldehyde is the most widely employed method for the synthesis of BODIPYs with this moiety [55- 57].

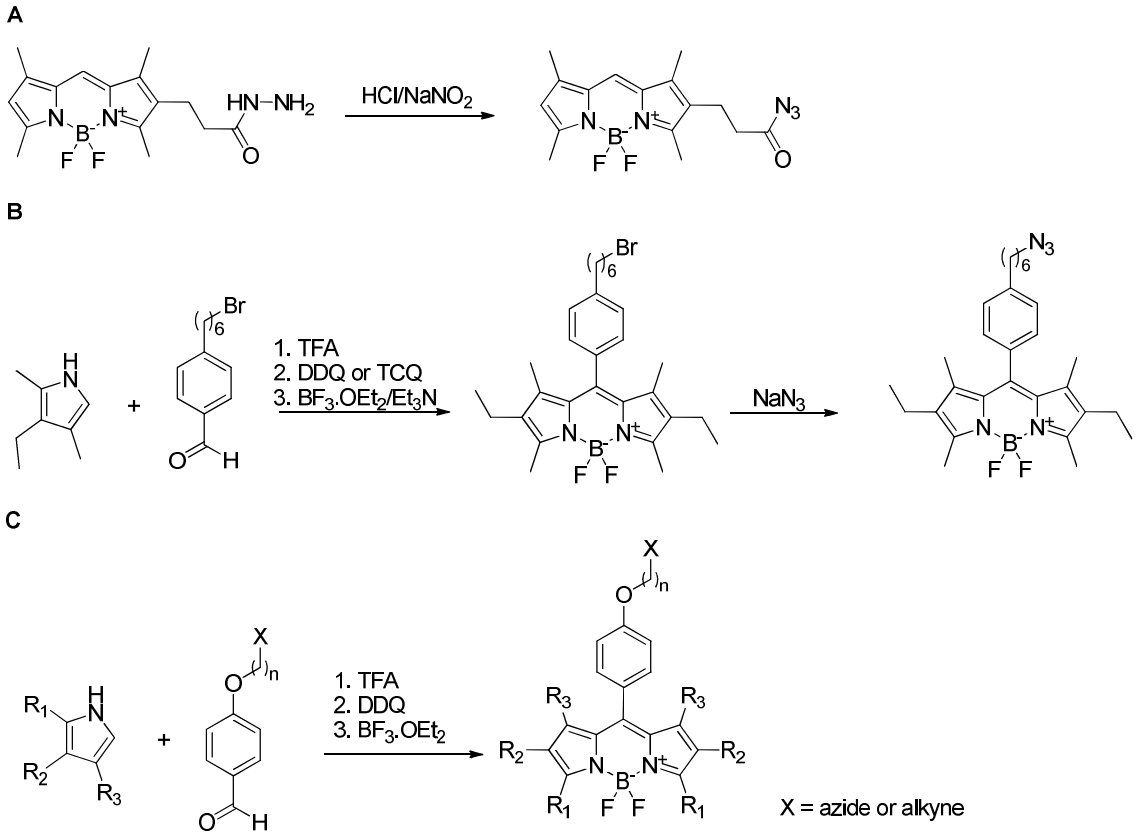

Figure 26. **A**: Synthesis of the azido-BODIPY shown in a patent by molecular probes [5]. **B:** Application of bromohexyl benzaldehyde to obtain an azido-BODIPY. **C:** Direct synthesis of azido-BODIPY and alkynyl-BODIPY using the respective functionalized benzaldehydes.

Brominating and chlorinating agents have also been successfully employed in the synthesis of azido-BODIPYs (Figure 27). It was recently shown that the reaction of methylated BODIPYs with NBS yields brominated BODIPYs with the halogen at the methyl group linked to one or both C_2 depending on the stoichiometric relationship between the reagents. These compounds were used to obtain azido-BODIPY derivatives from their reaction with sodium azide and alkyne-BODIPYs by reaction with propargyl alcohol [58]. The chlorinating agent NCS has been shown to generate chlorinated dipyrromethanes directly at C_2. After aromatization and complexation with difluoroboryl, the chlorinated BODIPYs react with sodium azide to yield the respective azido-BODIPY [59] (Figure 27).

Azido alkylamines can be obtained from the reaction of bromo alkylamine hydroboride with sodium azide or from a similar reaction with N-phthalimido bromo alkylamine followed by amine deprotection with hydrazine (Figure 28). The coupling of these amines via an amide linkage with commercially available succinimidyl ester-BODIPYs has been applied to synthesize azido BODIPYs [60, 61]. A similar approach involves the use of an azidocarboxylic acid to couple, via an ester linkage, with a BODIPY containing a hydroxyl group, which was obtained from the deacetylation of a commercialy available material (Figure 28).

Another useful strategy is the Knoevenagel condensation, which is a very powerful reaction for modifying BODIPYs, and is the most widely used method for tuning their photophysical properties. In this reaction, aromatic aldehydes are used to add allyl aromatic substituents to the methyl positions at C2 of the BODIPYs. This method allows researchers not only to modify photophysical properties but also to insert functionalities. This method had been employed

for the addition of both azido [52, 62, 63] and alkyne functionalities to the BODIPY core in reactions catalyzed by acetic acid and piperidine (Figure 29).

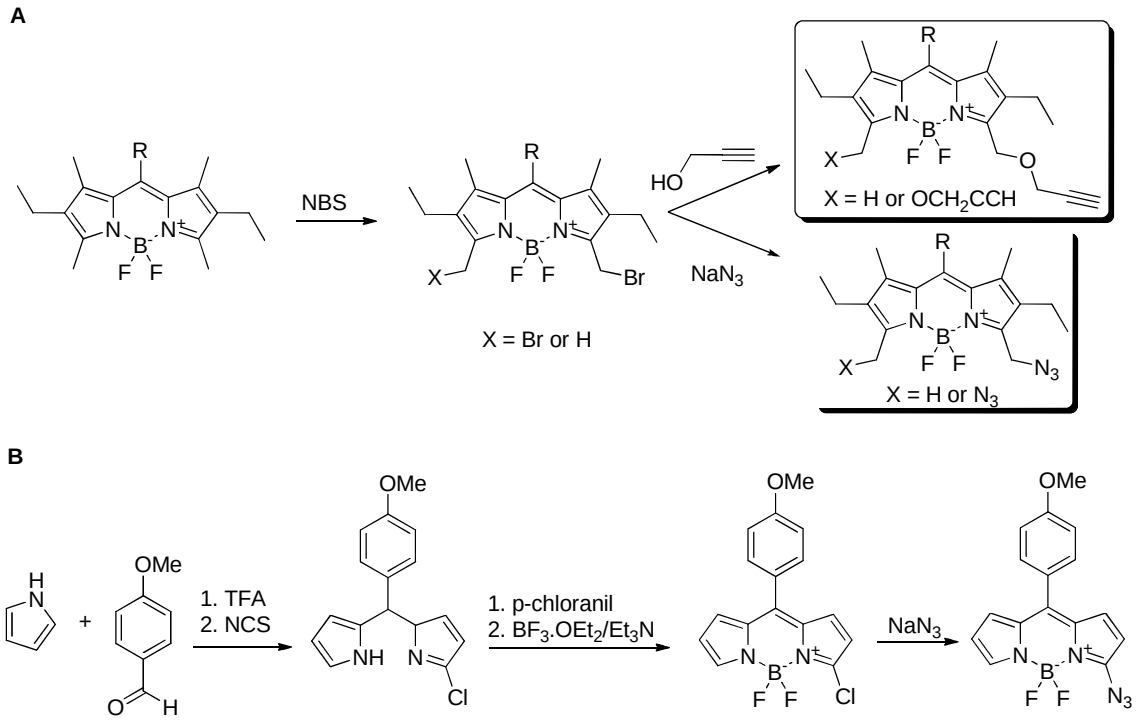

Figure 27. **A**: Bromination of the methyl groups on the BODIPY core using NBS followed by synthesis of alkynyl-BODIPYs and azido-BODIPYs. **B:** Direct chlorination of meso-substituted dipyrromethanes using NCS followed by azido-BODIPY synthesis from application of sodium azide.

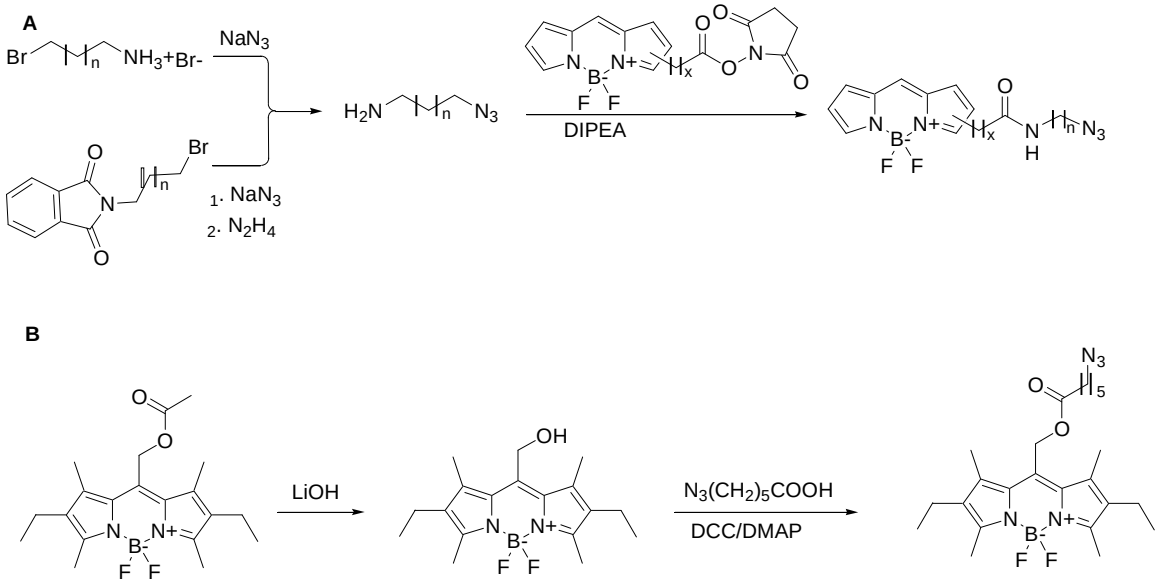

Figure 28. **A**: Application of azido alkylamines in the synthesis of azido-BODIPYs. **B:** Ester coupling of an azidocarboxylic acid to a deacetylated commercial BODIPY.

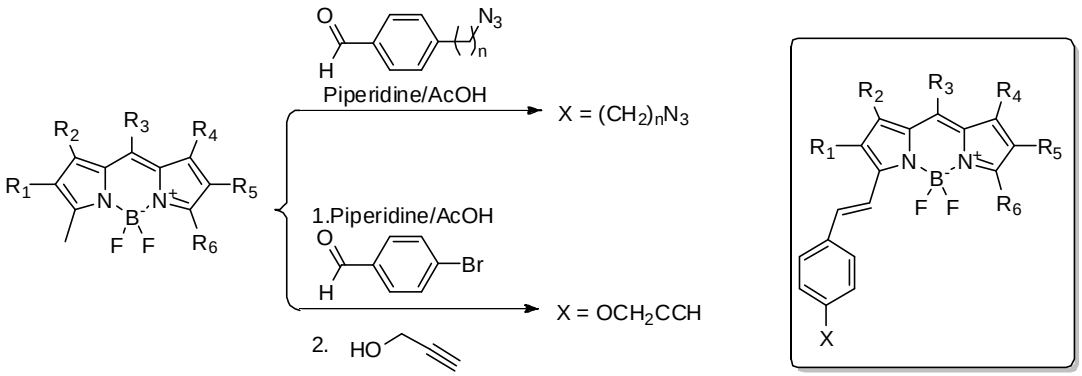

Figure 29. Application of the Knoevenagel condensation to the synthesis of alkynyl-BODIPY and azido-BODIPY.

8. OTHER BODIPY DYES

The syntheses of alternative BODIPY dyes deserves to be mentioned in this review. In 1993, a BODIPY with an imidazole heterocycle was synthesized by a group at Northeastern University, and it was named BO-IMI. In an EDC-catalyzed reaction with a phosphate group, this compound would yield a stable phosphorimidazolide linkage, while the same reaction with a carboxyl group would afford an easily hydrolyzed acylimidazole linkage (Figure 30). Therefore, BO-IMI could be used as a phosphate-reactive probe [64].

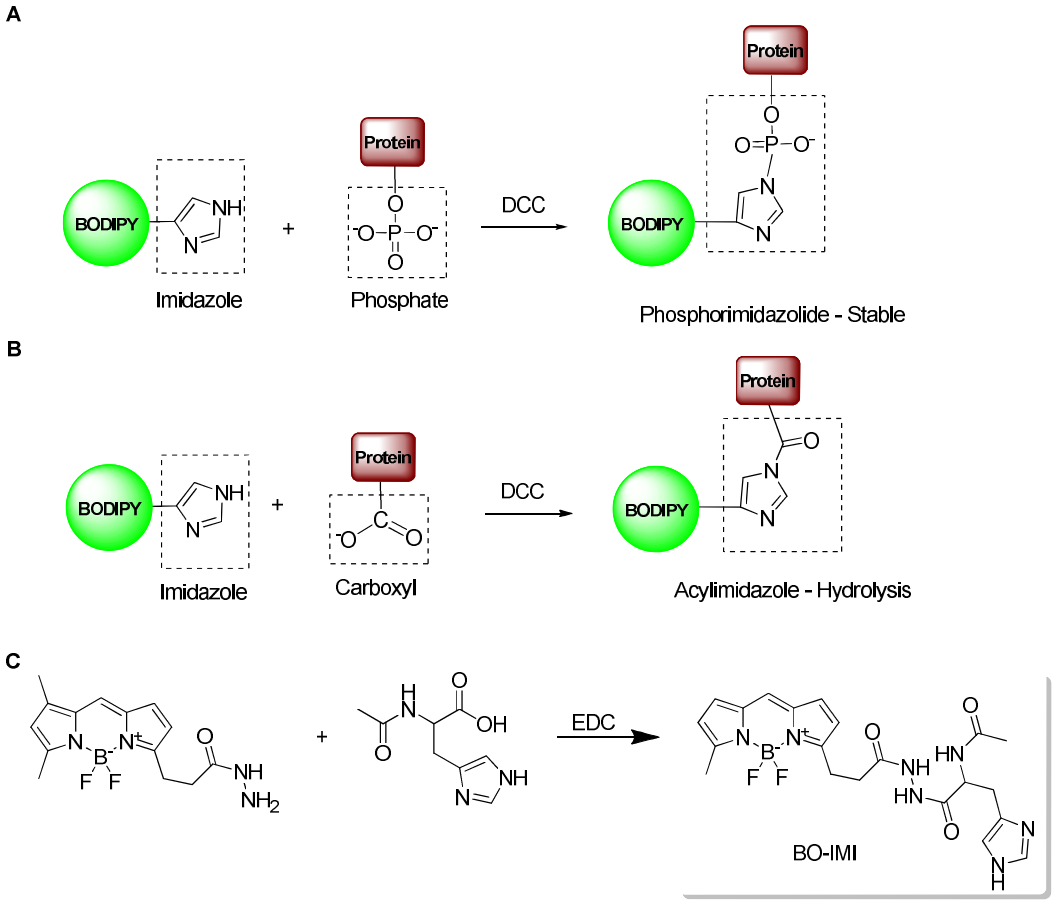

Figure 30. **A**: Coupling between a phosphate group and imidazole yielding a stable phosphorimidazole linkage. **B**: Coupling between a carboxyl group and imidazole yielding an unstable acylimidazole linkage. **C**: Synthesis of BO-IMI.

BO-IMI was synthesized from the EDC-catalyzed coupling of a commercially available hydrazide-BODIPY and N-acetyl-L-histidine [64] (Figure 30). This probe was successfully employed for the labeling of pepsin, which is a protein containing a phosphate moiety linked to its structure. BO-IMI was incubated for 14 hours with EDC and pepsin in an MES/NaOH buffer at pH 5.5. The same coupling procedure using a pepsin sample that was pre-treated with a phosphatase resulted in a severe loss of fluorescence, which suggested selective linking to the phosphate moiety [65].

Diacrylate BODIPY is another interesting probe synthesized to label proteins [66]. A BODIPY with two acrylates conjugated to the fluorescent core was synthesized for use as a marker for proteins linked to an "RC" peptide tag (Arg-Cys-X-X-Cys-Arg). The idea is that the double bonds in the acrylate moieties would covalently bind to the sulfhydryl group of the cysteines and that the carboxyl groups would form an ionic interaction with the guanidinum moiety of arginine. Once the probe links to the protein, the conjugation extension is reduced, resulting in a decrease in the emission wavelength, which enables the differentiation between the emission of the free BODIPY and the protein-linked BODIPY.

The probe was synthesized from a meso-substituted dipyrromethane obtained by a TFA-catalyzed reaction of benzaldehyde derivatives and pyrrole. A carbonyl group is added to C2 and C10 at the dipyrromethane via a Vilsmeier reaction. Application of the Wittig reaction of the dipyrromethene followed by aromatization with DDQ and complexation with a difluoroboryl unit affords the diacrylate-BODIPY (Figure 31). The capacity to stain tagged proteins was studied in protein samples using SDS-PAGE, and the synthesized BODIPYs were shown to specifically label RC-tagged proteins. Fluorescence microscopy experiments in transfected live cells expressing tagged H2B histone resulted in clear nuclear staining, which illustrated the specificity of the dye to tagged proteins.

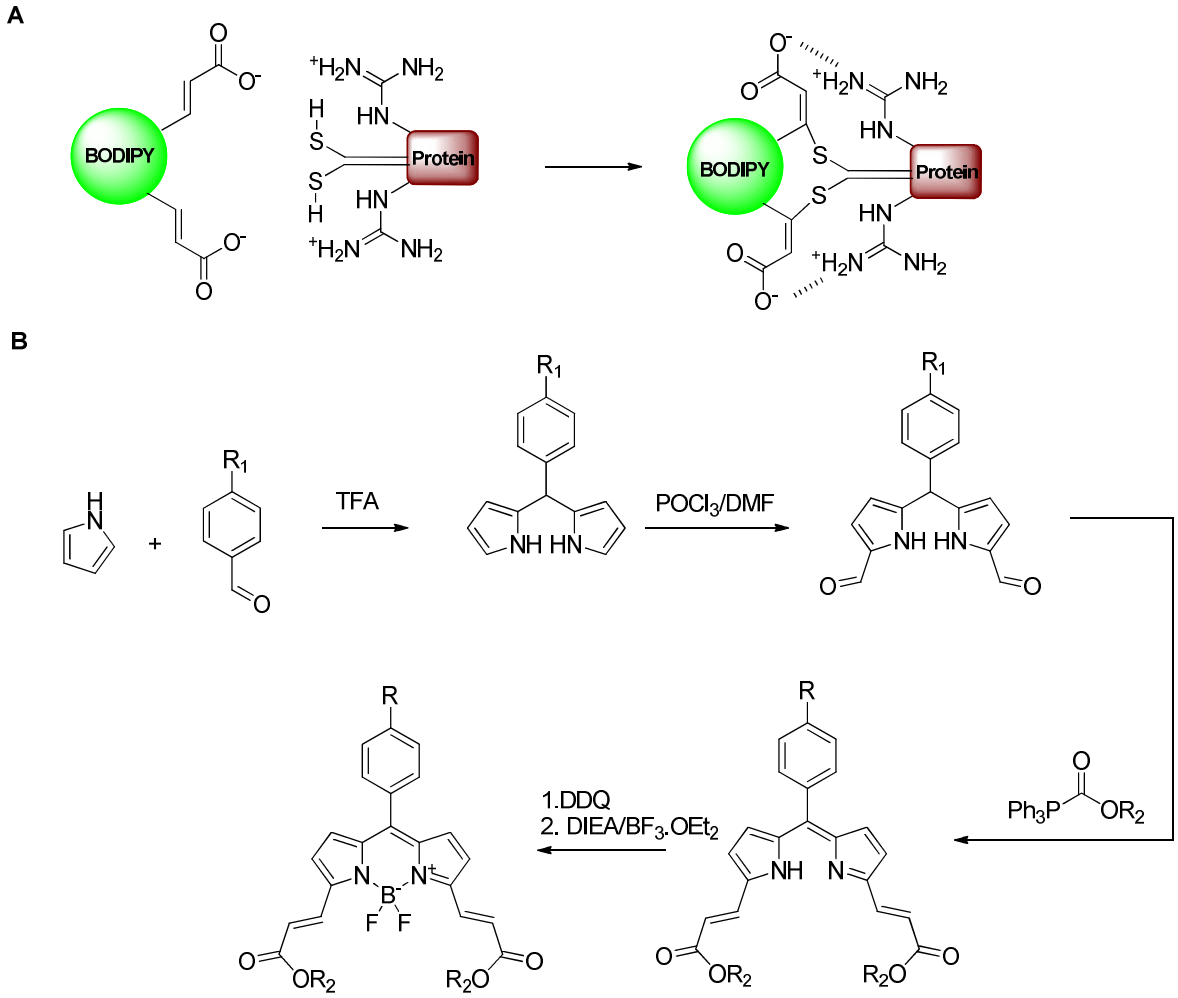

Figure 31. **A**: Interaction between the diacrylate moiety and the RC-tagged proteins **B**: Synthesis of diacrylate BODIPYs.

9. CONCLUDING REMARKS

BODIPYs are highly valuable compounds in the field of biomolecule labeling due to their chemical stability and photophysical properties. As a consequence of their relatively easy synthesis and chemical modification, this class of compounds was the subject of a wide range of studies both in the area of biological labeling and chemical synthesis. Herein, we reviewed studies focusing on both subjects. By studying the available synthetic methods for the preparation of BODIPYs for protein labeling, we have provided a review of the state of the art in this area. We found many underexplored synthetic methods that can be employed to produce reactive BODIPYs for protein labeling. It is also important to note that the field of bioorthogonal labeling of biomolecules is on the rise and few BODIPYs possessing chemical motifs applicable in this area have been explored. Finally, due to the increasing number of fluorescent-based techniques, interest in novel high-yielding synthetic procedures for the synthesis of BODIPY dyes with variable chemical groups and photophysical properties will continue to grow.

10. REFERENCES AND NOTES

[1] Valeur, B.; Berberan-Santos, M. N., *J. Chem. Educ.* **2011**, *88*, 731. [CrossRef]

[2] Valeur, B., Molecular Fluorescence: Principles and Applications, Weinheim: Wiley-VCH, 2001;

[3] Lakowicz, J. R., Principles of Fluorescence Spectroscopy 3rd ed. Singapore: Springer, 2006.

[4] Treibs, A.; Kreuzer, F. H. *Liebigs Ann. Chem.* **1968**, *718*, 208. [CrossRef]

[5] Haugland, R. P.; Kang, H. C. US pat. 4,774,339 1988.

[6] Boens, N.; Leen, V.; Dehaen, W. *Chem. Soc. Rev.* **2012**, *41*, 1130. [CrossRef]

[7] Anderson, G. W.; Callahan, F. M.; Zimmerman, J. E. *J. Am. Chem. Soc.* **1964**, *86*, 1839. [CrossRef]

[8] Hoagland, P. D.; Boswell, R. T.; Jones, S. B. *J. Dairy Sci.* **1971**, *54*, 1564. [CrossRef]

[9] Folsch, G., *Acta Chem. Scand.* **1970**, *24*, 1115. [CrossRef]

[10] Bolton, A. E.; Hunter, W. M. *Biochem. J.* **1973**, *133*, 529.

[11] Müller, G. H. *J. Cell. Sci.* **1980**, *43*, 319.

[12] Demushki, V. P.; Budowsky, E. I. *FEBS Lett.* **1972**, *22*, 89. [CrossRef]

[13] Weston, S. A.; Parish, C. R. *J. Immunol. Methods* **1990**, *133*, 87. [CrossRef]

[14] Thompson, V. F.; Saldaña, S.; Cong, J.; Goll, D. E. *Anal. Biochem.* **2000**, *279*, 170. [CrossRef]

[15] Schade, S. Z.; Jolley, M. E.; Sarauer, B. J.; Simonson, L. G. *Anal. Biochem.* **1996**, *243*, 1. [CrossRef]

[16] Diemel, R. V.; Bader, D.; Walch, M.; Hotter, B.; van Golde, L. M.; Amann, A.; Haagsman, H. P.; Putz, G. *Arch. Biochem. Biophys.* **2001**, *385*, 338. [CrossRef]

[17] Meltola, N. J.; Wahlroos, R.; Soini, A. E. *J. Fluoresc.* **2004**, *14*, 635. [CrossRef]

[18] Li, J. S.; Wang, H.; Cao, L. W.; Zhang, H. S., *Talanta.* **2006**, *69*, 1190. [CrossRef]

[19] Wang, D.; Fan, J.; Gao, X.; Wang, B.; Sun, S.; Peng, X. *J. Org. Chem.* **2009**, *74*, 7675. [CrossRef]

[20] Riggs, J. L.; Seiwald, R. J.; Burckhalter, J. H.; Downs, C. M.; Metcalf, T. G. *Am. J. Pathol.* **1958**, *34*, 1081.

[21] Meltola, N. J.; Soini, A. E.; Hanninen, P. E. *J. Fluoresc.* **2004**, *14*, 129. [CrossRef]

[22] Malatesti, N.; Hudson, R.; Smith, K.; Savoie, H.; Rix, K.; Welham, K.; Boyle, R. W. *Photochem. Photobiol.* **2006**, *82*, 746. [CrossRef]

[23] Yamane, T.; Hanaoka, K.; Muramatsu, Y.; Tamura, K.; Adachi, Y.; Miyashita, Y.; Hirata, Y.; Nagano, T. *Bioconjug. Chem.* **2011**, *22*, 2227. [CrossRef]

[24] Ziessel, R.; Bonardi, L.; Retailleau, P.; Ulrich, G. *J. Org. Chem.* **2006**, *71*, 3093. [CrossRef]

[25] Smythe, C. V. *J. Biol. Chem.* **1936**, *114*, 601.

[26] Hermanson, G. T., Bioconjugate Techniques. 2nd ed. Waltham: Academic Press, 2008.

[27] Baker, G. A.; Pandey, S.; Kane, M. A.; Maloney, T. D.; Hartnett, A. M.; Bright, F. V. *Biopolymers.* **2001**, *59*, 502. [CrossRef]

[28] De Taeye, B.; Compernolle, G.; Declerck, P. J. *J. Biol. Chem.* **2004**, *279*, 20447. [CrossRef]

[29] Dansen, T. B.; Pap, E. H. W.; Wanders, R. J. A.; Wirtz, K. W. A. *Histochem. J.* **2001**, *33*, 65. [CrossRef]

[30] Guminski, Y.; Grousseaud, M.; Cugnasse, S.; Brel, V.; Annereau, J. P.; Vispé, S.; Guilbaud, N.; Barret, J. M.; Bailly, C.; Imbert, T. *Bioorg. Med. Chem. Lett.* **2009**, *19*, 2474. [CrossRef]

[31] Friedmann, E.; Marrian, D. H.; Simonreuss, I. *Br. J. Pharmacol. Chemother.* **1949**, *4*, 105. [CrossRef]

[32] Gregory, J. D. *J. Am. Chem. Soc.* **1955**, *77*, 3922. [CrossRef]

[33] Haugland, R. P.; Kang, H. C. US pat. 5,248,782 1993.

[34] Hill, B. G.; Reily, C.; Oh, J. Y.; Johnson, M. S.; Landar, A. *Free Radic. Biol. Med.* **2009**, *47*, 675. [CrossRef]

[35] Matsumoto, T.; Urano, Y.; Shoda, T.; Kojima, H.; Nagano, T. *Org. Lett.* **2007**, *9*, 3375. [CrossRef]

[36] Yang, J.; Chen, H.; Vlahov, I. R.; Cheng, J.-X.; Low, P. S. *J. Pharmacol. Exp. Ther.* **2007**, *321*, 462. [CrossRef]

[37] Lewis, C. A.; Munroe, W. A.; Dunlap, R. B. *Biochemistry.* **1978**, *17*, 5382. [CrossRef]

[38] Owenius, R.; Osterlund, M.; Lindgren, M.; Svensson, M.; Olsen, O. H.; Persson, E.; Freskgard, P. O.; Carlsson, U. *Biophys. J.* **1999**, *77*, 2237. [CrossRef]

[39] Hainfeld, J. F.; Foley, C. J.; Maelia, L. E.; Lipka, J. J. *J. Histochem. Cytochem.* **1990**, *38*, 1787. [CrossRef]

[40] Loo, T. W.; Bartlett, M. C.; Clarke, D. M. *J. Biol. Chem.* **2003**, *278*, 50136. [CrossRef]

[41] Haugland, R.; Kang, H. C. US pat. appl. publ. US2005/0250957 A1 2005.

[42] Barrera, F. N.; Fendos, J.; Engelman, D. M. *Proc. Natl. Acad. Sci. USA.* **2012**, *109*, 14422-7. [CrossRef]

[43] Berghuis, B. A.; Spruijt, R. B.; Koehorst, R. B. M.; van Hoek, A.; Laptenok, S. P.; van Oort, B.; van Amerongen, H. *Eur. Biophys. J.* **2010**, *39*, 631. [CrossRef]

[44] Kalai, T.; Hideg, K. *Tetrahedron.* **2006**, *62*, 10352. [CrossRef]

[45] Pantoja, R.; Rodriguez, E. A.; Dibas, M. I.; Dougherty, D. A.; Lester, H. A. *Biophys. J.* **2009**, *96*, 226. [CrossRef]

[46] Sletten, E. M.; Bertozzi, C. R. *Angew. Chem. Int. Ed.* **2009**, *48*, 6974. [CrossRef]

[47] Yi, L.; Sun, H.; Wu, Y.-W.; Triola, G.; Waldmann, H.; Goody, R. S. *Angew. Chem. Int. Ed.* **2010**, *49*, 9417. [CrossRef]

[48] Dilek, O.; Bane, S. L. *Tetrahedron Lett.* **2008**, *49*, 1413. [CrossRef]

[49] Xiong, X.-J.; Wang, H.; Rao, W.-B.; Guo, X.-F.; Zhang, H.-S. *J. Chromatogr. A* **2010**, *1217*, 49. [CrossRef]

[50] Rayo, J.; Amara, N.; Krief, P.; Meijler, M. M. *J. Am. Chem. Soc.* **2011**, *133*, 7469. [CrossRef]

[51] Kostereli, Z.; Ozdemir, T.; Buyukcakir, O.; Akkaya, E. U. *Org. Lett.* **2012**, *14*, 3636. [CrossRef]

[52] Bozdemir, O. A.; Erbas-Cakmak, S.; Ekiz, O. O.; Dana, A.; Akkaya, E. U. *Angew. Chem. Int. Ed.* **2011**, *50*, 10907. [CrossRef]

[53] Li, L.; Han, J.; Nguyen, B.; Burgess, K. *J. Org. Chem.* **2008**, *73*, 1963. [CrossRef]

[54] Jose, J.; Ueno, Y.; Castro, J. C.; Li, L.; Burgess, K. *Tetrahedron Lett.* **2009**, *50*, 6442. [CrossRef]

[55] Perez-Ojeda, E. M.; Trastoy, B.; Lopez-Arbeloa, I.; Banuelos, J.; Costela, A.; Garcia-Moreno, I.; Luis Chiara, J. *Chem. - Eur. J.* **2011**, *17*, 13258. [CrossRef]

[56] Li, Z.; Bittman, R. *J. Org. Chem.* **2007**, *72*, 8376. [CrossRef]

[57] Erbas, S.; Gorgulu, A.; Kocakusakogullari, M.; Akkaya, E. U. *Chem. Commun*. **2009**, *7*, 4956. [CrossRef]

[58] Ulrich, G.; Ziessel, R.; Haefele, A. *J. Org. Chem.* **2012**, *77*, 4298. [CrossRef]

[59] Wang, C.; Xie, F.; Suthiwangcharoen, N.; Sun, J.; Wang, Q. *Sci. China: Chem.* **2012**, *55*, 125.

[60] Willems, L. I.; Li, N.; Florea, B. I.; Ruben, M.; van der Marel, G. A.; Overkleeft, H. S. *Angew. Chem. Int. Ed.* **2012**, *51*, 44. [CrossRef]

[61] Cunningham, C. W.; Mukhopadhyay, A.; Lushington, G. H.; Blagg, B. S. J.; Prisinzano, T. E.; Krise, J. P. *Mol. Pharmaceutics* **2010**, *7*, 1301. [CrossRef]

[62] Hoogendoorn, S.; Blom, A. E. M.; Willems, L. I.; van der Marel, G. A.; Overkleeft, H. S. *Org. Lett.* **2011**, *13*, 5656. [CrossRef]

[63] Vedamalai, M.; Wu, S. P. *Org. Biomol. Chem.* **2012**, 10, 5410. [CrossRef]

[64] Wang, P. G.; Giese, R. W. *Anal. Chem.* **1993**, *65*, 3518. [CrossRef]

[65] Wang, P. G.; Giese, R. W. *J. Chromatogr. A* **1998**, *809* (1-2), 211. [CrossRef]

[66] Lee, J. J.; Lee, S. C.; Zhai, D.; Ahn, Y. H.; Yeo, H. Y.; Tan, Y. L.; Chang, Y. T. *Chem. Commun (Camb).* **2011**, 47, 4508. [CrossRef]